Investigations on the use of circular RNA for effective inhibition of protein biosynthesis in plants and fungi

Dissertation zur Erlangung des Doktorgrades (Dr. rer. nat.) der Agrarwissenschaften, Ökotrophologie und Umweltmanagement der Justus-Liebig-Universität Gießen

durchgeführt am Institut für Phytopathologie

vorgelegt von:
M. Sc. Moammar Hossain
aus Bangladesh

Gießen, 2024

Board of Examiners

Vorsitzende: Prof. Dr. Lühken

Gutachter: Prof. i. R. Dr. Karl-Heinz Kogel

Gutachter: Prof. i. R. Dr. Albrecht Bindereif

Gutachter: Prof. Dr. Patrick Schäfer

Prüfer: Prof. Dr. Volker Wissemann

Prüfer: Prof. Dr. Marc F. Schetelig

Selbstständigkeitserklärung

Ich erkläre, dass ich die vorgelegte Dissertation selbstständig und ohne unerlaubte fremde Hilfe und nur mit den Hilfen angefertigt, die ich in der Dissertation angegeben habe. Alle Textstellen, die wörtlich oder sinngemäß aus veröffentlichten Schriften entnommen sind, und alle Angaben, die auf mündlichen Auskünften beruhen, sind als solche kenntlich gemacht. Ich stimme einer evtl. Überprüfung meiner Dissertation durch eine Antiplagiat-Software zu. Bei den von mir durchgeführten und in der Dissertation erwähnten Untersuchungen habe ich die Grundsätze guter wissenschaftlicher Praxis, wie sie in der „Satzung der Justus-Liebig-Universität Gießen zur Sicherung guter wissenschaftlicher Praxis “ niedergelegt sind, eingehalten.

Datum: 05.06.2024 Unterschrift

Parts of this work already has been or will be published.

Hossain M, Kogel KH, Imani J. (2021) "The use of non-coding RNA (circRNAs) for disease control in plant production" Workshop, Molecular Plant Breeding with an annual general meeting, Organised by the Society for Plant Biotechnology, 6th - 07th September 2021, Germany.

Hossain M, Pfafenrot C, Imani J, Secic E, Sede A, Galli M, Heinlein M, Bindereif A, Ladera-Carmona M, Kogel KH. (2023). Designer antisense circRNA$_{GFP}$ reduces GFP protein abundance in transgenic Arabidopsis protoplasts in a sequence-specific manner and independent of RNAi pathways (Submitted).

Table of contents

Abbreviations

AGO	Argonaute
APS	Ammonium persulfate
AS	Antisense
At	*Arabidopsis thaliana*
Bc	*Botrytis cinerea*
CaMV	Cauliflower mosaic virus
cDNA	Complementary DNA
circRNA	Circular RNA
Col-0	*At* wild-type Columbia-0
DCL	DICER-LIKE
ddH_2O	Double-distilled water
dpi	Days past infection
dsRNA	Double-stranded RNA
E. coli	*Escherichia coli*
EVs	Extracellular vesicles
h	Hours
HIGS	Host-Induced Gene Silencing
LB	Lysogeny broth
miRNA	micro RNA
mRNA	messenger RNA
MS	Murashige & Skoog
MVB	Multivesicular Body
PBS	Phosphate buffered saline
PTI	Pattern-triggered immunity
PTGS	Post-transcriptional gene silencing
qRT-PCR	quantitative real-time PCR
RBP	RNA-binding protein
RISC	RNA-induced silencing complex
RNAi	RNA interference
SDS	Sodium dodecyl sulfate
SDS-PAGE	SDS polyacrylamide gel electrophoresis
SIGS	Spray-Induced Gene Silencing
siRNA	small interfering RNA
SNA-agar	Synthetic nutrient-poor agar
TBS	Tris Buffered Saline
TEM	Transmission Electron Microscopy
TGS	Transcriptional Gene Silencing
VIB	Vesicle Isolation Buffer
WT	Wild-Type

1. Introduction

1.1 Plant pathogen interaction

Food security due to climate change is a major issue in the recent world. The production of staple grains including wheat, barley, and rice is decreasing due to the invasion of new pests and pathogens. Most importantly diseases e.g. Fusarium head blight, grey mold, and rice blasts are destroying huge amounts of grain and other commercial food products in recent times. It has been reported up to 40% of crop losses ensued due to the invasion of pathogens each year worldwide (Alexander et al. 2017; Oerke & Dehne 2004).

In recent times, chemical fertilizers and commercial pesticides have become the most widely used methods to increase the production of grain. However, those are effective methods in a way where the environmental pollutants are also risks to human health nowadays. To minimize those problems scientists are looking for different and sophisticated approaches.

Besides, commercial chemical products, plants themself struggle against pathogens by using their immune system (Jones & Dangl 2006). Due to the lack of specific immune cells in plants, like animals, plants fight against pathogen invasion by using their own cellular response. Perhaps such responses are regulated due to their hormonal homeostasis and protein biosynthesis process (Druege et al. 2016). A different intracellular signaling pathway is responsible for the activation of the plant immune system against pathogens which results in a successful defense reaction cascade. However, pathogens can also overcome the plant defense by targeting distant components of the host plant (Jones & Dangl 2006; Lapin & Van den Ackerveken 2013). There are two different defense layers, that exist in the plant immune system, where the cells recognize and respond against the external signals immediately at infection sites (Jones & Dangl 2006). Those kinds of external signals are termed PAMPs, MAMPs, and DAMPs (Pathogen-, Microbe, and Damage-associated molecular patterns), which are perceived by the plant's pattern recognition receptors (PRR). Pattern-triggered immunity (PTI) is a first-layer defense system in the plant that can restrict the initial pathogens' invasion. However, pathogens can overcome PTI by using effector molecules that can interfere with the PTI process. In the next step, virulence effectors can be perceived through intracellular immune receptors that result in ETI (Effector-triggered immunity) against the pathogens (Macho & Zipfel, 2014). There is a short detail about the immune response by plant cells

described in the following figure 1. Furthermore, many effector molecules are involved throughout the process to gain immunity and combat invasive pathogens.

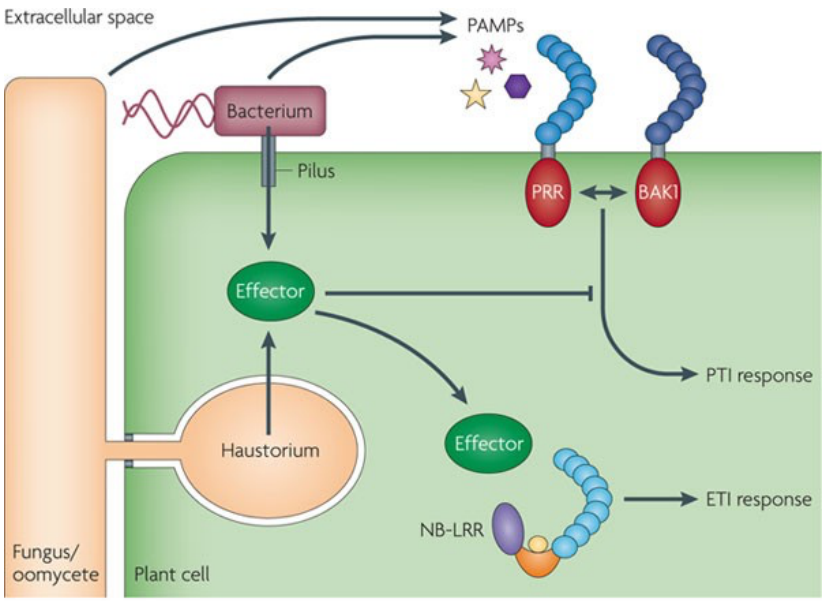

Figure 1: Immune response of plant against different pathogens. Bacterial, fungal, and oomycete invasion with hyphae into the plant cell. Haustoria that can directly penetrate to the plant cell wall. Different molecules released by pathogens inside the extracellular space, e.g., lipopolysaccharides, flagellin, chitin, etc. detected by cell surface PRRs and evoke PTI activation. BAK1 (BRASSINOSTEROID INSENSITIVE 1-ASSOCIATED KINASE-1) and other interactors of PRRs initiate the PTI signaling pathway. On the other hand, the NB-LRR receptors (Intracellular nucleotide binding) induce ETI (Dodds & Rathjen, 2010).

1.2 Protein biosynthesis and immunity

Protein biosynthesis or protein translation, refers to the cellular process where proteins are produced using the information contained within mRNA. In plant immunity, protein synthesis is vital to control a variety of proteins that act as key components in the defense system of the host. There are several functions involved regarding the biosynthesis of protein including the detection of pathogens, resistant protein expression to initiate defense response, initiation of signal transmission protein, defense gene expression, as well as post-transcriptional modification (Zheng et al. 2015). In summary, protein biosynthesis is necessary for plant immunity which can control numerous types of proteins intricate in detecting pathogens,

transmitting signals, initiating defense responses, and regulating gene expression. Based on those strategies of the plant immune system it's possible to develop innovative strategies for crop resistance against pathogens and boost agricultural productivity (Yang et al. 2022).

1.3 Conventional plant protection strategy

Ensuring the health of plants and sustaining yields through the protection of crops is essential, which aligns with the ecological balance. The selection of a plant protection approach depends on the specific crops cultivated and the nature of potential threats, whether they are diseases, insects, or weeds. It is crucial, that these measures are implemented on time and, whenever possible, in a preventive fashion. Contemporary crop protection methods heavily incorporate digital solutions, facilitating precise assessments of soil and plant conditions, as well as delivering accurate insights into external factors such as weather conditions. Simultaneously, these solutions enable the optimization of resource utilization. Consequently, farmers can save their crops, enhance profitability, and minimize adverse environmental impacts.

However, conventional plant protection strategies have been used since the beginning of the agricultural era. It refers to the traditional use of the available component to save the crop plant from various pathogens and also from animals. Recently, the invasion of different pests and pathogens has made those techniques a bit difficult to enrich the production of crop plants as aspected in quality and amount. Several commonly used strategies are implicated all over the world are mentioned below.

i. Chemical pesticides: Until now, chemical crop protection has been the most successful way to protect the plant. Herbicides, insecticides, and fungicides are increasingly used in the crop field to ensure a higher amount of production. However, the environment and human health are ignoring which needs to be considered for side effects of chemical uses (Srivastava et al. 2020).
ii. Biological control: Approaches to crop protection through biological control encompass a range of products originating from living organisms. Serving as a valuable complement to chemical methods, these biological solutions offer enhanced defense against pests, diseases, and weeds. While some biological plant protection products can be chemically synthesized, their formulation closely resembles that of natural products (Waage et al. 1988).
iii. Resistance breeding: Utilizing immune receptors for the development of disease-resistant cultivars proves to be a viable and sustainable method for managing crop

diseases. Nonetheless, the success of this approach heavily depends on the rapid identification and transfer of beneficial resistance genes ("R" gene) from the source to commercially cultivated crop varieties. In the past two decades, significant strides have been achieved in identifying R-genes, both from crop species and their wild counterparts, owing to advancements in DNA sequencing, molecular markers, and genotyping techniques (Huang et al. 2023).

iv. Cultural practices and crop rotation: Cultural control measures can successfully diminish the activity of pests, one of which is precision irrigation techniques. For instance, adjusting the irrigation supply can reduce weeds by limiting their access to adequate moisture while simultaneously raising root health. On the other hand, crop rotation can be a very practical way to enhance the production of many cereal crops. For instance, corn can be cultivated in the same spot for a consecutive period of five years. In contrast, rye, wheat, and sugar beet exhibit adverse reactions to consecutive planting but can achieve increased yields when subjected to appropriate rotation practices (Sainju et al. 2017).

v. Integrated pest management: Integrated pest management (IPM) holds significant potential in decreasing crop losses, leading to productivity, and mitigating environmental pollution and health risks. In recent times, IPM has been used particularly in developing crop varieties resistant to pests, implementing biological control strategies against invasive species, substituting traditional inorganic pesticides with biopesticides, exploring new export market avenues, and incorporating innovative tools in biotechnology. It's a new concept for increasing crop productivity, which still has limitations in the larger production of cereal crops (Nwilene et al. 2008).

1.4 Alternative solution to reduce pathogen-related diseases in plant production

There are lots of molecular mechanisms already well known for the protection of crop plants. Among them, pathogen recognition is very common and widely studied until now (Mogensen. 2009). Treatment of plants with beneficial microbes is a known biological concept, where plants engage in a beneficial symbiotic relationship with such kinds of fungi and bacteria. As a result, plants can benefit and enhance their resistance by getting nutrients from beneficial microbes (Finkel et al. 2017). On the other hand, signal transduction pathways exist in the plant cell which can be activated and recognize pathogenic molecules. In this process, signaling molecules such as salicylic acid, jasmonic acid, and ethylene play very important roles in the defense mechanism of plants (Kachroo & Kachroo. 2007). The production of secondary

metabolites and cell wall reinforcement is another way of defense mechanism of plants against pathogens. In the last two decades, RNA interference (RNAi) and small RNA molecules have been discussed to integrate into the crop protection process. Those small RNAs regulate the defense mechanisms in crop plants by targeting specific mRNA molecules of the pathogens to limit their invasion and infection process. Moreover, the production of small RNA or dsRNA inside the plant (HIGS) and artificially sprayed (SIGS) showed significant advancement in the plant protection perception (Koch et al. 2019). On the other hand, genome editing using CRISPR-Cas9 showed significant advancement in plant protection techniques where plant genes are directly modified by editing the desired genome of plants to enhance resistance against specific fungal pathogens (Borrelli et al. 2018). In a nutshell, the molecular basis of crop protection systems is vital for developing different strategies to enhance the resistance capability of plants. Consequently, it's possible to reduce the dependency on chemical use and possible to increase plant health and productivity. Ongoing research in the field of plant protection needs to uncover new molecular techniques for sustainable and effective plant protection.

1.4.1 RNA interference (RNAi)

At the end of last century, in 1998, it was reported that exogenously provided dsRNA can effectively downregulate target gene in the model organism *C. elegens*. After that, the potentiality of RNAi has been established and revolutionized in molecular biology. RNAi a conserved biological process exists in the eukaryotic system where dsRNA (double-stranded RNA) inhibits a specific gene of interest, or it may inhibit the translation process (Fire. 1999; Alder et al. 2003). On the other hand, RNAi is considered as a vital part of the immune-related response to viruses which can be observed in most of the eukaryotes (Cerutti & Casas-Mollano. 2006). RNAi begins with DICER, a RNAse III enzyme, that slices the dsRNA into small interfering RNAs (siRNAs) duplexes of 20-25 nt in length (Borges & Martienssen. 2015; Papp et al. 2003). The antisense strand is exactly complementary to the target mRNA sequence. A sense strand that is identically similar to the target mRNA could be degraded and doesn't show any function inside the RNAi mechanism. Afterward, the antisense strand will be loaded onto ARGONAUTE (AGO) proteins to generate an active RNA-induced silencing complex (RISC), it may include other proteins as well. Due to the sequence complementarity, the antisense strand and target mRNA bind together which causes the target mRNA degradation by the action of AGO proteins (Pratt & MacRae. 2009). In

addition, translational inhibition can be proceeded due to the non-degradation of mRNA (Borges & Martienssen. 2015; Majumdar et al. 2017; Pratt & MacRae. 2009). Furthermore, it was also reported, that RNAi can be triggered endogenously by viral dsRNA, pre-microRNA, or maybe by foreign DNA molecules (Nosaka et al. 2012; Plasterk. 2002). Moreover, RNAi is regarded as a precious tool in molecular biology due to the introduction of foreign dsRNA as a triggering tool. Likewise, RNAi was also used in functional genomics for loss-of-function phenotypes study in different organisms including plants and other eukaryotes (Lu et al. 2003; Nybakken et al. 2005; Hamakawa & Hirotsu. 2017; Pratt & MacRae. 2009).

1.4.2 CRISPR/Cas for genome editing in plants

The mechanism of CRISPR/Cas system begins with the bacteriophage attack on bacteria, inserting their genetic material into the bacterial genome and exploiting them as a source for generating new phages. After surviving a viral confrontation, it apprehends fragments of the external DNA, incorporating them into its own genome sequences. The preserved foreign DNA sequence, implicated in the defense system of prokaryotic organisms against viruses, is termed CRISPR (clustered regularly interspaced short palindromic repeats). In the event of a subsequent attack by a similar bacteriophage, the bacterium quickly produces an RNA copy from the CRISPR archive (crRNA) and loads it into a CRISPR-associated endonuclease protein (Cas). The RNA-loaded Cas then evaluates the bacterium's interior for complementary DNA or RNA sequences. Upon finding a proper counterpart, it activates and excises the target, rendering it ineffective and continuing to protect the bacterium (Horvath and Barrangou. 2010).

The CRISPR/Cas system rose to prominence as a genome editing technology when scientists realized that the crRNA sequence could be programmed to target any sequence in an organism (Doudna and Charpentier. 2014). The current categorization distinguishes CRISPR/Cas systems into two primary classes including interference mediated by multiple small proteins forming the effector complex, and another one is a single, large protein with multiple domains that generates the double-strand break (DSB). Each class is further subdivided into various subtypes, with distinct Cas proteins targeting single- and double-stranded DNA or RNA (Koonin et al. 2017).

CRISPR/Cas9 type II system from Streptococcus pyogenes (SpCas9) has become the most widely used CRISPR tool for genome editing. To achieve interference, only a

target-specific crRNA, a target-independent tracrRNA (transactivating crRNA), and a dual RNA-directed DNA endonuclease Cas enzyme (SpCas9) are necessary. It has been demonstrated that the dual tracrRNA:crRNA can also be constructed as a single guide RNA chimera (gRNA) to facilitate sequence-specific Cas9-dsDNA cleavage, streamlining the genome editing process (Jinek et al. 2012). A crucial prerequisite for Cas-directed DNA cleavage is the presence of a conserved 2 to 6 bp (base pair) protospacer-adjacent motif (PAM) downstream of the target sequence. In SpCas9, the PAM typically carries the sequence 5'-NGG-3', where "N" denotes any nucleobase and "G" represents guanine (Anders et al. 2014).

The development and application of the CRISPR/Cas9 method for genome editing have been effectively utilized in plant genomes nowadays (Demirer et al. 2021). The knockout mutants in higher crop plants were not widely available compared to dicotyledonous plants *Arabidopsis thaliana*. The efficiency of CRISPR/Cas9 enables the production of mutants in many monocotyledonous species, including wheat, rice, and barley (Chen et al., 2019; Lawrenson and Harwood, 2019).

1.5 Sustainable way of crop protection techniques over the recent approaches

The scientific consensus and legal requirements in most states emphasize minimizing the use of synthetic pesticides, including herbicides, in agricultural practices. While alternative crop protection methods are under development, their effectiveness in intensive production systems is rarely demonstrated, and their dependence on environmental factors remains poorly investigated.

Recent discoveries suggest that treatments involving RNAs hold promise for reducing diseases in plants, animals, and even humans. RNA, a fundamental component in genetic templates, has evolved into a central molecule for storing, transmitting, and modifying genetic information. It also plays a crucial role in communication between interacting organisms, a phenomenon known as cross-kingdom RNA interference.

Artificial RNAs, such as small RNA duplexes or dsRNAs, have shown potential to protect plants from biotic stress. Strategies such as HIGS involve producing RNA in transgenic plants, while SIGS applies exogenous RNA. Although HIGS is scientifically effective and environmentally superior, it faces political challenges in many European countries. SIGS applications, while adaptable to diverse biotic stresses, have concerns such as RNA degradation and genetic cross-resistance.

In the pursuit of innovative RNA-based solutions, circular RNA (circRNA) has been explored for plant protection. Unlike linear RNA molecules, circRNAs, formed through a process called back-splicing, have a closed-loop structure, making them more stable and resistant to degradation. While circRNAs have been extensively studied in animals, their functions in plants are still emerging. Artificial circRNAs are considered promising for agronomic applications due to their structural stability and potential roles as microRNA sponges and translation regulators. The details of circRNA from their sources, types, and biogenesis are discussed further in a broad aspect.

1.6 Discovery of circular RNA (circRNA) and their short histography

Continuous discovery of new types of RNA opens the era of new research in the field of RNA biology. Along with the messenger RNA (mRNA), several other types of noncoding RNAs including miRNA, dsRNA, siRNA, and lncRNAs function have been partially explored in recent times. The detailed function of many RNAs is still undefined both in plant and animal kingdoms. One of the newly arrived non-coding RNAs is circRNA. circRNA was first discovered in 1976 in RNA viruses through electron microscopy but it was unnoticed for a long time (Sanger et al. 1976). Last decade, circRNA received the focus of researchers as a novel possibility in medical science (Arnaiz et al. 2019). As a member of non-coding RNA, it was expected that circRNA could not be translated into protein. However, extensive research conducted in the last 10 years explored many hidden functions of circRNA, including their translation into protein (Legnini et al. 2017; Pamudurti et al. 2017).

In addition, eukaryotic cells have shown expression of various non-coding RNA species with their functional capacity in the last few decades (Arnaiz et al. 2019). For the advantages of next-generation sequencing, the identification of different RNA has grown considerably. Surprisingly, circRNA exists in the cell in abundant amounts and is covalently linked in their 3′ to 5′ ends (Barrett & Salzman. 2016). Intended to the formation of circRNA, back-splicing has a crucial role in the splicing mechanism (Jeck et al. 2013; Zhang et al. 2014; Starke et al. 2015).

circRNA normally forms by alternative splicing of pre-mRNA when an upstream splice acceptor links to a downstream splice donor (Barrett et al. 2015; Starke et al. 2015; Schindewolf et al. 1996). Several studies have unveiled their numerous characteristics, expression patterns on eukaryotes, and conservation in mammals (Wang et al. 2014). Although, circRNA is expressed in a regulated manner which is different than the cognate linear isoform. Additionally, many unknown facts exist in circRNA research which may be explored by doing

extensive investigation. Table 1 shows a short histography of circRNA that was recently investigated.

Table 1 Short histography of circRNA discovery

Year of discovery	Example of discovered function	Source	References
1976	First circRNA observed in viroids	Plant	Sanger et al. 1976
1979	circRNA first noticed in cytoplasm of eukaryotic HeLa cells	Eukaryotic cell	Hsu & Coca-Prados. 1979
1986	circRNA in human, Hepatitis delta virus	Human	Kos et al. 1986
1988	circRNA found stable after injecting into fertilized egg	African-clawed frog *Xenopus laevis*	Harland & Misher. 1988
1991	Endogenous circRNA in human	Human	Nigro et al. 1991
1995	Modifying circRNA can be translated in vitro. For circularization inverted repeats are required	Human, Mouse	Chen & Sarnow. 1995; Dubin et al. 1995
1998	In vivo circRNA can proceed translation	*Escherichia coli*	Perriman & Ares. 1998
2006	Use of RNase R in circRNAs	*Escherichia coli*	Suzuki et al. 2006
2010	circANRIL expression related to atherosclerotic vascular disease (ASVD)	Human	Burd et al. 2010
2012	RNA sequencing to detect circRNAs	Human	Salzman et al. 2012
2013	circRNA functional analysis	Human, mouse, and nematode	Memczak et al. 2013; Hansen et al. 2013
2014	Alternative circularization by reverse complementary sequence	Human introns	Zhang et al. 2014
2015	Relation between circRNA and cancer	Mammals	Bachmayr-Heyda et al. 2015; Li et al. 2015
2017	Translation of endogenous circRNAs, loss of function in circRNA phenotype (in vivo)	Eukaryotes, Fly, Human transcriptome	Legnini et al. 2017; Pamudurti et al. 2017; Yang et al. 2017; Piwecka et al. 2017
2020	Aging regulated by insulin-dependent circRNA	Mutant flies	Weigelt et al. 2020
2021	Artificial antisense circRNA can modulate splicing regulatory network	Mammalian cell	Schreiner et al. 2021
2021	Antisense circRNA reduces virus proliferation in cell culture	SARS-CoV-2 coronavirus	Pfafenrot et al. 2021
2021	Antisense circular RNA regulates expression of RuBisCO	*Arabidopsis thaliana*	Zhang et al. 2021

1.7 Types of circRNA in different cellular systems

Based on biogenesis, structural feature, and composition, circRNA fall into four different categories namely exonic circRNA, intronic circRNA, exon-intron circRNA, and tRNA intronic circular RNAs (tricRNAs), the latter being produced by tRNA introns (Lu et al. 2015; Yang et al. 2020). Most of the identified circRNAs (approximately 80%) are exonic circRNA and are found in the cytoplasm (Jens. 2014; Jeck et al. 2013). Nevertheless, intronic circRNAs and exon-intron circRNAs predominantly exist in the nucleus (Zhang et al. 2013) and regulate gene transcription (Li et al. 2015). Recently, another type of circular transcript was found, called read-through circRNA, and formed by exons from a flanking region of a gene through back-splicing (Vo et al. 2019). Figure 2 illustrates different types of circRNA in the cytoplasm and other cellular subsystems.

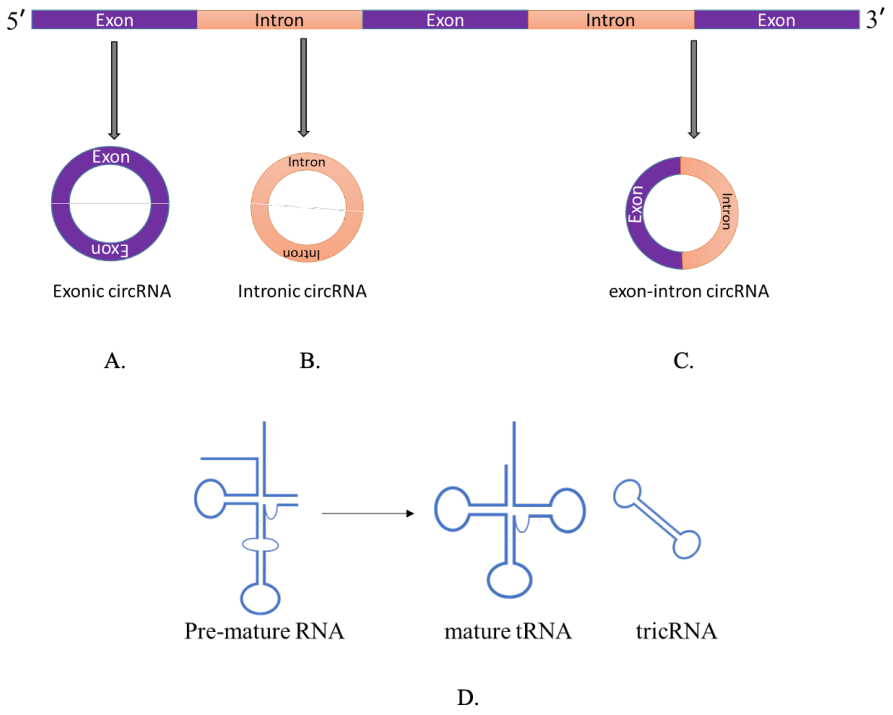

Figure 2: Illustration of different types of circRNA in cytoplasm and other cellular sub-systems. A. Exonic circRNAs, resulting in a back-splicing event in the RNA molecule, where the downstream exons and upstream exons are joined together. B. intronic circRNAs resulted in the same way by joining the intronic part, C. Exon-intron circRNAs resulting from the combination of exon and intron part of the RNAs, D. Pre-mature RNA which also creates another type of circular RNA named tricRNA.

1.8 Biogenesis of circRNA

According to the circRNA database, a few thousand of circRNAs have been identified and annotated (Glažar et al. 2014). From the previous studies, it has been found that circRNA biogenesis is slightly different from the long non-coding RNA (lncRNA) in the sense of covalently joined structure (Ashwal-Fluss et al. 2014; Quinn & Chang. 2016). CircRNA joined in the 3′ and 5′ end which gives them a complete circular structure without any open frame in the strand. Moreover, the generation of circRNA proceeds co-transcriptionally in the animal cells and their production rate depends on the intronic sequences (Ashwal-Fluss et al. 2014).

According to several studies, it has been found that circRNA derives from canonical splice sites. Due to the slowing down of pre-mRNA processing, newly appeared RNA pointed to alternative ways that facilitate back splicing (Legnini et al., 2017). In back splicing, intronic sequences connect to the downstream splice site (donor site) with the upstream splice site (acceptor site) and form a circular structure. Furthermore, the back spliced junction is an important feature of circRNA to detect and analyze their function in different developmental stages and their junctions are different from each other based on circRNA derivation. Three different models are proposed for circRNA loop formation. i. According to the intron pairing model, splicing is caused by reverse complementary sequences, for instance, ALU repeats, which are found in upstream and downstream introns. The loop is formed by splice donor and acceptor sites where they come into closed proximity. Mutation analysis found that only ~100 nt of each repeat is enough for the circularization (Bachmayr-Heyda et al. 2015; Kramer et al. 2015). Hence, the existence of intronic repeat is not always abundant to accelerate the back-splicing mechanism. ii. The exon skipping and intron lariat formation model, the 3′ ends of an exon attached to the 5′ ends of the same exon, also referred to as single-exon circRNA or connects to the upstream exon to form multiple-exon circRNA. iii. According to the RNA binding protein-mediated model, RNA binding proteins (RBPs) bind to each flanking introns to form a bridge that connects the splice donor and acceptor site closely to form a loop (Kramer et al. 2015). Quaking (QKI) binds to flanking introns and makes a dimer which brings the intervening splice sites into close proximity (Conn et al. 2015), whereas many intervening steps of circularization are still unexplored.

Furthermore, inhibition of the canonical spliceosome by isoginkgetin treatment results in the reduction of both linear and circular transcripts (Starke et al. 2015; Ashwal-Fluss et al. 2014). The reduction phenomena of a circular transcript can distinguish between forward and back splicing. However, the details mechanism are still unexplored (Salzman et al. 2013). Figure 3 shows the biogenesis process of circRNA in different conditions.

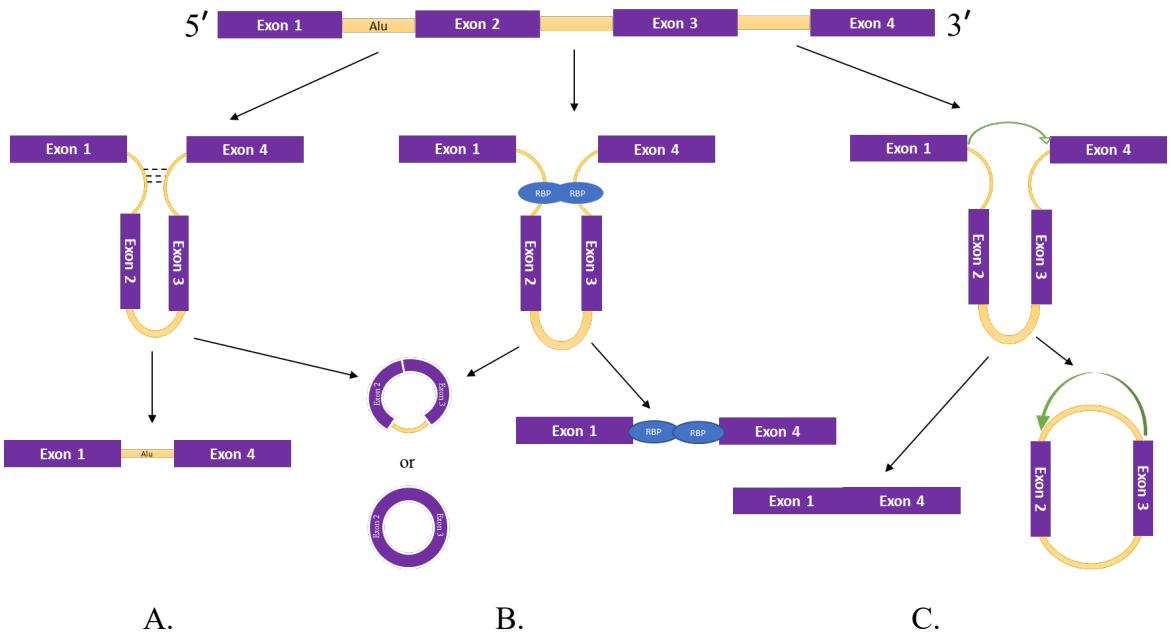

Figure 3: The biogenesis process of circRNA in three different ways. (A). Intron pairing-driven circularization occurs due to the pairing between downstream and upstream introns due to the driven of inverse-repeating sequences. In some instances, introns are completely removed or retained to form the circularity of RNAs, (B). RBP pairing driven circularization, RNA-binding proteins form the circRNA by connecting the downstream and upstream intronic region, and (C). Lariat-driven circularization occurs when pre-mRNA undergoes splicing, it creates a covalent link between the 3' end of the preceding exon and the 5' end of the following exon. This connection results in a lariat formation, which contains both exons and introns. The 2' hydroxyl group of the 5' intron then reacts with the 5' phosphate of the 3' intron which is followed by an interaction between the 3' hydroxyl group of the 3' exon and the 5' phosphate of the 5' exon, leading to the formation of circular RNA.

1.9 Biological significance and the roles of circRNA

circRNAs are present in most organisms including plants, animals, fungi, archaea, and metazoans (Zhang et al. 2013). Even RNA sequencing results revealed half of the total circRNA in mammals are tissue-specific (Yang et al. 2017). circRNAs are produced in the nucleus and subsequently transported into cytoplasm though the exact mechanism of this transfer is still unexplored. Recently it was reported that an ATP-dependent RNA helicase is

involved in the transport (Huang et al. 2018). Also, it may be transported through methyl-6-Adenosin (m6A) modification, but the mechanism is still not fully explored (Chen et al. 2019). As of today, some common functions have been found for circRNAs in different organisms including sponge formation, response against various stress, transcriptional regulation, protein binding, and miRNA binding (Hansen et al. 2013; Memczak et al. 2013).

i. miRNA - circRNA sponge formation

Earlier studies on animal cells represent the most intriguing function of circRNA, working as a miRNA sponge under certain conditions (Ebert et al. 2007). miRNA sponges are known as competing endogenous RNA in mammals and plants as target mimicry. Further studies on circRNA uncovered that it is involved in gene regulation through miRNA-regulated pathways. circRNA has several miRNA binding sites, and thus can also inhibit the activity of miRNA. Hence, circRNA can provide information about miRNA function while sponging (Ebert et al. 2007; Franco-Zorrilla et al. 2007). Additionally, higher stability over the linear RNA makes circRNA more vulnerable to forming miRNA sponges (Jeck et al. 2013). In the same way, miRNA activity can be affected by sponge formation, and the sponge is formed through binding with circRNA, for instance highly expressed circRNA in the mammalian brain acts as a ciRS-7 sponge. The circular transcript ciRS-7, also known as circRNA sponge for miR-7, contains 70 different target sites associated with AGO protein in miR-7 dependent manner. Also, another example in mammals showed that the sponge-forming effect is achieved by circRNA, which is regarded as a normal phenomenon. However, circRNA inhibits miRNA-mediated target destabilization and suppresses miR-7 activity which is followed by increased miR-7 targets. Compared to the animal model system, plant shows fewer miRNA binding sites in miRNA sponges (Hansen et al. 2013; Zuo et al. 2016). For instance, in Arabidopsis, 5% of circRNAs carry putative miRNA binding sites (Ye et al. 2015). Another report noted that 31 rice circRNAs contain more than one miRNA binding site out of 235 circRNAs which comprise miRNA binding sites (Ye et al. 2015; Lu et al. 2015). However, only one circRNA has been validated experimentally out of five detected in Arabidopsis flower (Capelari et al. 2019). Furthermore, it is not completely established whether circRNA is directly involved in different regulatory processes such as biotic, abiotic, metabolic, or developmental processes. Additionally, more experiments are required such as crosslinking immune precipitation sequencing (CLIP-seq) to prove their activity. CLIP-seq can identify circRNA that forms miRNA sponges, circRNA, and miRNA complexes. This technique has already

been successfully applied in the plant model system to identify circRNA accurately (Chi et al. 2009). Nonetheless, CLIP can also identify RNA binding proteins associated with circRNA functionality (Li et al. 2017; Chi et al. 2009).

ii. circRNA against different stress responses

Besides sponge formation, circRNA has been shown to respond to numerous stress conditions in different organisms especially in plants and few are also reported in animals (Litholdo & da Fonseca. 2018; Fischer & Leung. 2017; Hanan et al. 2020). Several reports elucidate various biotic and abiotic stress responses in such a different condition. However, most of the responses were found through data analysis of high throughput sequencing techniques. Even though experimental data also reported some of the stress-related information in mammals, as well as in plants (Zhang et al. 2019).

Pathogenic invasion produces circRNA expression in different tissues (Wang et al. 2017). As it has been reported, the expression of circRNA is cell, tissue, and developmental stage specific. The characteristic features suggest that circRNA is crucial for plant growth and development like the lncRNA (long non-coding RNA) or miRNA. Furthermore, the regulatory function and role of circRNA in plants need to be explored with various experiments besides bioinformatic data.

circRNA identified predominantly in the root and leaf as a result of different pathogenic invasions. For instance, the biotic stress responses in plant species kiwi (*Actinidia chinensis*), produced 584 circRNAs in response to invasion with *Pseudomonas syringae*. By network analysis from sequencing data, it has also been found that circRNA is responsible for plant defense (Wang et al. 2017). Additionally, circRNA does not work only as a positive regulator of the stress response, they are also responsible for different disease regulators found in tomato yellow leaf curl virus (TYLCV) in cultivated tomatoes (Yang, et al. 2018). On the other hand, circRNA which is expressed differentially, plays a crucial role in Verticillium wilt disease caused by *Verticillium dahliae* in cotton. After gene ontology analysis it has been assumed that circRNA has a regulatory effect on disease resistance process in cotton (Xiang et al. 2018).

Similarly, maize circRNAs have a role in plant cell regulation and they increase in response to Iranian mosaic virus (MIMV) (Ghorbani et al. 2018). On the other hand, circRNA was also found in several types of abiotic stress conditions, such as salt tolerance, light, nutrient deficiency, drought, chilling (Ye et al. 2015; Zuo et al. 2018; Zhu et al. 2019; Wang Lin, et al. 2018). Most of them has been found through the sequencing analysis of several root

sample. Moreover, the circRNA first identified in Arabidopsis under different light conditions. As well as phosphate deficiency produces circRNA response in the rice roots. However, the resulting condition was the upregulation and downregulation of the distinct circRNA (Ye et al. 2015). Also, the chilling effect reported on tomato fruit and grape leaves (Zuo et al. 2016; Gao et al. 2019). By using the circRNA in cold responding on grape, further applied to improve the cold tolerance in *Arabidopsis thaliana* through merging with stimulus-responsive gene. Many other examples are existing in wheat maize and Arabidopsis in response to dehydration (Zhang et al. 2019; Wang et al. 2017).

Furthermore, different stress conditions may change the circRNA length, circularized exon number, and alternative circularization in *Arabidopsis thaliana* (Pan et al. 2018). In the sense of stress responding circRNA, research on animals shows only a few examples compared to plants. Most of the stress-related circRNA were found in plants until now by sequencing result analysis.

iii. Gene expression regulation by circRNA

circRNA derives from a splicing process. In humans, it has been discovered, the combination of exon and intronic-derived circRNA increases the transcription process in the host gene through combination with U1 snRNP. Exon-intron circRNA was first found in plant species and has a role in gene regulation (Zhao et al. 2017). As well as circRNA has also shown a role in the modification of the splicing process to increase the efficiency of cognate exon skipped mRNA. In Arabidopsis, circRNA derived from exon 6 of the SEPALLATA3 (SEP3) gene can be able to bind to DNA locus and form RNA: DNA hybrid, also known as R-loop but linear RNA also can make the R loop which is weaker and pause the transcriptional process (Conn et al. 2017).

Previously it was thought that circRNA is untranslatable, but research shows a different strategy to translate circRNA. Different reports explored the translation process mediated by IRES and m6A RNA modification (Abe et al. 2015; Yang et al. 2017; Meyer et al. 2015). Tang et. al. showed that the circRNA with ORF and m5A modified start codon in junction sequence, has protein coding potentiality (Tang et al. 2020). Most fascinating, N6-methyladenosine RNA modification on circRNA confers immunity in humans (Chen et al. 2019). However, the direct translation of circRNA is still not known to the scientific source but in plant Arabidopsis m6A modification has been reported and still is in further progress to find out the exact function and proper biogenesis process (Zhou et al. 2017).

iv. circRNA serves as a biomarker

A biomarker is normally defined as an indicator of a biological process, which can indicate a certain development in a system. Successfully those are used in science to measure the severity of disease, amount, and progression of the process. There are several types of biomarkers used in the last few decades, for example, DNA, Protein, RNA, etc (Buyse et al. 2011). In recent decades, many non-coding RNAs have been used as biomarkers in medical science for disease diagnosis. circRNA has currently been discovered as a non-coding RNA, which could be used as a biomarker through certain modifications. They are circular and more stable than their linear counterpart which gives them a specialty for different biological approaches (Pfafenrot & Preußer, 2019). As of their characteristic feature, cell and tissue specificity and specific expression patterns make circRNA a potential biomarker. Several reports depicted, that circRNA participates in various pathophysiological processes in cancer disease, cardiovascular, neurological, and diabetes patients' cellular level which provides more practical information on circRNA to be used as a biomarker for the diagnosis and treatment of various diseases (Qin et al. 2016; Zhao et al. 2017; Grapp et al. 2013). Notably, it has also been found in fruit fly Drosophila where circRNA isoforms intensify in CNS aging. Later, circRNA in Drosophila was used as an aging biomarker in 2014 (Westholm et al. 2014). On the other hand, in crop science, to accelerate crop production biomarker is a valuable tool. In the last decades, it was successfully used in different breeding programs (Yang et al. 2011). In plant molecular biology, circRNAs are implied as biomarkers to detect the alternative splicing variant (Conn et al. 2017). Nevertheless, circRNA may be used as an excellent and highly effective biomarker for genetic crop development against heat or drought in harsh environments all over the world (Zhang et al. 2019).

v. circRNA and immune response

The immune system of an organism falls into two different category, namely innate and adaptive immunity. There are two major immune responses found which include immune surveillance and immune defence. Depending on the factor, the immune system can respond as antiviral or antibacterial. However, many factors are related to the immune system to accelerate the immunity of an organism (Russell et al. 2017; O'Sullivan et al. 2019). Innate immunity, which is known as a first-line defense, may include natural killer cells, macrophages, dendritic cells, etc in the animal cell. Depending on the innate immunity, antigen-specific adaptive immunity rises. However, it has been found that

circRNA directly or indirectly influences the immune system by creating a different immune response against many diseases. More specifically circRNA produces an immune response in animals against autoimmune disease, antiviral immunity, and different types of tumor immunity (Martin et al. 2020).

It has also been reported that in systemic autoimmune disease Rheumatoid arthritis (RA), circRNA forms a sponge with microRNA (miR181d) to suppress the development of the disease RA, however, it can also work as an inducer of the biogenesis of RA (Zheng et al. 2017). Further investigation proved that circRNA is directly involved in the immune response. In the mammalian cell, in-vitro-generated circRNA after transfecting induces innate immunity and confirms immune protection against viral infection (Chen et al. 2017). Likewise, another finding shows endogenous circRNA can form RNA duplex and work as an inhibitor of dsRNA-induced protein kinase (PKR) in innate immunity. Due to viral infection, PKR is activated as a result of degrading circRNA by RNase L. However, the overexpressed dsRNA tagging circRNA in T cell can improve the abnormality of the activation cascade of PKR, which provides the correlation between circRNAs and systemic lupus erythematosus (SLE) (Liu et al. 2019).

As of today, it has been published, that circRNA can bind to miRNA to form miRNA sponges in animals, but in plants, circRNA needs to be verified using more experiments. Bioinformatic analysis reveals a lot of circRNA-miRNA sponging, but eventually, through the experiment, it has found a very small amount of binding site for miRNA (Guo et al. 2014). It has also been reported after genome-wide analysis, only a small percentage of circRNA works as an active target mimic for miRNA in Arabidopsis (5%) and Rice (6.6%) (Ye et al. 2015). Hence, in-silico analysis and molecular analysis could be contradictory in the sense of right binding sites, for instance in rice circRNA, where RT-qPCR shows different results than the bioinformatic analysis compared to wild-type plants (Lu et al. 2015). Recently, it has been investigated that overexpression of miR477-3p (sponges of exonic circular RNA circRNA45 and circRNA47) in tomatoes results in disease gene expression due to infection by *Phytophthora infestans*. It has been suggested that two circRNA can regulate miRNA-mRNA expression levels and work as a positive inducer of tomato resistance (Hong et al. 2020). As a miRNA sponge, circRNA can accumulate huge amounts of miRNAs together, in extreme conditions miRNA can be separated from the complex, probably the process could probably regulate the immunity efficiently.

1.10 Translational gene silencing or inhibition of protein synthesis by circRNA

Besides miRNA sponging, circRNA has another crucial function in making circRNA-protein interactions. A common feature of circRNA is that can interact with RNA-binding proteins (RBP). RBPs have a great role in the cellular process which interacts with the RNA molecules to proceed with the transportation, translation, and maturation. Furthermore, they form ribonucleoprotein complexes (Conlon & Manley. 2017; Li et al. 2017; Yang et al. 2022). In humans, circANRIL binds to 60S ribosomal assembly factor PES1 and proceeds pre-rRNA and ribosome biogenesis in atherosclerosis. Consequently, circRNA binds to a RBP and alters RNA function to escape from the disease (Holdt et al. 2016). Another example of the protein binding capability of circRNA induces cell proliferation and accelerates autophagy by interacting among circDNMT1, p53, and AUF1. As a result, highly expressed circRNA (circDNMT1) could bind to oncogenic proteins and regulate their function (Du et al. 2018).

1.11 Commonly used methods for circRNA identification

There are several ways of circRNA identification method has been successfully implemented over the last few decades. The details procedure from in silico to the molecular levels are mentioned below:

1.11.1 Database for circRNA

Over periods, circRNA databases are getting enriched as an important research tool for scientists. Not only for animal science but also for plant science, which has been enhanced by the collection of huge amounts of circRNA data. Currently, available online databases are the primary source of research in the circular RNA world. That information provides advanced knowledge for the detection and characterization of new circRNAs in different species as well. The most used databases include CropcircDB, GreencircRNA, AtCircDB, etc. Different databases are established based on the different characteristics of identification, which provides enormous information to proceed the further research (Wang et al. 2019; Zhang et al. 2020; Ye et al. 2019).

1.11.2 Molecular and biological methods for identification of circRNA

There are several methods involved in molecular biology to identify the circRNA from a particular cell and tissue system. Among them, the enzymatic digestion method provides the easiest way to identify them. Due to the circular structure, circRNA shows higher stability and resistance to enzymatic digestion over linear RNA (You & Conrad 2016). The

overall process of identification includes different enzymes for instance RNase R, 5′ end exonuclease, nicotinic acid phosphatase, etc., which are able to destroy the linear RNA. Due to the lack of open ends enzymes keep the circRNA in a native form (Jeck & Sharpless. 2014; Suzuki et al. 2006). Northern blot analysis is another technique used for the identification of circRNA. Hence, it has been reported that the circRNA can run through the weak crosslinked gel slower than the longer linear RNA. Consequently, the difference between the various RNAs, and circRNA can easily be detected. Even the gel extraction process also helps to isolate the circRNA for further use (Tabak et al. 1988). Additionally, the localization of a circRNA can be detected at the cellular level through the in-situ hybridization method (Zhang et al. 2013; Li et al. 2017). To generate the molecular library of circRNA, the most effective procedure is to remove the linear RNA using RNase R treatment (Ebbesen et al. 2016).

1.11.3 circRNA detection by microarray analysis

circRNA microarray is regarded as a newly efficient tool for detecting specific circRNA by comparing normal and infected circRNA, for example, carcinogenic or normal cell-derived circRNA. The microarray technique used a kind of special probe, which can only bind to the reverse splice site of circRNA and make differences between the linear and circular forms of RNA (Lü et al. 2017). It is a very effectively used technique for profiling circRNA by targeting the reported back splice sites in a specific sample. Moreover, it has also been regarded as a more efficient technique than RNA sequencing (Li et al. 2018).

1.11.4 Sequencing technology for circRNA detection

Up to date, the RNA sequencing method is mostly used for circRNA detection in different organisms. Unfortunately, traditionally used RNA sequencing is not able to identify circRNAs from the linear RNAs. For that reason, it's necessary to use further developed sequencing technologies (You & Conrad. 2016). According to Jeck et al whole genome sequences have been analyzed through bioinformatics and their assessment has been done by using different sequence alignment algorithms, which are followed by the identification of cirRNA (Jeck et al. 2013). Another approach is the direct detection of circRNA from cDNA, where templates are designed with multiple sequence splice joints (Hoffmann et al. 2014). In the last few years, many algorithms have been used for the prediction of circRNA such as Acfs, CIRI2, and FUCHS (You & Conrad. 2016; Metge et al. 2017; Gao et al. 2018). Acfs is well known for its wide application for characterizing the circRNA from various

organisms. It can accurately identify circRNA and takes less time than other renowned techniques. It can also be able to find circRNA from a single as well as pair-ended RNA sequencing data (You & Conrad. 2016). FUCHS system detects the circular form of RNA within variable shear, it is based on long sequencing read and can provide much information to interpret accurately (Metge et al. 2017). CIRI2 is another tool for circRNA identification. The advantage of this tool is the filtering process which can remove false positives and mapping error results from the repetitive sequence (Gao et al. 2018). It provides reliable data depending on multiple seed matches (Ebbesen et al. 2016).

1.11.5 Important parameters for designing circRNA primer

To amplify the abundant circRNA and their presence in the subcellular system, primer designing is an important part which is followed by molecular biology. Because the contribution of circRNA is getting enlarged it is necessary to conduct the experiments accurately. Unlike other PCR primers, the circRNA primer design is a bit different and has special criteria. For the identification of exonic circRNA, primers are designed for the back splicing site. For circRNA primers initially target the cross-cleavable sites and are designed for intron regions. Furthermore, sequence position transfection and amplified product length must not be more than 100 base pairs (Panda & Gorospe. 2018). The amplification effect should be determined experimentally. Although, for qPCR, the length of amplification is determined by experiment. Yet, to amplify the abundant circRNA, a circRNA-specific primer is utilized which is known as a divergent primer. Divergent primer is only specific to circRNA, not to linear RNA (Jeck & Sharpless. 2014; Suzuki et al. 2006).

1.12 Aim of the study

This study aimed to investigate the potential of artificial exogenous circRNAs in targeting endogenous genes in plants and phytopathogenic fungi, as well as to understand the core mechanism / target (protein biosynthesis) of circRNA.

As a proof of concept, a GFP (Green Fluorescence Protein) antisense circRNA, and a vector carrying GFP sequences were cotransfected to protoplasts of the fungus *Botrytis cinerea* to evaluate the silencing effect of circRNAs regarding GFP protein accumulation.

On the other hand, as another proof of concept, artificially designed circRNA was applied in the *A. thaliana* plant protoplast (transiently) system, and in stable *GFP* expressing *Arabidopsis thaliana* leaves to understand the accumulation of reporter *GFP* in sequence and isoform-specific manner.

Additionally, using the mutants that are compromised in Dicer-like (DCL) and Argonaute (AGO) functions, we wanted to show whether the activity of circRNA depends on canonical RNAi or is independent of the RNAi pathways.

2. Material and Methods

2.1 Plant and fungal materials and growth conditions

Plants used in this study were grown under different conditions:

Arabidopsis thaliana, wild type, and their mutants *ago1-27* (Δ*Atago1*), *ago2-1 (*Δ*Atago2*), *ago4-1* (Δ*Atago4*), *dcl1-11* (Δ*Atdcl1*), *dcl2,3,4* (Δ*Atdcl2,3,4*) (Obtained from NASC, https://arabidopsis.info/) and *AtW33* (*At35S:GFP*, Provided by Dr. Steinbrenner) were grown in a climate chamber at 18°C/ 14°C (light/dark) with 60% relative humidity, with a photoperiod time of 16 h and a photon flux density of 240 µmol m^{-2} s^{-1}.

2.2 Fungi and different bacteria components

The strain of *Botrytis cinerea* (Bc, B05.10) was cultivated on Hansen's Agar (HA) medium, The following components were used for the medium listed in table 2.

Table 2: Chemical composition of Hansen's Agar (HA) medium (Doehlemann, Berndt, and Hahn. 2006).

Chemical components	Amounts
Malt extract	1%
Yeast extract	0.4%
Glucose	0.4%
Milli-Q H_2O and pH	Added until 1L and pH adjusted to 5.6
Agar (solid medium)	1.5%

For different cloning purposes, *Escherichia coli* (*E. coli*) was used and grew on LB medium (Tryptone 10 g/L, NaCl 10 g/L, Yeast extract 5 g/L, agar-agar 15 g, pH 7.0) and their incubation was at 37°C in the incubator. Moreover, the only bacterial strain used for the cloning of all plasmids was *Escherichia coli* DH5α.

A. thaliana mutant plants including the Argonaute and DCL play a crucial role in the RNAi process respectively guiding the RISC complex to target mRNA facilitating the degradation of mRNA sequence and cutting longer dsRNA into smaller versions of siRNA or miRNA to target the specific sequence of mRNA. Specifically, the Δ*Atago1* mutants lack a gene in no 27 (Δ*Atago1-27*) which is responsible for encoding an RNA slicer that recruits siRNAs and

miRNAs (Morel et al. 2002). ∆*Atago2* promotes the binding of sRNA molecules to the RISC complex (RNA-induced silencing complex). Additionally, *ΔAtago4* mutants are involved in the RNA-directed DNA methylation process (RdDM) to preserve DNA methylation which leads to a proper gene silencing process. On the other hand, the dicer-like gene Δ*Atdcl1* has the most important function in the RNAi process that encodes a Dicer homolog which is an RNA helicase involved in microRNA processing. Δ*Atdcl 2,3,4,* a triple mutant that contributes to the maintenance of gene regulation and genome stability in *A. thaliana* (Yao et al. 2016). Plant mutants that were used for the study are listed below in table 3.

Table 3: List of different mutants and sources

Plant	Mutant name	Stock no./Source	Disposition
Arabidopsis thaliana	∆*Atago1-27*	Morel et al. 2002	Protoplasting
Arabidopsis thaliana	∆*Atago2-1*	N503380	Protoplasting
Arabidopsis thaliana	∆*Atago4-1*	N16395	Protoplasting
Arabidopsis thaliana	∆*Atdcl1-11*	N3828	Protoplasting
Arabidopsis thaliana	∆*Atdcl2,3,4*	N16391	Protoplasting
Arabidopsis thaliana	*AtW33*	Harvey et al. 2022 (Collected from Jens Steinbrenner)	Topical RNA application

Table 4: List of plasmids used for this study. For the plasmid maps see figure 04.

Plasmid Name	Function
pGY1-35S-GFP	*GFP* expression
pBGgHg	*GFP* expression
LMBP 8054-ppK2	Cloning of *GFP*
pGY1-35S-gpdA::GFP-35S-Ter	*GFP* expression
pGY1-35S::GFP:RFP	*GFP* and *RFP* expression

The maps of different plasmids are as follows in figure 04.

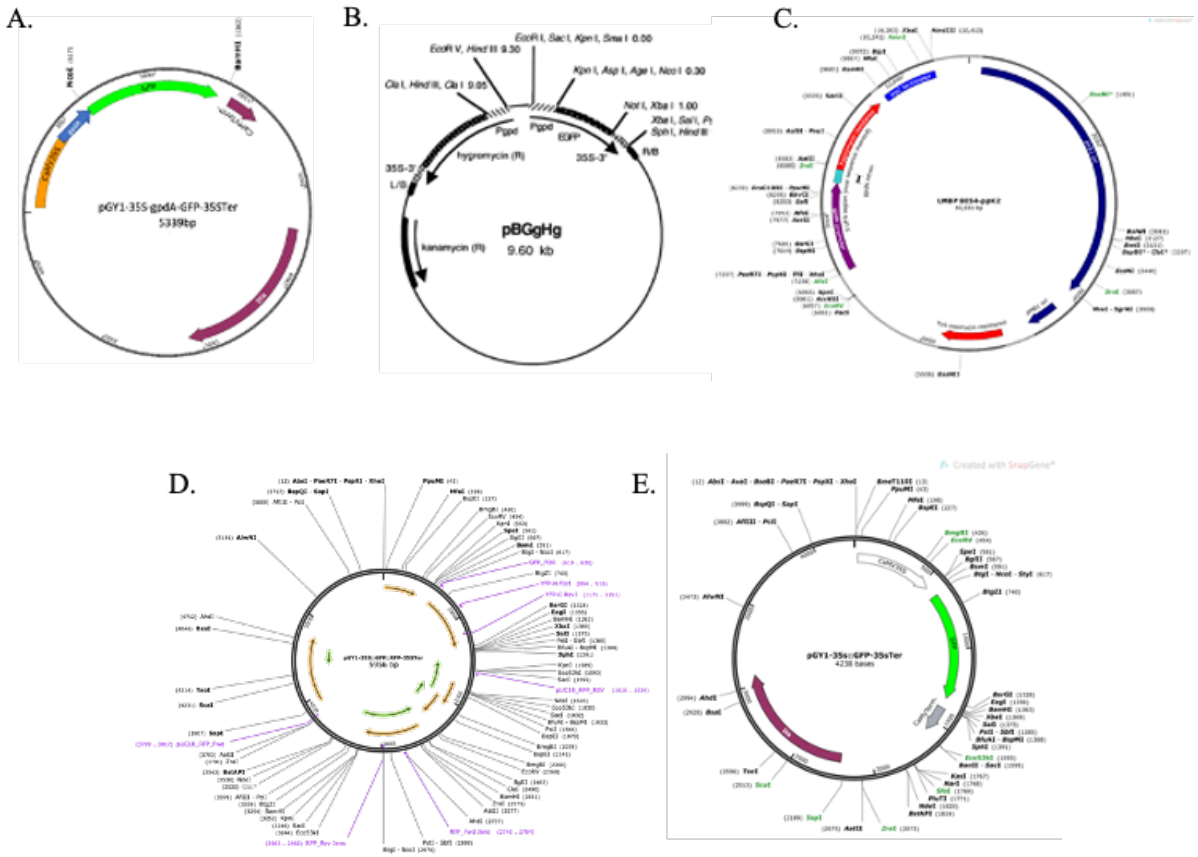

Figure 4: Organization of different plasmids. (A). Plasmid pGY1-35S-pgpd-GFP-35STer, containing *GFP* and express under 35S promoter of CaMV, size of the plasmid 5359 bp in total; (B). Arrangement of the binary vector pBGgHg or pBGgHg-pgpd::GFP involves a 9.6 kb construct containing the kanamycin resistance (*R*) gene. The hygromycin resistance and *eGFP* genes are located between the border sequences, each connected to the *A. bisporus* glyceraldehyde-3-phosphate dehydrogenase promoter (Pgpd) and the cauliflower mosaic virus terminator; (C). LMBP 8054-ppK2, the vector used for the cloning of different plasmids with desired promoter and termination, is used for the fungi *B. cinerea*; (D). pGY1-35S::GFP:RFP-35STer Plasmid containing *GFP* and *RFP* with the 35S promoter and terminator from CaMV, size 5,956 bp in total; (E). pGY1-35S::GFP-35STer Plasmid containing *GFP* with the 35S promoter and terminator from CaMV, size 4,238 bp in total.

The primers which are used throughout the study were synthesized by Eurofins Scientific Germany.

Table 5: List of Primers.

Primers Name	Sequences of used Primer	Application
*GFP*_F	5'-GACGTAAACGGCCACAAGTTC-3'	qPCR
*GFP*_R	5'-AAGTCGTGCTGCTTCATGTG-3'	qPCR
*Bc-β-tubulin*_F	5'-GTTACTTGACATGCTCTGCCATT-3'	qPCR
*Bc-β-tubulin*_R	5'-CACGGCTACAGAAAGTTAGTTTCTACAA-3'	qPCR
*At Actin*_F	5'-GGAAGGATCGTACGGTAAC-3'	qPCR
*At Actin*_R	5'-TGTGAACGATTCCTGGACCT-3'	qPCR
*At Ubiquitin*_F	5'-GCTTGGAGTCCTGCTTGGACG-3'	qPCR
*At Ubiquitin*_R	5'-CGCAGTTAAGAG GACTGTCCGGC-3'	qPCR
*Vi_CLP1*_F	5'-GAAGGCAATTCTCCCGACGTG-3'	dsRNA production
*Vi_CLP1*_R	5'-GATTCAGGCCAGAGAGTGCG-3'	dsRNA production
*Vi_CLP1T7*_F	5'-TAATACGACTCACTATAGGGAGAGAAGGCAATTCTCCCGACGTG-3'	dsRNA production
*Vi_CLP1T7*_R	5'-TAATACGACTCACTATAGGGAGAGATTCAGGCCAGAGAGTGCG-3'	dsRNA production
Antisense_circRNA _ORF_F	5'-TAATACGACTCACTATAGGGAGTAAGCTCGTGCTGCTTCATGTGGTCGGGGTAGCGGGCTTACAGTA-3'	circRNA production
Antisense_circRNA_ORF_R	5'-TACTGTAAGCCCGCTACCCCGACCACATGAAGCAGCACGAGCTTACTCCCTATAGTGAGTCGTATTA-3'	circRNA production
Antisense_circRNA _5'UTR_F	5'-TAATACGACTCACTATAGGGAGTAAGCCCAAGCTTACTTAGATCGCAGATCTACTAGTATGATGGCTTACAGTA-3'	circRNA production
Antisense_circRNA _5'UTR_R	5'-TACTGTAAGCCATCATACTAGTAGATCTGCGATCTAAGTAAGCTTGGGCTTACTCCCTATAGTGAGTCGTATTA-3'	circRNA production
$circRNA_{CTR1}$_F	5'-TAATACGACTCACTATAGGGAGTAAGCAGATGCGCACCGCACAGATGCGCACGCTTACAGTA-3'	circRNA production

circRNA$_{CTR1}$_R	5'-TACTGTAAGCGTGCGCATCTGTGCGGTGCGCATCTGCTTACTCCCTATAGTGAGTCGTATTA-3'	circRNA production
circRNA$_{CTR2}$_F	5'-TAATACGACTCACTATAGGGAGTAAGCAAAAGTCAGTGAGTCAGTGTAATACGGGAGGATACCCGCTGTCAAAGCTTACAGTA-3'	circRNA production
circRNA$_{CTR2}$_R	5'-TACTGTAAGCTTTGACAGCGGGTATCCTCCCGTATTACACTGACTCACTGACTTTTGCTTACTCCCTATAGTGAGTCGTATTA-3'	circRNA production
Oligo (dT) Primer	TTTTTTTTTTTTTTTT	cDNA synthesis
T7 Promoter	TAATACGACTCACTATA	In-vitro transcription

2.3 PCR (Polymerase chain reaction)

PCR was used for genotyping of different transgenic *Arabidopsis thaliana* protoplasts using DCS-Taq DNA Polymerase (DNA cloning service, Hamburg, Germany). 20 µL of PCR reaction approach and temperature protocol were followed throughout the process (table 6 and 7). Depending on the primer melting temperature and length of the template, annealing temperature and elongation times were adjusted.

Table 6: PCR reaction mix with DCS-Taq DNA Polymerase.

Chemical components	Amounts
BD buffer (10x)	2.5 µL
$MgCl_2$	2.5 µL
dNTPs (2mM)	2.5 µL
Forward Primer (10 pmol)	1 µL
Reverse Primer (10 pmol)	1 µL
DCS Taq DNA Polymerase	0.5 µL
DNA template	up to X µL
Milli-Q water	Until 20 µL

Table 7: Temperature protocol for DNA amplification process.

Temperature (°C)	Time	Cycle
95	5 min	
95 60 ± 2 72	30 sec 30 sec 1 min/kb	39x
72	5 min	
4	∞	

2.4 DNA sequencing

For sequencing, plasmid DNA and other DNA specimens, used for the study were sent to LGC Genomics according to the manufacturer's instructions. After receiving the DNA sequencing result, it was analyzed by Snap Gene viewer and other bioinformatic tools e.g. Clustal Omega (https://www.ebi.ac.uk/Tools/msa/clustalo/).

2.5 DNA extraction process

Organisms' biomass was collected and frozen immediately into the liquid nitrogen to keep their entire DNA undegradable. Tissues were broken down to fine powder form by using Tissue Lyzer II (Qiagen, Germany). Around 500 mg tissue materials (different samples may vary in amount) were mixed and incubated by adding 500 µL DNA extraction buffer for 10 min (Extraction buffer is a combination of (250 mM NaCl, 200 mM Tris-HCl pH 7.5, 0.5% SDS, and 25 mM EDTA). After adding 500 µL chloroform to the mixture solution, samples were centrifuged for 10 min at 12,500 rpm. Then the supernatant was transferred to a new 1.5 ml Eppendorf tube and 500 µL isopropanol was added and followed by incubation for 30 min at -20ºC and centrifuged for 10 min at 12,500 rpm. Finally, the pellet was washed with 1 mL 75% (v/v) ethanol and dried for 20 min under sterile conditions. Then DNA was dissolved into 50 µL millique water and the final concentration was measured using a NanoDrop Spectrophotometer (Peqlab Biotechnology GmbH, Germany) and stored at -20ºC for further use.

2.6 RNA extraction process

After preparing the cell/tissue extract by using a grinder or by using a pipette tip (for plant/fungi protoplast), total RNA was extracted according to the protocol of Direct-zol™ RNA Microprep kit (Zymo Research Europe GmbH, Germany) following the manufacturer's instructions. First, an equal volume of ethanol (95-100%) was added to the sample lysed in TRI Reagent and mixed properly. Then the mixture was transferred to the Zymo-Spin™ IC Column and centrifuged to discard the flow-through.

Then the remaining was washed with 400 µL RNA Wash Buffer. Afterward, DNase I treatment was continued by adding 5 µL DNase I and 35 µL DNA Digestion Buffer. Then the mixture was incubated for 15 min at room temperature. 15 minutes later, the column was washed with 400 µL Direct-zol™ RNA PreWash two times. Finally, 700 µL RNA Wash Buffer was added and centrifuged for 1 min. All the centrifugation speed was maintained at 12.500 rpm for 30 sec and in the final step, it was increased to 1 min. Moreover, in the last step of extraction, 10 µL of DNase/RNase-Free water was added into the column matrix directly and centrifuged in a new tube for collection. After measuring the RNA concentration using a NanoDrop Spectrophotometer (Peqlab Biotechnology GmbH, Germany), RNA was stored at -80ºC immediately.

2.7 DNase-I digestion and cDNA synthesis from total RNA

DNase-I digestion was performed to eliminate DNA contaminant, completely from the RNA sample. 2 µg RNA was mixed with 1 µL DNase-I (Fermentas, Germany) and 0.25 µL RNase inhibitor (Fermentas, Germany). Then incubated at 37°C for 30 min and the reaction was stopped by adding 2 µL EDTA at 70°C for 10 min.

cDNA synthesis was performed in two different methods, one of them was followed by a qScriptTM cDNA Synthesis kit (Quanta Biosciences, Gaithersburg, USA). By following this kit 4 µL of 5X qScript reaction mix, 1 µL of qScript reverse transcriptase, and 1 µg of RNA were mixed and incubated, by adding up to 20 µL of ddH_2O. Subsequently, the reverse transcription program was performed with the following setup including 22°C for 5 min, 42°C for 30 min, 85°C for 5 min, and finally, held at 4°C for unlimited time.

2.8 Single-stranded cDNA synthesis using oligo-dT

There was an optimized protocol established to generate single-stranded cDNA to use in the RT-qPCR. The following components according to table 8, were prepared in a sterile condition and left on ice.

Table 8: cDNA synthesis with oligo-dT.

Template RNA	Total RNA	0.1µg - 5µg
Primer	Oligo dT	100 pmol
DEPC-treated deionized water (**dH_2O**)		Until 12.5 µL

For the GC-rich template or in the presence of any secondary structures, mixed gently, centrifuged, and incubated at 65°C for 5 min. Then cool it down and again centrifuged. Afterward, add the following components according to table 9, and mix gently, and centrifuge.

Table 9: Chemical components for cDNA synthesis according to the kit.

Chemical components	Amounts to be added
Reaction buffer (5x)	4 µL
RNase inhibitor	0.5 µL
dNTP mix	2 µL
Revert aid reverse transcriptase	1 µL
Total volume	20 µL

After the mixing, there are two different temperatures were followed depending on the primer. For oligo-dT primer, 60 min at 42°C and for random hexamer primer 19 min at 25 °C, followed by 60 min at 42°C was incubated. For GC rich RNA, transcription temperature could be increased up to 45°C. At the end, the whole reaction was terminated at 70°C for 10 min. Finally, cDNA was used immediately for further analysis through PCR and qRT-PCR.

2.9 Quantitative real-time PCR (qRT-PCR)

qRT-PCR was performed to determine the target gene expression in the QuantStudio 5 Real-Time PCR system (Applied Biosystems) by using SYBR® green JumpStart Taq Ready Mix (Sigma-Aldrich, Germany) in 384 well plates. For each sample, three replicates were conducted, and target transcript levels were analyzed using the $2^{-\Delta\Delta Ct}$ method (Livak & Schmittgen, 2001). In this experiment target transcript was normalized to the reference transcript. Reaction assembly includes SYBR® Mix 5 µL, forward primer 0.25 µL, reverse

primer 0.25 µL, cDNA 10 ng in 1.5 µL, ddH_2O up to 3 µL and preset temperature protocol for qRT-PCR was applied for the whole reaction process.

2.10 Protein isolation from protoplasts and leaf

Isolation of protein from different sources including leaf, protoplast, etc., was performed by 4x Laemlli buffer (4mL 1M Tris-HCl pH 6.8, 50% glycerol, 4% SDS, 0.02% bromophenol blue, 200 µL 1M DTT). 200 µL protoplast (100 mg plant leaf extract) was used for the protein extraction process, where 50 µL 4x Laemlli buffer was added and mixed with pipette tip properly. Afterward, centrifuged for a few seconds and let them heat for 5 min at 95°C in the closed incubator. After finishing the heating process, protein tubes were centrifuged at 12.500 rpm for 2 min and the supernatant was stored at -20°C or immediately ready for the SDS-PAGE and Western Blot analysis.

2.11 SDS-PAGE (Sodium dodecyl sulfate-polyacrylamide gel electrophoresis)

For protein separation from a complex mixture of protein, discontinuous polyacrylamide gels were used carrying a 3% stacking gel and a 12% resolving gel. The components for the two gels are shown in the following table 10.

Table 10: Chemical components for two different SDS gels.

Components	Resolving gel / Lower gel	Stacking gel / Upper gel
30% acrylamide	4mL	1mL
1 M Tris-HCl pH 6.8	-	600 µL
1.5 M Tris-HCl pH 8.8	2.5 mL	-
dH_2O	3.4 mL	3.6 mL
10% SDS	100 µL	50 µL
10% APS	100 µL	50 µL
TEMED	10 µL	10 µL

After the extraction of protein, total protein was loaded into the well of the SDS gel. For the same amount of protein loading Bradford Ultra assay was performed. The separation of gel was conducted at 80V for 2 to 2.5 h until the gel ran below the end of the chamber, but the gel should not exit the gel cast.

2.12 Bradford Ultra assay for protein quantification

The Bradford protein assay, regarded as Bradford assay is an extensively used colorimetric method to determine the concentration of protein content in a complex mixture of protein. The updated version of the Bradford assay known as a Bradford Ultra assay, is a fast and ready-to-use method based on coomassie binding, a colorimetric technique for total protein quantitation in solution. It's more sensitive than the traditional Bradford assay which can measure up to 0.1% low protein range. Additionally, Bradford Ultra indicates excellent linearity for a detailed spectrum of protein concentration and exhibits less protein-protein alteration than the other coomassie-type assay. Moreover, in the acidic medium coomassie dye binds to the protein of interest and indicates a shift of absorption from 465 nm to 595 nm with a visible color change from brown to blue. The whole process is used to find out the concentration of unknown protein samples using some calculations based on the spectrophotometer data. For the calculation of a protein sample concentration following steps would be followed.

Firstly, the protein sample which is in the Laemmli buffer with less than 1% SDS, needs to be compared with a known protein concentration and usually for that reason BSA was used widely. In the beginning, a stock solution of BSA was prepared using dH_2O with a concentration of 100 mg/ml in a 1.5 ml Eppendorf tube. Then the following BSA standard series was prepared from the stock solution with 1x SDS buffer which is in a combination as following table 11.

Table 11: Combination of different concentrations of BSA standard.

	Concentration of BSA (mg/ml)	**Volume of stock solution (µL)**	**Volume of 1xSDS (µL)**	**Final Volume (µL)**
BSA Standard 1	10	50	450	500
BSA Standard 2	5	25	475	500
BSA Standard 3	2.5	12.5	487.5	500
BSA Standard 4	1.25	6.25	493.75	500
BSA Standard 5	0	0	500	500

After preparing the standards, they were diluted 10 times using dH_2O to minimize the detergent concentrations, otherwise, all the standards will provide the same data reads at OD-595. If the

protein is slightly higher in range, then it would be covered by dilution. The following table 12 shows the dilution of standard BSA protein for further calculation.

Table 12: Different BSA standard dilution (1:10).

Dilution (1:10)	Concentration of BSA (mg/ml)	Volume of standard to take (µL)	Volume of dH_2O (µL)	Final Volume (µL)
BSA Standard 1	1	50	450	500
BSA Standard 2	0.5	50	450	500
BSA Standard 3	0.25	50	450	500
BSA Standard 4	0.125	50	450	500
BSA Standard 5	0	50	450	500

Afterward, 1:10 dilution of each sample was prepared in a final volume of 200 µL by combining 180 µL of dH_2O and 20 µL of each sample of interest. Then the Bradford Ultra reagent was mixed gently (no shaking) by inverting the chemicals and the desire amount was taken and rest of them stayed at 4ºC which is very important to maintain the quality of Bradford assay. Then, Bradford Ultra reagent was directly put into the sample in a ratio of 1:15 where the sample must be 50 µL and 750 µL of Bradford Ultra reagent. The final volume of 800 µL was maintained for each of the samples in the cuvette. Immediately after mixing in a cuvette, the solution was directly measured at OD-595 at room temperature. At least three times the read was taken for each sample and the average was considered as a desired protein concentration. Each sample read was normalized against the blank by subtracting the blank (BSA standard 5) data from each of the reads found in the spectrophotometer. After collecting all the data in an Excel file, was calculated to generate a standard curve by applying the equation Y=bX (Y = absorption, X = Concentration, b = constant). After calculating the data, it was multiplied by 10 to get the proper concentration of the sample. Finally, the loading concentration in a certain µg was measured using the formula; V = µg/Concentration. Moreover, if it's necessary the standard curve can be slightly changed to keep the data accurate.

Immuno-blotting

After separating by SDS-PAGE, immunodetection was continued. For immunodetection, proteins were transferred by applying an electric tension from the SDS gel to a polyvinylidene

difluoride (PVDF) membrane (CarlRoth, Germany), which is a naturally hydrophobic, unsupported transfer membrane. it has been used for its high binding capacity; low background noise and it inhibits protein from fleeting through the membrane. The blot was prepared in a sandwich process where it was arranged from bottom to top by 6x Whatman paper, PVDF membrane, SDS-Gel, and again 6x Whatman paper (GE Healthcare, USA). Firstly, the Whatman paper was dipped into the Towbin buffer (25 mM Tris, 192 mM Glycine, 20% Methanol for 1 liter). Additionally, the PVDF membrane was dipped into the methanol to activate the membrane and then dipped into the Towbin buffer before transferring. Then, the protein was transferred using BioRad TransBlot Turbo with an electric tension of 25V (Volt) and 1.0A (Ampere) for 30 min. before continuing with the immunodetection, the membrane was blocked for 1h at room temperature using 5% (w/v) milk powder (CarlRoth, Germany) and 1xTBS Tween buffer. After blocking the PVDF membrane, it was cut into two pieces according to the position of the protein to incubate in different antibody solutions. For the detection of GFP protein, the membrane was incubated with primary GFP antibody (Living colors Monoclonal antibody JL-8: 1:5000, Takara Bio Inc) diluted in 5% Milk powder mixed in 1x TBS-Tween. On the other hand, half of the upper membrane was incubated with a primary Actin antibody (Agrisera, Sweden) mixed with 5% Milk powder and 1xTBS-Tween. Then both membranes were incubated at 4°C in a shaker overnight. After overnight shaking, membranes were washed 4 times with 1x TBS-Tween buffer. Afterward, two different membranes were incubated separately with secondary antibodies (Anti-Mouse IgG-peroxidase conjugate 1:5000~10000, Sigma and Goat anti-rabbit IgG HRP 1:25000) for 1.5 h to 2 h at room temperature. After incubation, membranes were washed again separately with 1x TBS-Tween buffer for 4 times each 7 to 10 minutes. Finally, chemiluminescent substrates (Solution A and Solution B) were applied onto the membrane according to the manufacturer's recommendation. Bio-rad ChemiDoc MP imaging system was used to take several images at different time points until 1 to 20 min for both membranes.

2.13 Microscopic analysis

There were various sorts of microscopes used in this whole study for analyzing different purposes and evaluating samples from tissues, cells, and protoplasts.

Stereo microscope:

Transgenic Nicotiana, Barley, and Arabidopsis leaves were examined by stereo microscope (MZ16F, Leica, Germany) in different conditions. Arabidopsis protoplasts were examined

using different filters and different laser excitation between λ_{em} 480 nm to λ_{em} 510 nm and λ_{em} 470 nm to λ_{em} 525 nm.

Inverted microscope:

In the inverted microscope (Leica DM IL, Germany), the light source and condenser are located on the top, and the stage is located at the down position, where the turret and objectives are at below. This type of microscope is very important to examine the living objects. In this study, fungal protoplasts were extensively studied for their proper observation under different conditions.

Confocal laser scanning microscopy (CLSM):

CLSM, also known as a confocal laser-scanning microscope (TCS SP8, Leica, Germany) was used to investigate the GFP expression in different parts of the fungal mycelium. Fungal pictures were taken by confocal microscope under the λ_{em} 488 nm laser excitation.

2.14 Protoplast isolation and transfection

For transient gene expression and functional genomics studies, protoplast isolation and transfection are extensively used techniques. In plant cells, cell walls were removed enzymatically to make them flexible for the uptake of foreign plasmids or DNA. A combination of a huge amount of chemicals is necessary to get the highest amount of healthy protoplast.

The following listed stock solutions in table 13 are prior requirements to proceed through the culture and isolation of protoplast.

Table 13: Stock solution for protoplast isolation and transfection.

Stock solution	Quantity (L)	Process of sterilization
1M $CaCl_2$	1	Autoclave
1M NaCl	1	Autoclave
1M KCl	1	Autoclave
1M $MgCl_2$	1	Autoclave
0.8M D-Mannitol	1	Autoclave
0.5M MES pH 5.7 (adjusted by KOH)	1	Filter sterilization
10% BSA	0.1	Filter sterilization
Milli-Q H_2O	1	Autoclave

After preparing the stock solution, it is necessary to prepare the individual solution as follows at table 14.

Table 14: Different buffers for protoplast preparation.

Enzyme solution	W1 Buffer	W5 Buffer	MMg Buffer
0.4M D-Mannitol	0.5 M D-Mannitol	154 mM NaCl	0.4 M Mannitol
20mM KCl	20 mM KCl	125 mM $CaCl_2$	15 mM $MgCl_2$
20mM MES, pH 5.7	4 mM MES, pH 5.7	5 mM KCl	4 mM MES, pH 5.7
ddH_2O until 50 mL	ddH_2O until 50 mL	2 mM MES, pH 5.7	ddH_2O until 50 mL
		ddH_2O until 50 mL	

After preparing all the above solutions, it is necessary to prepare the enzyme solution for protoplasting on the day of transfection. Otherwise, if the solution is prepared outside a clean bench, it can be contaminated easily by environmental bacteria, fungi spores, or molds. To prepare the enzyme solution, 1% Cellulose R10 and 0.25% Macerozyme R10 were added to the previously prepared enzyme solution. Then the solution was heated for 10 min at 55°C. After that 10mM $CaCl_2$ and 0.2% BSA were added to the solution. After mixing for a while, the total solution was sterilized by using a 45 µm filter. After filtration, the enzyme solution was used immediately otherwise enzyme solution would lose its activity over time.
For transfection purposes, PEG (Polyethylene glycol) solution was used. Always fresh PEG is recommended for the transfection. Over time PEGs also lose their transfection activity. To prepare 10ml PEG solution 4g PEG 4000 (Sigma Aldrich, Germany), 0.8 M 2.5 mL D-Mannitol, and 1M 1mL of $CaCl_2$ were mixed and kept into the 4°C for transfection purposes.

2.15 Protoplast isolation from *Arabidopsis thaliana*

For the isolation of protoplasts, 4 to 5-week-old wild-type *Arabidopsis thaliana* (Col-0) plants were selected. After preparing the enzyme solution, 10 to 12 leaves of epidermis were carefully pealed using the Tape sandwich method and immediately left in the 10 mL enzyme solution. The pealed surface was placed facing down to the solution. The whole petri dish was closed with a lid and aluminum foil to keep them in the dark for 60 min at a shaker speed of 50-60 rpm. An hour later, 10 mL cold W5 buffer solution was added to the protoplast very carefully and swirled around gently on one side. Then a 180 µM nylon mesh was attached to the 50 mL

falcon tube and 5 mL W5 solution was added to make the mesh wet. Wet mesh helps protoplasts to slide into the tube without any damage. Then all the protoplasts were added to the falcon tube gently through the filter. At the end of filtration, 5 mL of W5 buffer solution was added to take all the protoplasts from the petri dish and refilter. After collecting all the protoplasts were put on ice and then centrifuged at 4℃ for 3 min at a speed of 100x g. After centrifugation, the supernatant was removed and 10 mL of cold W5 solution was added. During the 30 min incubation time, the protoplast yield was counted by a hemocytometer. Counting of the protoplast was done by the Fuchs-Rosenthal Counter. After counting protoplasts were centrifuged again at 4℃ for 3 min at the same speed. After counting with the following formula, a certain amount of RT MMg buffer was added for further use.

Count = Average x 5000 x 10 mL W5, and Final Volume = (Count x 0,1)/5000.

2.16 PEG-mediated protoplast transfection

In this experiment, we used PEG-mediated transfection which is a very simple and efficient strategy to deliver the exogenous DNA or plasmid into the cellular system, allowing high yields of transfected cells with high survival rates. For the co-transfection process, a 2mL tube was taken where 20 µg plasmid (pGY1-35S::GFP, Schweizer et. al 1999) and circRNAs were taken and mixed together up to 20 µL. Then 200 µL of protoplasts (50,000 protoplasts/100 µL) were mixed into the 2 mL tubes. Afterward, the same amounts of (220 µL) previously prepared cold PEG solution were added and mixed properly. Incubated the mix for 15 minutes. 15 min later 1 mL W5 solution was added to the Eppendorf tubes to stop the transfection. After that, the protoplasts mixture was centrifuged at 150x g for 2 min under room temperature. Then the supernatant was removed and washed two times with 500 µL with W5 buffer. Finally, 6 well plates were coated with 5% BSA for 1 min, then the BSA was completely removed, and 1.5 mL W1 buffer solution was added. Protoplasts were resuspended in the W1 buffer and left inside the dark until 18 h.

After 18 h later protoplasts were harvested using W5 solution at room temperature. 6 well plate was filled with 2 mL W5 buffer and waited until 2 min to mix them properly. After that protoplasts were collected with gentle pipetting for several times and centrifuged at 450x g at RT. After collection, all the protoplasts proceeded to mRNA isolation and protein extraction for further experimental process.

2.17 Plasmid DNA preparation

E coli, cells carrying the desired plasmid, were harvested between 16 h to 18 h later after culture and centrifuged down at 4000 rpm for 10 minutes at 4°C. Then the supernatant was completely removed from the falcon tubes. Afterward, 8 mL resuspension buffer (PureYield™ Plasmid Midiprep System, Promega, Germany) was added to the pellet separately and vortexed at a high speed to mix them properly. After that same amount of cell lysis buffer was added to the suspension and gently inverted a few times by hand. Then it remained incubated at room temperature for 5 min. The filters including the column were soaked with 12 mL equilibration buffer. Then neutralization buffer was applied to the previously prepared bacterial lysis, mixed properly until the blue color completely turned into white, and loaded into the column slowly. In the first washing step 5mL equilibrium buffer was added to the edges of the filter and the filter was removed completely whenever all the fluid passed through the column. Then 8 mL of wash buffer was added to the column in the second wash. Finally, 5 mL elution buffer was added to elute the plasmid DNA from the column. Then, 3.5 mL of isopropanol was added to enhance the precipitation of plasmid DNA and mixed properly. The collection tube was centrifuged at 4°C for 30 minutes at 15.000x g. After centrifugation, the supernatant was removed carefully to keep the pellet. The plasmid DNA pellet was washed with 1 mL of 70% ethanol and centrifuged at room temperature for 5 min at a speed of 12,000x g. After removing the supernatant carefully, plasmid DNA was air dried at room temperature for 10 min. It's always recommended not to keep them for a longer time, otherwise, it would be very hard to dissolve. Finally, 50 µL ddH_2O was added to the plasmid DNA, and the concentration measured was measured by using NanoDrop (Peqlab Biotechnology GmbH, Germany).

2.18 Preparation of enzyme solution for *Botrytis cinerea* and isolation of protoplasts

Different types of lysing enzymes were used throughout the experiment including enzymes from *Trichoderma harzianum* (Sigma, Germany), Macerozyme, Driselase, and Pectolyse. The enzyme solution also contains Gamborg B5 medium including vitamins. For the preparation of 20 mL enzyme solution $CaCl_2$, MES, Mannitol, and ddH_2O were added according to table 15. The enzyme solution was filtered through a 22 µm filter and collected for protoplast preparation.

Mycelium of *B. cinerea* was collected and dissolved in the enzyme solution. Afterward, mycelium was shaken for 2.5 h to 3.5 h at 25°C. Following 3 h, mycelium was observed under the inverted microscope (Leica DMC 2900, Germany) for the yield of protoplasts. After getting the proper production of protoplasts into the Petri dishes, it was collected by using a 25 µm

filter in a new tube very carefully. Then the collected protoplasts were centrifuged at 4°C for 7 min at 150x g. Protoplasts waere washed two to three times using a B5 washing solution (Gamborg B5 medium, D-Mannitol, and adjusted pH 5.8) to remove the enzyme completely. Finally, the supernatant was discarded, and the protoplast was collected in a new buffer for further use.

Table 15: Components used for enzyme solution to extract protoplasts from *B. cinerea* are listed below.

Chemical components	Amount
Lysing Enzyme from *Trichoderma harzianum*	2.5 %
Macerozyme	0.5 %
Pectolyase	0.5 %
Driselase	1 %
D-Mannitol	0.45 M
Gamborg B5 Salt	0.0634 g/ 20mL
$CaCl_2$	10mM
MES	3mM

2.19 dsRNA synthesis

siRNA-Finder commonly known as Si-Fi (Lück et al. 2019), is an open source software for designing RNAi-target and the off-target predictor. In this study, it was used to select the target sequence for RNAi design. Here, the Nicotiana gene *MgChl1* is used as a template for the synthesis of desired dsRNA. DsRNA was prepared using the MEGAscript T7 Transcription Kit (Thermo Fisher Scientific, Germany) according to the manufacturer's protocol by following several steps. First, thaw all the reagents to assemble the transcription reaction. Combine all the reagents according to the following table 16 at room temperature.

Table 16: Chemicals to assemble the transcription reaction.

Chemical components	Amount	Chemical components	Amount (µL)
Template DNA	1-2 µg	T7 Reaction Buffer (10X)	2
ATP Solution	2 µL	CTP Solution	2
GTP Solution	2 µL	UTP Solution	2
T7 Enzyme Mix	2 µL	Nuclease free H_2O	Fill until 20

After incubation whole mixture of chemicals was incubated at 37°C for 2 to 4 h. Incubation time varies depending on the template size and transcriptional efficiency. Assembled RNase digestion according to the following table 17 on ice and incubate for 1 h at 37°C.

Table 17: Chemical components for RNase digestion.

Chemical components	Amount (µL)
dsRNA	20
Nuclease free H_2O	21
Digestion buffer (10x)	5
DNase 1	2
RNase	2

Purification of dsRNA started with the assembling of dsRNA binding mix including 50 µL dsRNA, 50 µL binding buffer (10x), 150 µL nuclease-free H_2O, 250 µL ethanol (100%). The whole mixture of dsRNA (500 µL) was pipette through the filter cartridge and centrifuged to remove the flow-through. Then the filter cartridge was washed with 2x 500 µL wash buffer and manifold for up to 30 sec. Afterward, a maximum of 100 µL elution buffer was applied to the cartridge and incubated in a heat chamber for 2 min at 65°C. finally centrifuged for 2min at higher speed. Then the dsRNA concentration was measured by Nanodrop (Peqlab Biotechnology GmbH, Germany) and stored at -80°C for further use.

2.20 Statistical analysis

For statistical analysis, different statistical tests like Student's t-test, one-way ANOVA, and Kruskal Wallis (for non-normally distributed data) were used to determine if the results were

statistically significant compared to control samples. In this thesis, all the experiments were conducted at least three times.

2.21 Restriction digestion of Plasmid

Generally, plasmids exist in a circular shape, we linearize them using restriction enzymes named Sal-I. The reaction mixture contains cut smart Buffer, high fidelity restriction enzyme Sal-I, and DNase-free water. The tubes were incubated at 37°C for 2 h followed by 65°C for 15 min to inactivate the restriction enzyme. Then the linearized plasmid was run into gel to confirm the digestion process.
The chemical composition for the digestion of plasmid before transfection is listed in table 18.

Table 18: Chemical composition for the digestion of plasmid.

Chemical composition	Amount (µL)
Plasmid DNA	4,6
Cut smart buffer	5
SAL1 (Enzyme)	3
Milli-Q H_2O	37,4

2.22 Antisense circRNA design and synthesis strategies

2.22.1 AS-circRNA design against *GFP*

The antisense target sequence for the endogenous gene *GFP* was retrieved from the secondary structure of *A thaliana* ORF region by using bioinformatic analysis. Also, the *GFP* sequence was used for both plant and fungi transfection processes. On the other hand, sequence elements were present including the overhang sequence, stem sequence, start and stop codons, etc. Besides the target sequence, randomized sequences were selected to use as a control and their length was maintained according to the length of the antisense circRNA sequences. The sequences were flexible, and it was assured the stem-loop formation in both the antisense and control sequences. Moreover, the sequences of oligonucleotides were industrially organized

including the T7 promoter (Sigma-Aldrich, Germany). These were then annealed to produce templates suitable for the in-vitro transcription process.

2.22.2 In vitro transcription, circularization, and gel purification of circRNAs

Synthesizing of RNA was followed by the in vitro transcription method from annealed DNA oligonucleotide templates using HighScribe T7 high-yield RNA synthesis kit (NEB) along with ATP, CTP, UTP, GTP (7.5 mM each), GMP (30 mM, Merck), and RNaseOut (Thermo Fisher Scientific, Germany) at 37°C for 2 hours. Then the template DNA was digested using RQ1DNase treatment (Promega, Germany) followed by incubation at 37°C for 30 minutes. By using a Monarch RNA purification kit (New England Biolabs GmbH, Germany), transcripts were purified, and the amount of RNA was measured by Qubit™ RNA broad-range assay kit (Thermo Fisher Scientific, Germany). For the circularization of transcribed RNA, RNA was mixed with T4 RNA ligase (100 U per 100 µL-reaction; Thermo Fisher Scientific, Germany) in 1× T4 RNA ligase buffer in a combination of 0.1 mg/ml BSA and RNaseOut overnight at 16°C (Thermo Fisher Scientific, Germany) and the volume was adjusted to 200 µL. Finally, RNA was extracted through the phenol/chloroform extraction method (CarlRoth, Germany) and ethanol precipitation process. Afterward, gel purification was performed by desaturating polyacrylamide gels.

To confirm the circularity of RNAs, 250 ng of circular form or linear form of RNA was treated with or without 2 U of RNase R enzyme for 25 min at 37°C (Biozym, Germany). Finally, 200 ng of RNAs were run on the 10% denaturing polyacrylamide gel for the separation and was observed by using ethidium bromide staining.

2.23 Antisense circRNAs designing against *GFP* sequence

To develop new approaches against herbicide and microbial pathogen-related diseases in plants, the following antisense circRNA was designed against the *GFP* sequence as a proof of concept. The circRNA targets the *GFP* sequence in the *ORF* region of *GFP*. Here, we tested antisense circRNAs against the *GFP*-ORF sequence to observe its functionality in gene expression after the translation process. Moreover, the significance of *ORF* also shows its role in protein production. It functions as an important sequence, which can be translated into a functional protein acting as the basis of the cell's machinery to synthesize the desired protein. Also, it's possible to identify a lot of gene functions by analyzing the *ORF* region of the gene. *ORF* region as read by the ribosomes to proceed the protein production. In a nutshell, the *ORF*

region contains necessary genetic information for the synthesis of correct functional protein production.

For the functionality test, the *GFP* reporter system was used for different targets in the sequences. Out of that *ORF* was regarded as a vital target site for targeting endogenous genes in plants as well as in fungi. Here, we selected the precise position of the antisense sequences based on the existing secondary structure model of the Open Reading Frame (ORF). circRNA designing process also indicated that for stable interaction over 30 nucleotides can provide a perfect base-pairing between circRNA and target. Additionally, as a control for *GFP*, one non-specific circRNA was used in this experiment, which comprised a randomized nucleotide sequence of 45 nucleotides instead of the antisense sequences.

3. Results

3.1 Structure prediction and designing of *GFP*-antisense circRNAs

The ORF region of a gene stands out as a crucial target side for antisense circRNAs (Pfafenrot et al. 2021). As a potential novel tool for directing exogenous RNA towards plant and fungal genes, we designed a circRNA specifically targeting the ORF of a *GFP* reporter gene. Precise positions for the antisense sequences were chosen based on the existing secondary structure model of the mRNA. The designing of an artificial antisense circRNA termed circRNA$_{GFP}$ carried a total length of 50 nucleotides, which included a 30-nucleotide complementary sequence derived from the *GFP* gene. To serve as a control for circRNA$_{GFP}$, non-specific circRNAs were designed. These circRNAs featured randomized sequences of 25 nucleotides (lacking any target in the *GFP* gene) and a 20-nucleotide backbone, resulting in circRNA$_{CTR1}$ (45 nucleotides). Fig. 5 shows the structure of *GFP* gene for designing antisense circRNAs.

>ORF_GFP_718_bp

…TTTGGAGAGGACAGGGTACCCATCATACTAGTAGATCTGCGATCTAAGTAAGCTTGGCATTCCGGTACTGTTGGTAAAGCCACC**ATG**GTGAGCAAGGGCGAGGAGCTGTTCACCG
GGGTGGTGCCCATCCTGGTCGAGCTGGACGGCGACGTAAACGGCCACAAGTTCAGCGTGTCCGGCGAGGGCGAGGGCGATGCCACCTACGGCAAGCTGACCCTGAAGTTCATCTGC
ACCACCGGCAAGCTGCCCGTGCCCTGGCCCACCCTCGTGACCACCTTGACCTACGGCGTGCAGTGCTTCGC**CCGCTACCCCGACCACATGAAGCAGCACGA**CTTCTTCAAGTCCGC
CATGCCCGAAGGCTACGTCCAGGAGCGCACCATCTTCTTCAAGGACGACGGCAACTACAAGACCCGCGCCGAGGTGAAGTTCGAGGGCGACACCCTGGTGAACCGCATCGAGCTGA
AGGGCATCGACTTCAAGGAGGACGGCAACATCCTGGGGCACAAGCTGGAGTACAACTACAACAGCCACAAGGTCTATATCACCGCCGACAAGCAGAAGAACGGCATCAAGGTGAAC
TTCAAGACCCGCCACAACATCGAGGACGGCAGCGTGCAGCTCGCCGACCACTACCAGCAGAACACCCCCATCGGCGACGGCCCCGTGCTGCTGCCCGACAACCACTACCTGAGCAC
CCAGTCCGCCCTGAGCAAAGACCCCAACGAGAAGCGCGATCACATGGTCCTGCTGGAGTTCGTGACCGCCGCCGGGATCACTCTCGGCATGGACGAGCTGTACAAG**TAA**CTCGACT
AGAGTCGGGGCGGCCGGGGATCCTCTAGAGTCGACCTGCAGGCATGCCGCTGAAATCACCAGTCTCTC…

Figure 5: Nucleotide sequence of the *GFP*-ORF region with color coding. The 30-nucleotide target sequence of the 50-nucleotide GFP antisense circRNA$_{GFP}$ is indicated in red. The CaMV35S promoter sequence is highlighted in blue, the 5'-UTR in yellow. The start codon (ATG) is indicated in black bold, the stop codon (TAA) in black bold, the 3'-UTR in green, and the terminator sequence is indicated in grey color.

Moreover, circRNAs predominantly exist as single-stranded RNA molecules as a result of their lack of free ends. It also does not exhibit extensive base-pairing like other linear RNAs. Nevertheless, circRNAs have the potential to form secondary structures by complementary base pairing within their sequences (López-Carrasco et al. 2017). These secondary structures might involve interactions between distant regions of the circRNA, follow-on in the formation of structures like stem-loops or other secondary motifs. Additionally, it is worth noting that the binding of circRNAs within their secondary structure is predominantly persuaded by intramolecular base-pairing interactions. Also, complementary nucleotide sequences form

stable secondary structures through hydrogen bonding. These interactions are made possible by secondary structure elements, for example, hairpins, that exist within the circRNA sequence. The precise secondary structures of mRNAs are determined by several factors such as their sequence, length, and the existence of complementary regions. Two different mRNA structures were predicted by the RNAfold software for plant and fungal species and are shown in Fig. 6 (A) and Fig. 6 (B).

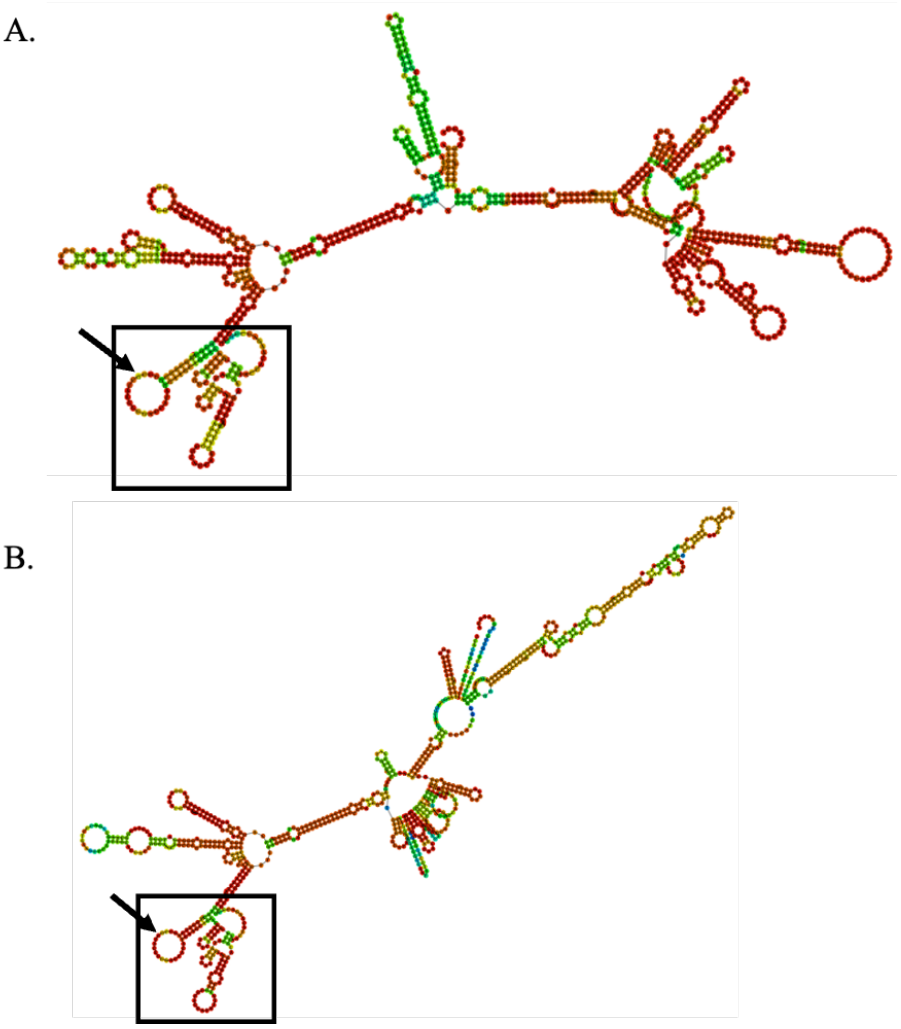

Figure 6: Secondary structure prediction of the *GFP* mRNA for *A. thaliana* (A), and *B. cinerea* (B), and their binding sites for circRNA$_{GFP}$ were determined by RNAfold. Inside the black box indicated with an arrow is the target site for the designated antisense circRNA$_{GFP}$. Antisense circRNA$_{GFP}$ is designed to be exactly bound to the plant and fungal *GFP* sequences indicated inside the box.

3.2 Determination of RNA accessibility by RNAup program

RNAup assesses the thermodynamics of RNA-RNA interactions through a two-step process (Vienna RNA Package, http://rna.tbi.univie.ac.at/cgi-bin/RNAWebSuite/RNAup.cgi). Firstly, it analyzes the possibility of a potential binding site remaining unpaired, which is equivalent to determining the energy required to open the site. Afterward, it combines this accessibility information with the interaction energy to derive the overall binding energy. These calculations involve computing partition functions inclusive of all possible conformations. Here, RNA sequences (including 5'-UTR, ORF, and 3'-UTR) with their antisense RNA sequences were used to determine the RNA accessibility by using RNAup. This analysis served as an orientation for the selection of sequence sections for the antisense circRNA design.

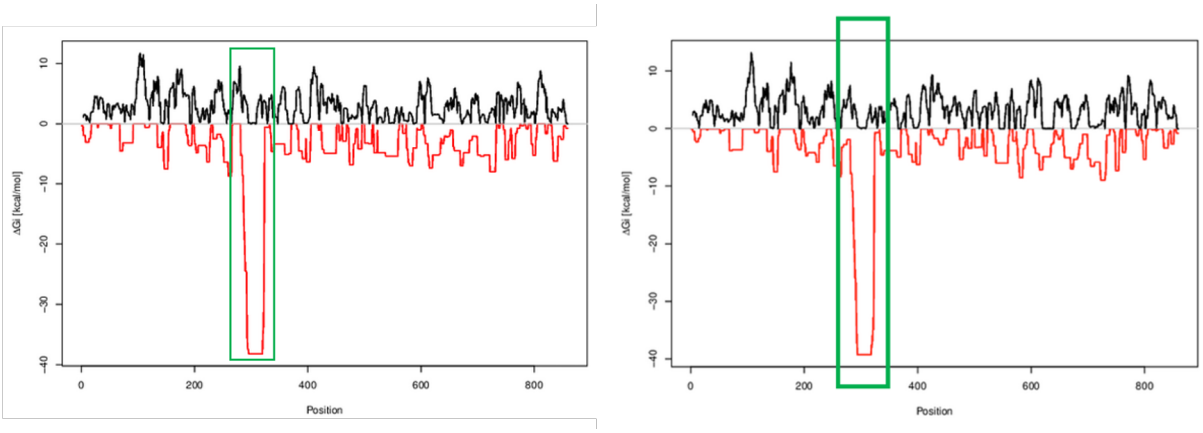

Figure 7: Analysis of RNA accessibility by the RNAup program. The antisense circRNA binds equally in both plants (left) and fungi (right). The mRNA sequence of *GFP*, including 5'-UTR, ORF, and 3'-UTR, was employed alongside its complementary antisense RNA sequence to assess RNA accessibility. The plot represents both the interaction-free energy (indicated in red as ΔGi) and the energy required to unfold pre-existing structures within the *GFP* sequence (indicated in black). The target region is indicated in the image (at the top of the graph carrying ΔGi value more than 0) and the whole range (at the bottom of the graph carrying ΔGi value less than 0). This analysis provided insights for choosing specific sequence segments for designing antisense circRNA. The target sequence of the antisense circRNA$_{GFP}$ is denoted by the green box. The RNAup program shows that antisense circRNA sequence can be used in both organisms for the highest inhibitory effect against the protein translation process.

3.3 Prediction of the secondary structure of circRNA via Mfold

The optimal and suboptimal secondary structures of the following antisense circRNA were predicted by the Mfold program (www.unafold.org; Zuker et al. 2003). It is followed by the minimum energy minimization. Depending on the energy-changing process, different optimal folding has been calculated. Mfold also shows many variations of the predicted structure, based on the energy consumption. As an example, certain segments of the RNA molecule that exhibit the same structure of helix in both optimal and suboptimal secondary structure predictions tend to be more accurately foreseeable compared to other regions that display higher variability. However, the following structures of circRNA have been predicted based on their low energy consumption and the reliability of binding sites. Mfold also writes the energy matrices as output data in a file which is read by another program named PlotFold. Likewise, RNA accessibility calculates the required energy to unfold a secondary structure of RNA, which was determined using the RNAup program. There are two different circRNA structures predicted in Fig. 8, where the circRNA shows a closed loop form by binding.

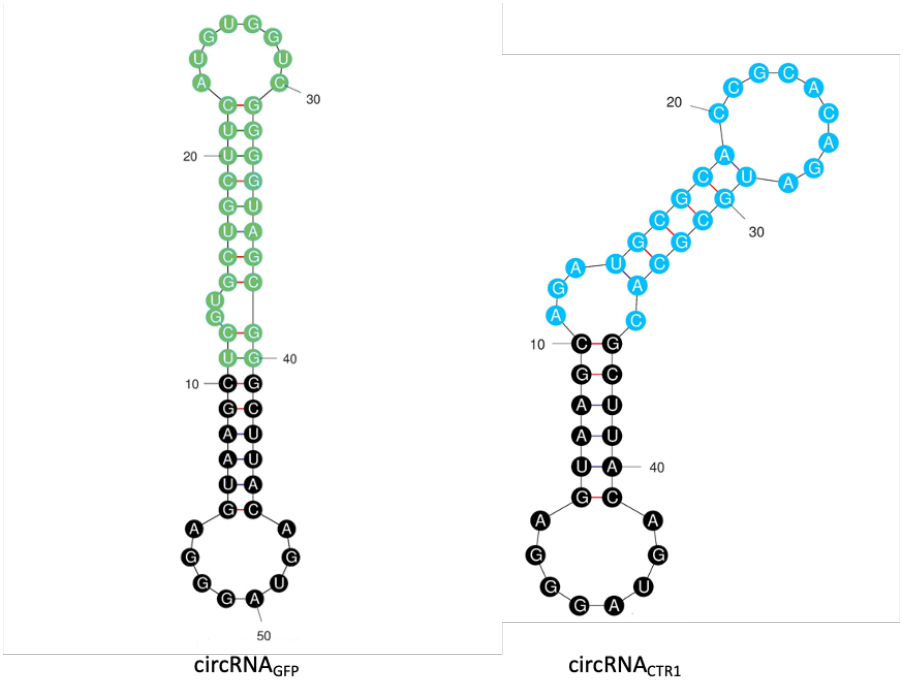

Figure 8: Secondary structure visualization of circRNA$_{GFP,}$ and circRNA$_{CTR1}$. The energy consumption of both circRNAs is minimal in a folding process, which was automatically calculated by using the program Mfold. The secondary structures were also determined with the same program Mfold (www.unafold.org; Zuker et al. 2003). The *GFP* target sequence is highlighted in green, whereas randomized control sequences are in blue.

3.4 Effect of antisense circRNAs on the *Botrytis cinerea* protoplasts upon PEG-mediated co-transfection

3.4.1 Microscopic analysis of *Botrytis cinerea* protoplasts

Enzymatic degradation of *B. cinerea* mycelium is the only procedure to produce a higher amount of high quality protoplasts in a short time. The protoplasts then were filtrated to remove extra debris including broken mycelium and conidia from the solution using a 22 µm filter. Protoplast sizes vary from 5 µm to 20 µm in the same buffer. Produced protoplasts were suitable and healthy for the transfection of foreign genes immediately after isolation. Fig. 9 shows the different sizes of extracted protoplasts immediately after incubation with a mixture of different enzymes.

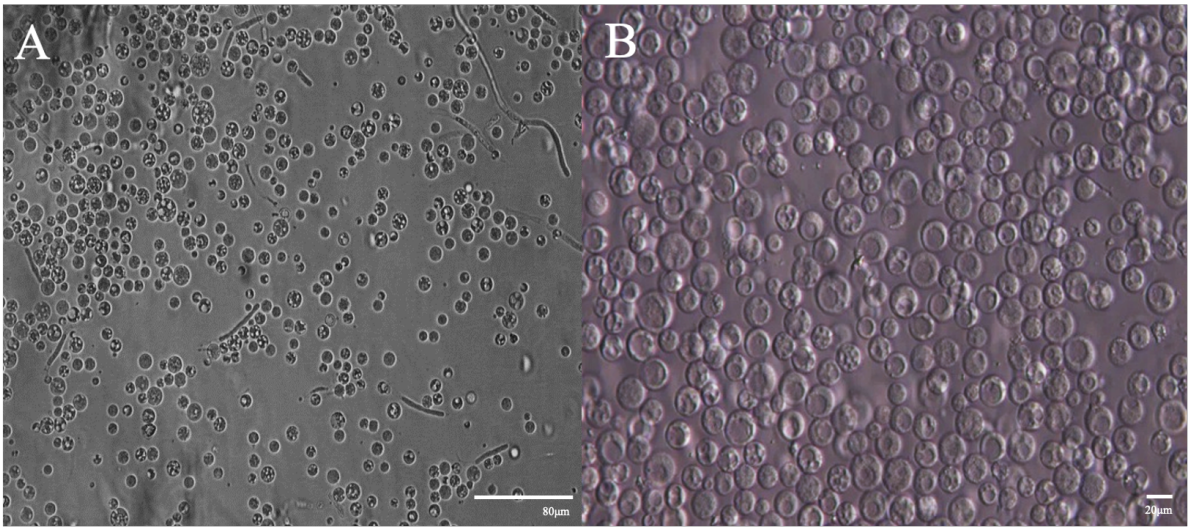

Figure 9: Imaging of *B. cinerea* protoplasts. Protoplasts were isolated within 3.5 h of incubation from the enzyme solution. Two different sizes of protoplast are shown from 10x (A) to 40x (B) magnification range. Here, the sizes of protoplasts varied from the smallest 5 µm to a maximum of 20 µm in the buffer. Images were captured with an inverted microscope (Leica DMC 2900, Leica, Germany).

3.4.2 Evaluation of co-transfected *Botrytis cinerea* protoplasts through fluorescence microscopy to confirm the transfection efficiency

After producing the fresh protoplasts from mycelium, they were transfected using two different sets of plasmids (pGY1-35S-pgpd::*GFP*-35sTer and pBGgHg-pgpd::GFP) to assess the transfection efficiency. Until 72 h, protoplasts were cultured in the same buffer carefully. The

expression of *GFP* was observed at 24 h post-transfection. Fig. 10 shows the transfection efficiency of the different plasmids.

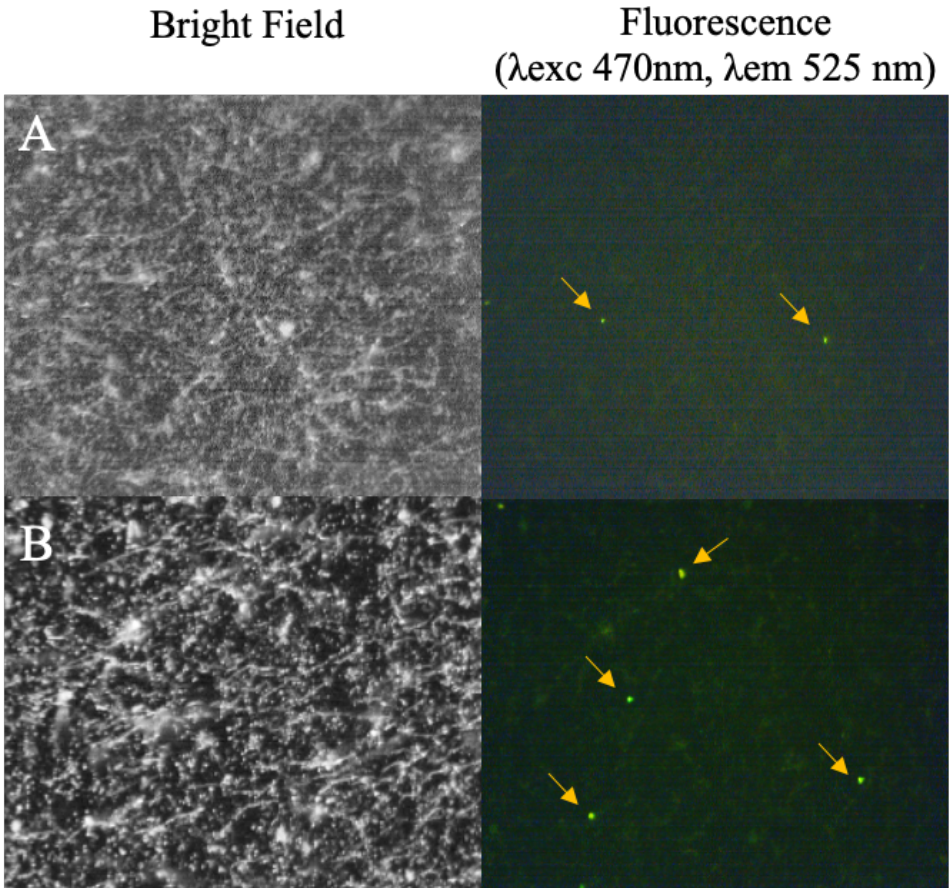

Figure 10: Transfection efficiency at 24 h after PEG-mediated post-transfection of plasmids (A) pGY1-35S-pgpd::*GFP*-35sTer and (B) pBGgHg-pgpd::GFP. The figure shows the transfected protoplasts from *B. cinerea* which turns into mycelium (left) in the bright field of microscopy and the expressed GFP protein (right) into the mycelium. Fungal protoplasts were inspected under the fluorescence microscope using the fluorescence filter from λexc 470 nm to λem 525 nm excitation range. The efficiency of GFP expression is different for both of the plasmids used for the transfection.

3.4.3 CLSM analysis of fungal protoplast and mycelium after co-transfection.

CLSM (Confocal laser scanning microscopy) is a widely used fluorescence microscope. It is commonly utilized in biological science as well as in the field of chemistry for capturing the high resolution of images. After hitting the fluoresce molecules with laser light, CLSM emits the light in lower energy to visualize the picture of different objects. It's also possible to create

3D images of substances by taking different pictures. CLSM is an advanced microscopic technique that can visualize the expression in different parts of an organism.

Fig. 11 shows the images of *B. cinerea* mycelium after 72 h of transfection with different plasmids. In the following images, the efficiency of *GFP* expression was observed inside the mycelium of *B. cinerea* without any staining procedure. The following results showed the expression of pBGgHg-pgpd::GFP, which was significantly higher than that of plasmid pGY1-35S-pgpd::*GFP*-35sTer. Therefore, pBGgHg-pgpd::GFP was selected for further experiment, and utilized for the transfection with fungal protoplast (Fig. 11).

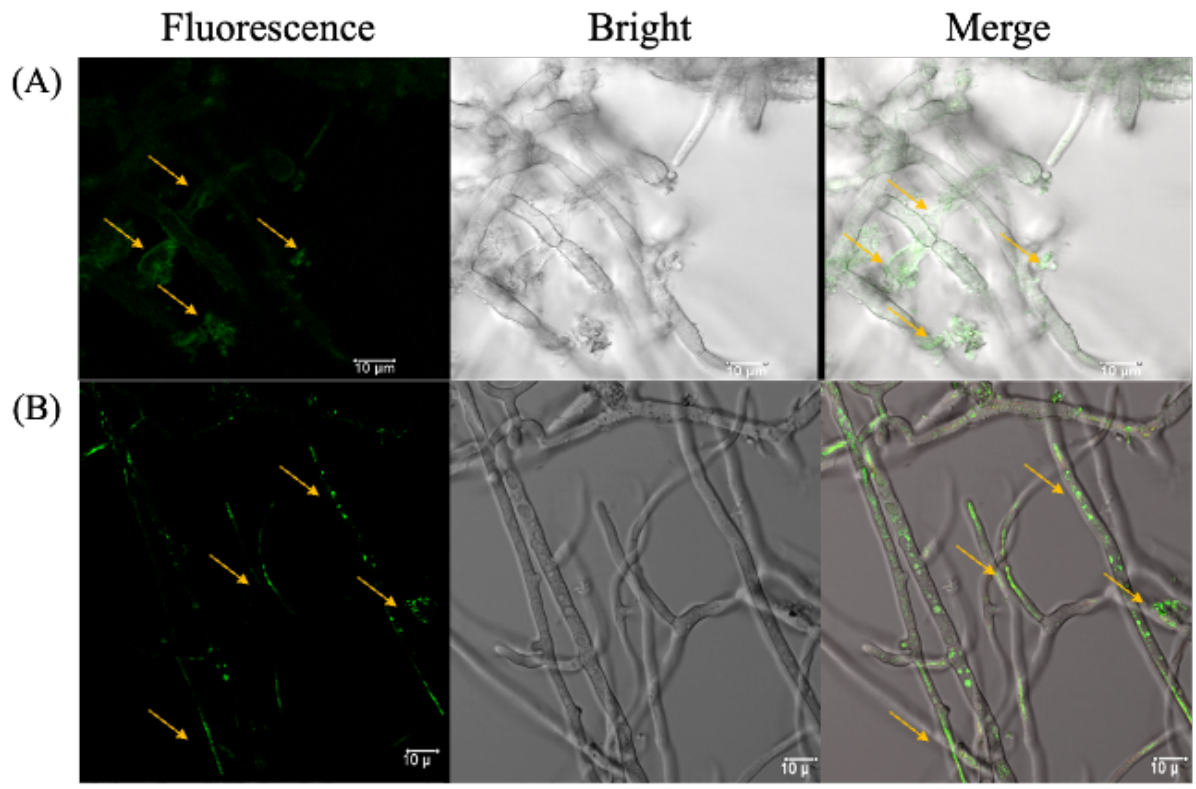

Figure 11: CLSM of *GFP* expressing *B. cinerea* mycelium at 72 h of transfection. (A) *GFP* expression from the plasmid pGY1-35S-pgpd::*GFP*-35STer after protoplast transfection. (B) *GFP* expression of plasmid pBGgHg-pgpd::GFP after protoplast transfection. The arrow sign in Fig. (A) and (B) represents the *GFP* expression inside the mycelium, and the *GFP* signal was detected under the fluorescence signal between 489 nm (λexc) to 508 nm (λem). The *GFP* expression was found in several distinct places inside the mycelium (Scale bars =10 µm).

3.4.4 Impact of circRNAs on *GFP* expression and protein inhibition in *Botrytis cinerea* protoplasts

The immunoblotting procedure was conducted using fungal protoplasts to assess the effectiveness of designer antisense circRNAs on the GFP protein expression. We transfected the protoplasts with plasmid (pBGgHg-pgpd::GFP) and co-transfected the protoplasts with circRNA and plasmid. Then the total protein was extracted from different treatments of the growing mycelium at 72 h post-transfection. As a negative control, non-target sequences of circRNA were co-transfected with the plasmid. Also, as a positive control, we used a protein sample from the transgenic fungus *Fusarium graminearum*, which produces GFP. Upon analyzing the immunoblotting results, it was observed that the transfected sample and co-transfected samples did not show any kind of GFP bands, except the positive (+) control (Fig. 12). These results suggested that the cotransfection of *B. cinerea* protoplast is not an ideal way to observe the protein inhibitory effect by circRNA.

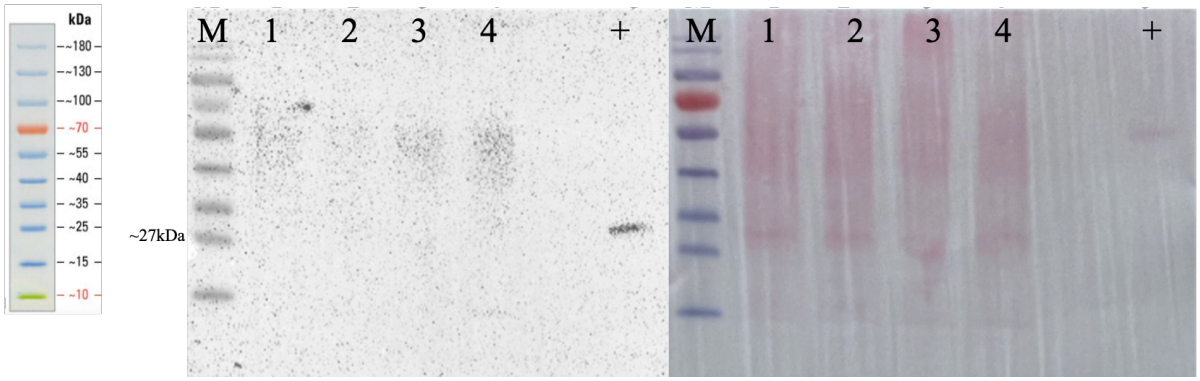

Figure 12: Immunoblotting analysis after co-transfection with plasmid pBGgHg-pgpd::GFP and circRNAs. In the left image, immunoblot analysis after SDS-PAGE using primary and secondary GFP antibodies (Primary antibody: living colors monoclonal antibody JL-8, Secondary antibody: anti-mouse IgG-peroxidase conjugate). The right image indicates the protein loading control (Ponceau-S staining).

M = Protein Marker, Lane 1 = Control (only protoplast), Lane 2 = pBGgHg-pgpd::GFP, Lane 3 = pBGgHg-pgpd::GFP + circRNA$_{GFP}$, Lane 4 = pBGgHg-pgpd::GFP + circRNA$_{CTR1}$, Lane + = Positive control for GFP protein. The size of the GFP protein is ~26.9 kDa and appears in the membrane after antibody detection.

3.5 Fluorescence microscopic analysis of co-transfected Arabidopsis protoplasts with plasmid pGY1-35S::GFP and circRNAs

Due to the lower expression level of *GFP* in the fungus, we continued the experiment of co-transfection using *Arabidopsis thaliana* protoplast. *A. thaliana* protoplasts are easier to extract, and it has been noticed that the protoplasts from *A. thaliana* can express *GFP* after co-transfection in a higher amount within a short period (18 h) compared to the fungal protoplast (starting from 24 h and up to 72 h). To explore the effect of designated antisense circRNAs against *GFP*, the following experiment was conducted to understand their inhibitory effect at an 18 h timepoint.

The isolated protoplasts from the wild-type *A. thaliana* were co-transfected with designer antisense circRNA against the *GFP* and additionally, another circRNA sequence that doesn't interact with the *GFP* sequence. After 18 h, protoplast number and transfection efficiency were calculated based on *GFP* fluorescence, which was compared and calculated to the total amount of protoplasts. Finally, the ratio between green and red pixels (representing GFP and total protoplast from chlorophyll autofluorescence) was calculated and statistically analysed.

To gain additional insights into the mechanism of action of a sequence-specific designer circRNA, we first conducted our experiment using wild-type *A. thaliana* protoplasts. After co-transfection with circRNA and plasmid into the protoplasts, we noticed less GFP fluorescence in $circRNA_{GFP}$ treated protoplast but not in $circRNA_{CTR1}$ treated protoplasts, indicating a sequence-specific inhibition (Fig. 13). Next, we wondered if GFP inhibition was due to RNAi. Therefore, we continued to investigate if the effectiveness of $circRNA_{GFP}$ is compromised in Arabidopsis mutants lacking essential genes for RNAi, specifically *dcl1-11* and *ago1-27*. The AGO1 encodes for an RNA slicer which leads to Ala to Val substitution, and the DCL1 generates 21-nt small RNAs (sRNAs) known as microRNAs from a partially double-stranded region that regulate the mRNA expression by complementary target sites. Meanwhile, the mutant *ago1-27* and *dcl1-11* lack AGO and DICER activity and, therefore cannot have 21 bp miRNAs to regulate their target genes.

After co-transfection with the plasmid and circRNA, we analyzed the microscopic images and the GFP inhibition by comparing the red and green pixels (Fig. 14, and Fig. 15).

As previously observed in WT protoplasts, the mutant protoplasts also showed a significant amount of GFP reduction in the $circRNA_{GFP}$ treated sample compared to the control, which was not treated with circRNA. These results suggest that $circRNA_{GFP}$ has an inhibitory effect on the expression of *GFP* and can be able to reduce GFP protein expression in a protein inhibitory manner.

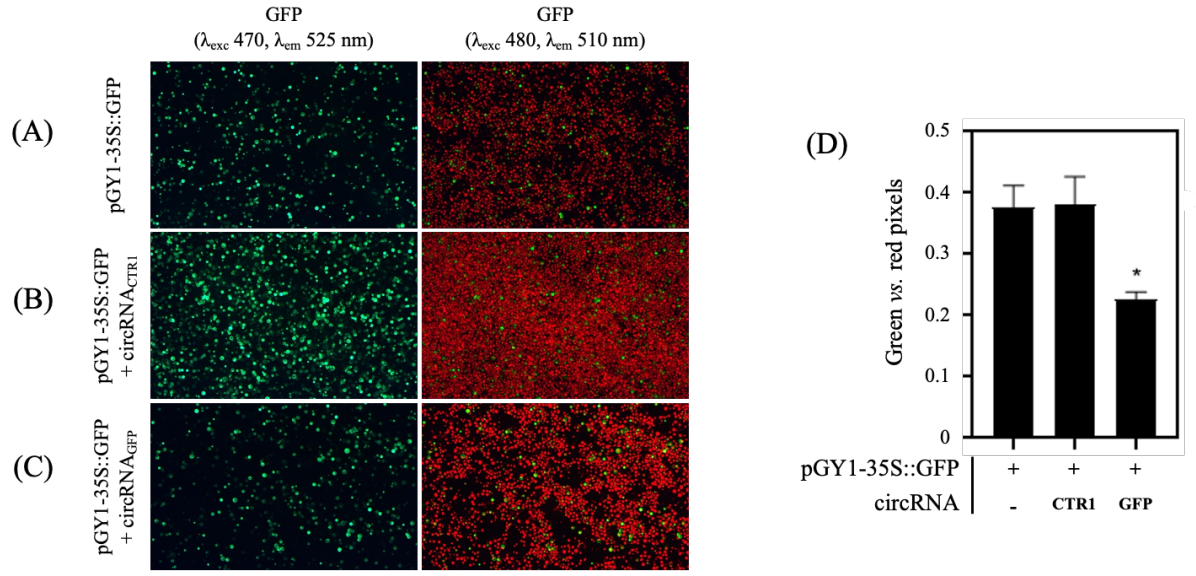

Figure 13: Microscopic images of *GFP* expressed WT *Arabidopsis thaliana* protoplasts after co-transfected with designated antisense circRNA$_{GFP}$. The GFP signal is visualized as green (left), while the red signal on the images (right) represents the total amount of protoplasts due to chlorophyll autofluorescence. The analysis was performed after 18 h of co-transfection. (A) The transfection of protoplasts was performed only with 20 µg of pGY1-35S::GFP plasmid. (B) The protoplasts were co-transfected with the same amount of plasmid and additionally 4 µg of antisense circRNA$_{GFP}$. (C) Co-transfection of protoplasts including 20 µg pGY1-35S::GFP and 4 µg of random nucleotide sequences of circRNA$_{CTR1}$ as an additional control. (D) The ratio between green and red pixels was measured using ImageJ software. Bars from the graph represent the measurement of three different pictures with SEM (Standard Error of Mean). Statistical analysis performed with one-way ANOVA, $p \leq 0.05$. * $p \leq 0.05$ compared to control protoplast (Dunnett's test).

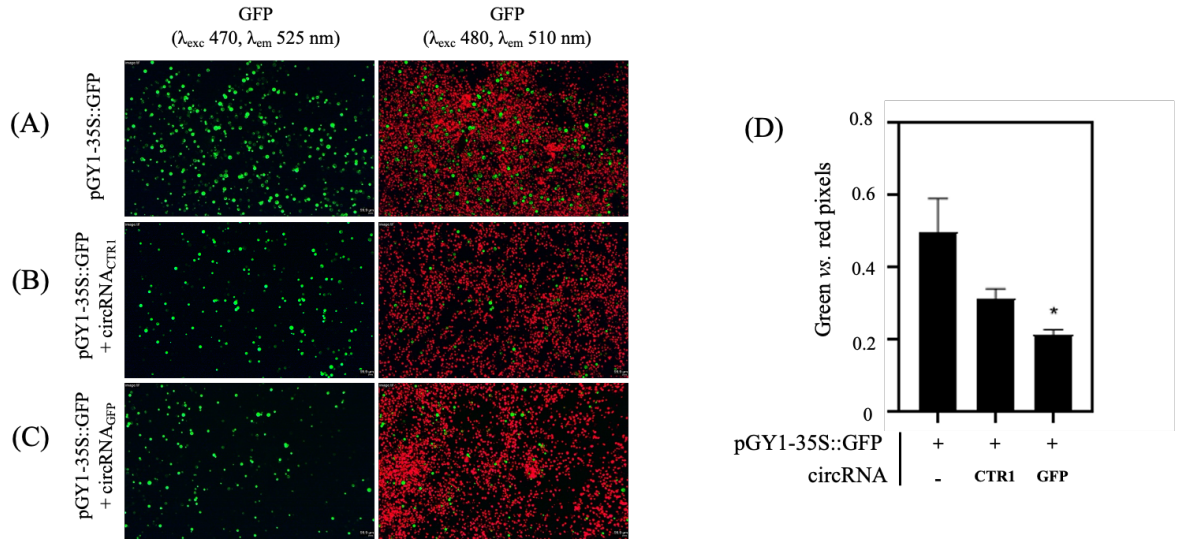

Figure 14: Images of *Arabidopsis thaliana* (Δ*Atago1*) protoplasts after transient expression. The images were analyzed after 18 h of post cotransfection where green images represent the GFP signal (left) and red signal (right) in the images represent the total number of protoplasts. (A) Protoplasts were co-transfected only with a concentration of 20 µg of pGY1-35S::GFP plasmid. (B) Co-transfection of protoplasts involved the same amount of pGY1-35S::GFP plasmid along with 4 µg of antisense circRNA$_{GFP}$, and (C) Co-transfection of protoplasts included the same amount of pGY1-35S::GFP plasmid and 4 µg of circRNA with a random nucleotide sequence (circRNA$_{CTR1}$) as an additional control, and (D) The ratio of green pixels (representing *GFP* fluorescence) and red pixels (representing total protoplasts) was calculated using an open source software ImageJ and bars represent the average measurements taken from at least 3 different images, with the standard error of the mean (SEM). For statistical analysis one-way ANOVA was performed, where (*) $p \leq 0.05$ significant compared to the control protoplasts (Dunnett's test).

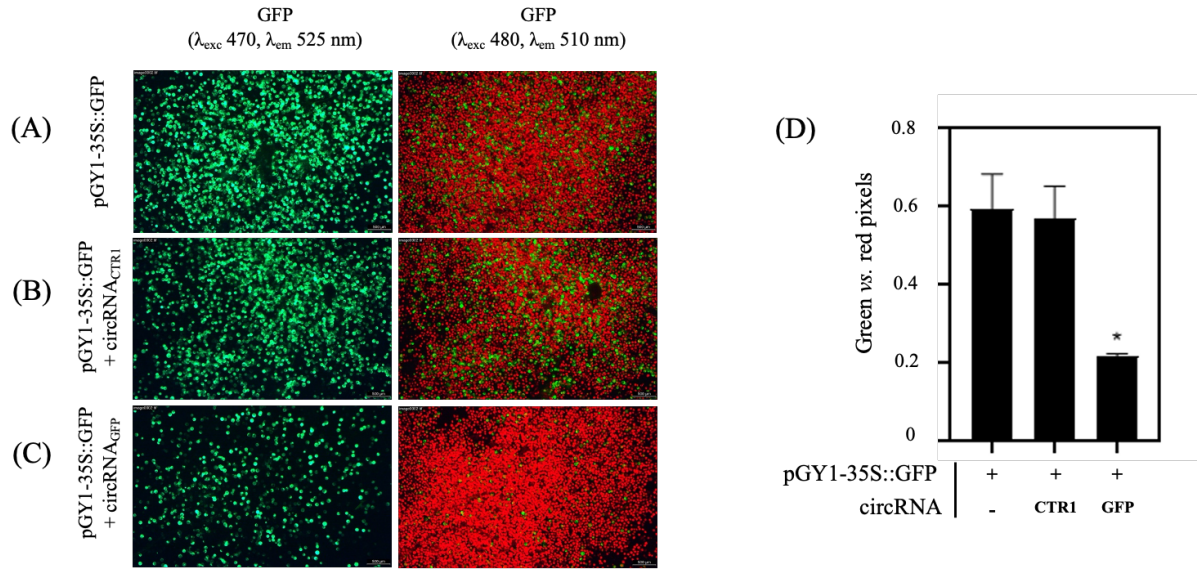

Figure 15: Microscopic analysis of images of *GFP* expressing *Arabidopsis thaliana* mutant Δ*Atdcl1* protoplasts after co-transfection with designated antisense circRNA$_{GFP}$. GFP as green signal on the left and as red signal on the right side of the images shows the total amount of protoplast. Analysis was performed after 18 h of post-cotransfection. (A) Protoplasts co-transfected only with 20 µg of pGY1-35S::GFP plasmid, (B) Protoplasts co-transfection by adding 20 µg pGY1-35S::GFP and 4 µg of antisense circular RNA (circRNA$_{GFP}$), (C) Co-transfection of protoplast by following same condition as (B) using random nucleotide sequence circRNA$_{CTR1}$ as control rather than circRNA$_{GFP}$, and (D) The bar from the graph represents the ratio between green (GFP fluorescence) vs. red pixel (total protoplast) from the 3 different areas of the protoplast image under the microscope, also SEM was calculated and statistical analysis was performed by one-way ANOVA, where (*) $p \leq 0.05$ significant compared to the control protoplast (Dunnett's test).

3.6 Quantification of protein content in co-transfected protoplasts by immunoblotting

To provide additional support for circRNA-mediated GFP reduction, we continued with the immunoblotting analysis to observe the alteration of GFP protein levels in response to the introduction of exogenous circRNAs.

The protoplasts transfection was carried out as before and afterward, they were collected for protein isolation. Then the proteins were analyzed by immunoblotting to observe the expression of GFP protein. In the quantification process, an anti-Actin antibody was used to measure the same amount of protein loading for the proteins of wild-type and different mutant plant protoplasts. The transfected protoplasts showed strong GFP accumulation while protoplasts

treated with circRNA$_{GFP}$ showed a GFP reduction of up to 78% compared to the control protoplast in the wild-type Arabidopsis protoplasts (Fig. 16A). Also, the two different mutant Arabidopsis protoplasts showed 49% (*ago1*) and 57% (*dcl1*) less GFP protein expression after cotransfection with antisense circRNA$_{GFP}$ (Fig. 16 (B) and (C), respectively).

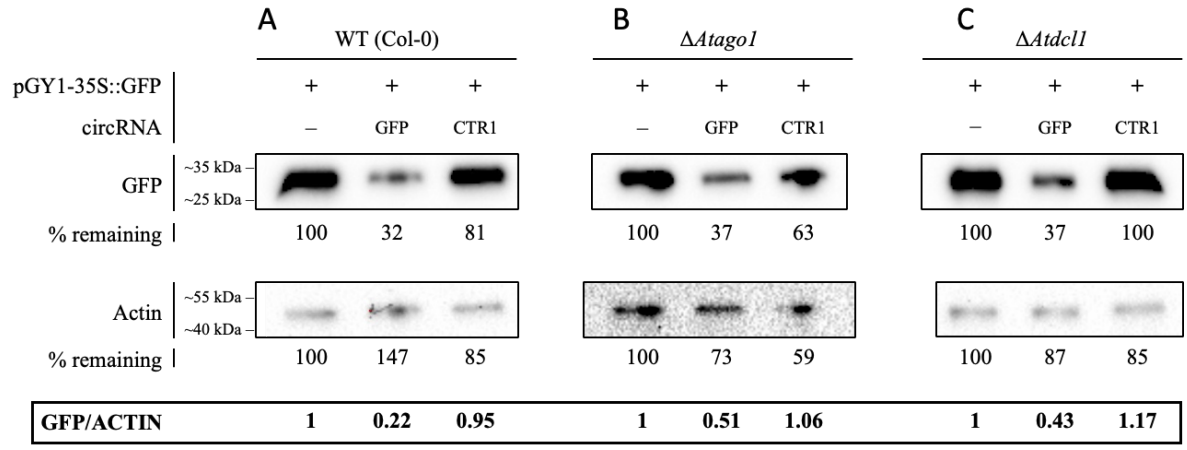

Figure 16: The effect of antisense circRNA on GFP expression in Arabidopsis protoplasts including those from RNAi mutants. Protoplasts were cotransfected with 4 µg of specific and unspecific circRNAs in each experimental procedure. Afterward, the protoplasts were collected, lysed, and equal amounts of protein were assessed using immunoblotting. The Actin protein was assessed by using an anti-Actin antibody as a loading control. (A), (B), and (C) represent the WT, Δ*Atago1,* and Δ*Atdcl1 Arabidopsis thaliana* protoplast samples, respectively. Imaging for two different antibodies was performed at two different times, where GFP protein appeared within 1 min of exposure (~26.9 kDa), and Actin appeared after 10 min of exposure (~45 kDa). The GFP and Actin protein expression ratio shows the amount of GFP protein downregulation in the experiment.

Additionally, three different Arabidopsis mutants including *dcl2,3,4; ago2-1*; and *ago4-1* were used to conduct the co-transfection with circRNA and plasmid by maintaining the same conditions as other WT and mutant plants. As a loading control, Ponceau S staining was used to measure the protein loading in a different sample. The mutant lines that are used have critical functions in the RNAi pathway. DCL2 and DCL4 function in dsRNA processing to produce 20 to 22 nucleotides of siRNA molecules. DCL3 participates in the formation of small RNA with 24 nt long repeat associated molecules referred to as heterochromatic siRNAs.

The triple mutant line DCL2,3,4 functions in gene regulation and the maintenance of genome stability in *Arabidopsis thaliana*. On the other hand, AGO2 is responsible for binding small RNA molecules (siRNAs) to the RISC complex leading to mRNA degradation (Kamthan et al. 2015). On the other hand, AGO4 functions in RNA-directed DNA methylation (RdDM), which is responsible for establishing and preserving DNA methylation involved in the regulation of transposons as well as the proper gene silencing process. Consistent with previous results, we also found the same type of inhibition in GFP protein in samples treated with antisense circRNA$_{GFP}$ compared to the control samples (Fig. 17). The results suggest that circRNA has an inhibitory effect on the GFP protein regardless of mutant plants.

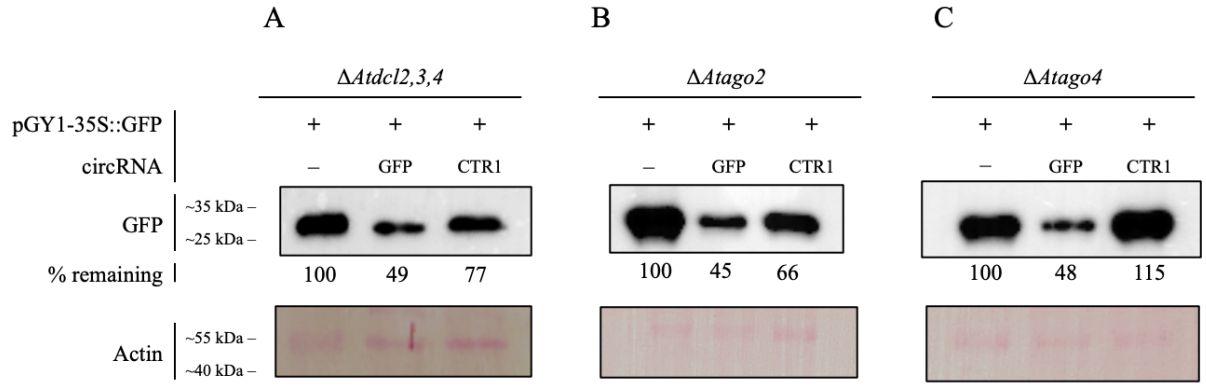

Figure 17: The impact of antisense circRNAs on GFP accumulation in protoplasts of various Arabidopsis mutants. Protoplasts were co-transfected with 4 µg of specific and unspecific circRNAs and with 20 µg pGY1-35S::GFP plasmid. Subsequently, the protoplasts were collected, lysed, and equivalent amounts of protein were assessed through Ponceau S staining. The anti-GFP antibody was employed to assess the GFP protein. Three sets of protoplast samples were represented as (A), (B), and (C), corresponding to the *dcl2,3,4; ago2-1*; and *ago4-1* of *A. thaliana* mutants. GFP protein, with a molecular weight of approximately ~26.9 kDa, was detected within 1 minute of exposure. In contrast, Ponceau S staining was conducted immediately after the GFP protein measurement to confirm the loading of the same amount of Actin protein in the membrane, which was visualized at around ~45 kDa. All the individual lanes of the membrane started with the transfection of the sample that contained plasmid (pGY1-35S::GFP), plasmid (pGY1-35S::GFP) + circRNA$_{GFP}$, and plasmid (pGY1-35S::GFP) + circRNA$_{CTR1}$ (Control; randomized non-target sequences of circRNAs) respectively.

3.7 Quantification of target *GFP* expression by qPCR upon co-transfection assay by applying circRNAs

According to the immunoblotting results, we hypothesized that the circRNAs may have a significant effect on the transcript level of the *GFP* gene. Therefore, the following experiment was conducted using the same condition of immunoblotting analysis. Different mutant plants including *ago1-27* and *dcl1-11* in addition to WT, were used to reveal the RNAi activity of circRNA$_{GFP}$. Our results found that the presence of both circRNAs had no obvious impact on the GFP transcript level in various protoplast types as shown in Fig. 18.

These findings strongly suggest that circRNA$_{GFP}$ specifically impedes the accumulation of the GFP protein without influencing the levels of the corresponding transcripts. Notably, this regulatory mechanism functions independently of canonical RNA interference (RNAi) pathways.

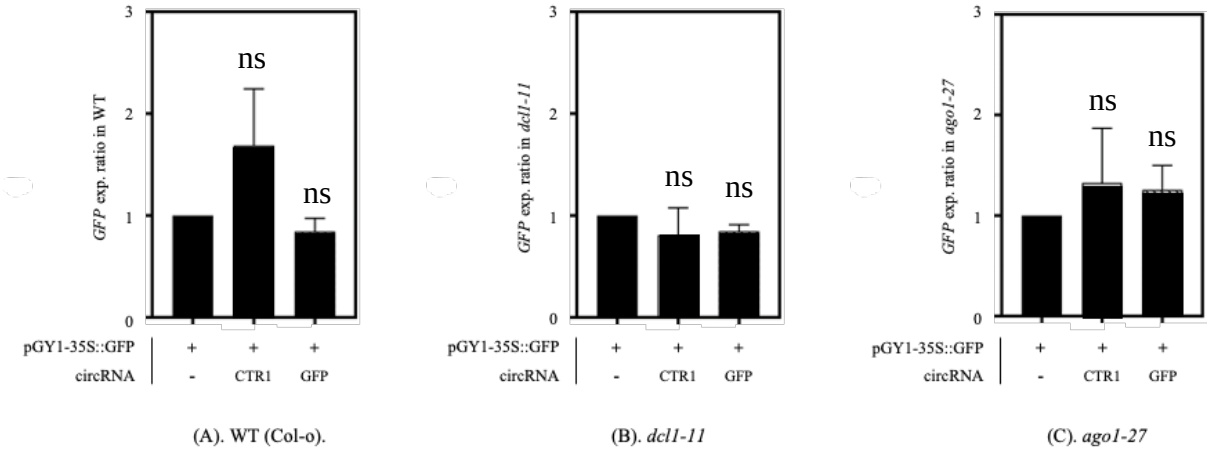

Figure 18: Expression of the *GFP* gene in *A. thaliana* protoplasts after PEG-mediated co-transfection with the plasmid (pGY1-35S::GFP) and circRNA (targeting and non-targeting circRNA sequences). Expression of the *GFP* gene was quantified by RT-qPCR and normalized to *A. thaliana* reference gene *Ubiquitin*. The error bars on the graph indicate the standard error of the mean (SEM), which was calculated from three different biological replications. (A) WT (wild type Col-0), (B) mutant *dcl1-11*, and (C) *ago1-27*, plant protoplasts were transfected by following the previous method. Between the treatments and genotypes, there were no statistically significant differences. Statistical analysis was conducted using one sample t-test ($p \geq 0.05$).

Additionally, we also conducted another experiment with three more mutant lines of Arabidopsis plants such as *dcl 2,3,4; ago2-1;* and *ago4-1*. After RT-qPCR analysis (Fig.19), we found the same type of results which suggest that there is no RNAi activity and $circRNA_{GFP}$ suppresses the accumulation of proteins in a sequence-specific manner, without influencing GFP transcripts.

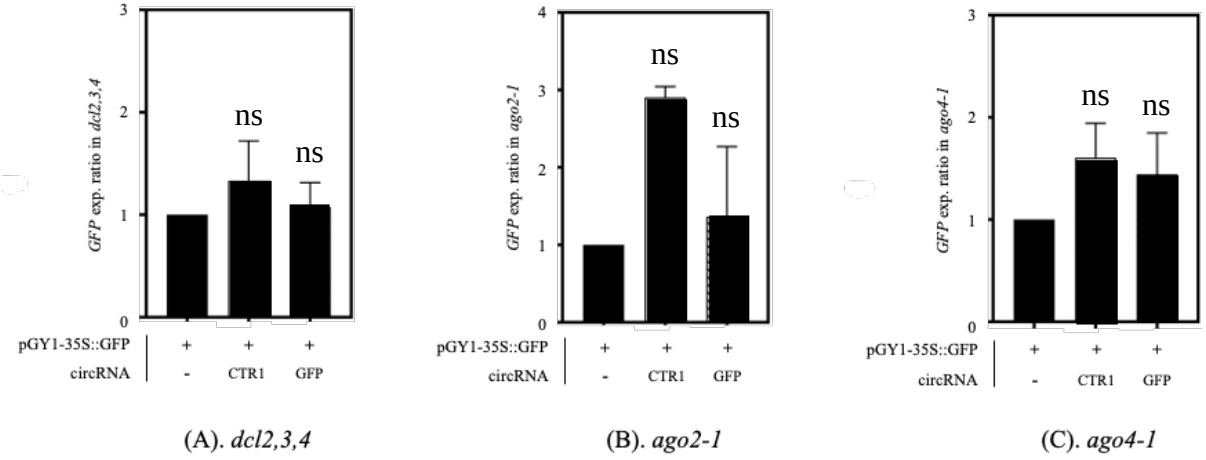

Figure 19: Relative expression of *GFP* determined by RT-qPCR in different mutant lines (*dcl 2,3,4; dcl4-1; ago2-1*) of *A. thaliana* after protoplast co-transfection. Co-transfection was conducted by using plasmid pGY1-35S::GFP and circRNAs. *GFP* quantification was normalized to *A. thaliana* reference gene *Ubiquitin*. Bars represent average of three different biological repetitions with SEM. Treatment was non-significant according to one sample t-test ($p \geq 0.05$). (A) mutant *dcl 2,3,4*, (B) mutant *ago2*, and (C) *ago4,* plant protoplasts were co-transfected with plasmid and circRNA by following the same method.

3.8 Analysis of microscopic images after using different doses of circRNAs in Arabidopsis protoplasts through PEG-mediated co-transfection assay

To assess the efficiency of circRNAs, different doses of circRNA were applied to determine GFP protein accumulation. It was followed by the same condition as before and different doses of circRNAs were applied, from 1 µg to 8 µg into the transfection process. At the constant time point of 18 hours, all the samples were analysed and imaged through a fluorescence microscope, and ImageJ software was used for GFP fluorescence quantification. According to Fig. 20, the GFP fluorescence showed a significant reduction in all protoplasts treated with $circRNA_{GFP}$, where no significant reduction was observed in protoplasts treated with the control $circRNA_{CTR1}$. Quantitative analysis of GFP fluorescence showed a significant reduction of the GFP fluorescence treated by $circRNA_{GFP}$ (Fig. 21). On the other hand, $circRNA_{CTR1}$ does

not reduce the GFP fluorescence, which suggests that circRNA$_{GFP}$ showed an inhibitory effect against GFP protein expression.

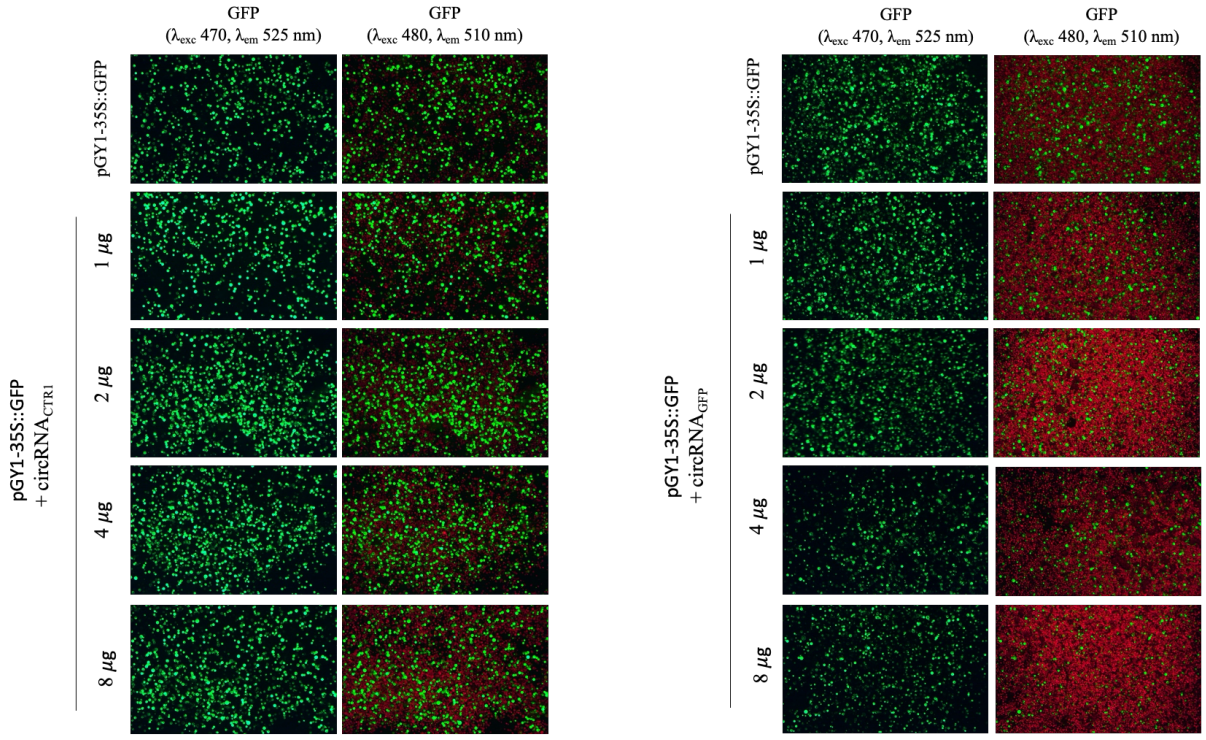

Figure 20: Microscopic analysis of different doses of circRNA$_{CTR1}$ and antisense circRNA$_{GFP}$ after the PEG-mediated co-transfection process in WT *A. thaliana* protoplast. Samples were co-transformed with 20 µg of plasmid (pGY1-35S::GFP) and doses of circRNA from 1 µg to a maximum of 8 µg for both types of circRNA. Subsequently, the GFP signal was visualized with a filter between λexc 470 nm to λem 525 nm, whereas another filter between λexc 480 nm to λem 510 nm wavelength was used to visualize the total protoplast content. Samples were analyzed after 18 hours of incubation after co-transfection.

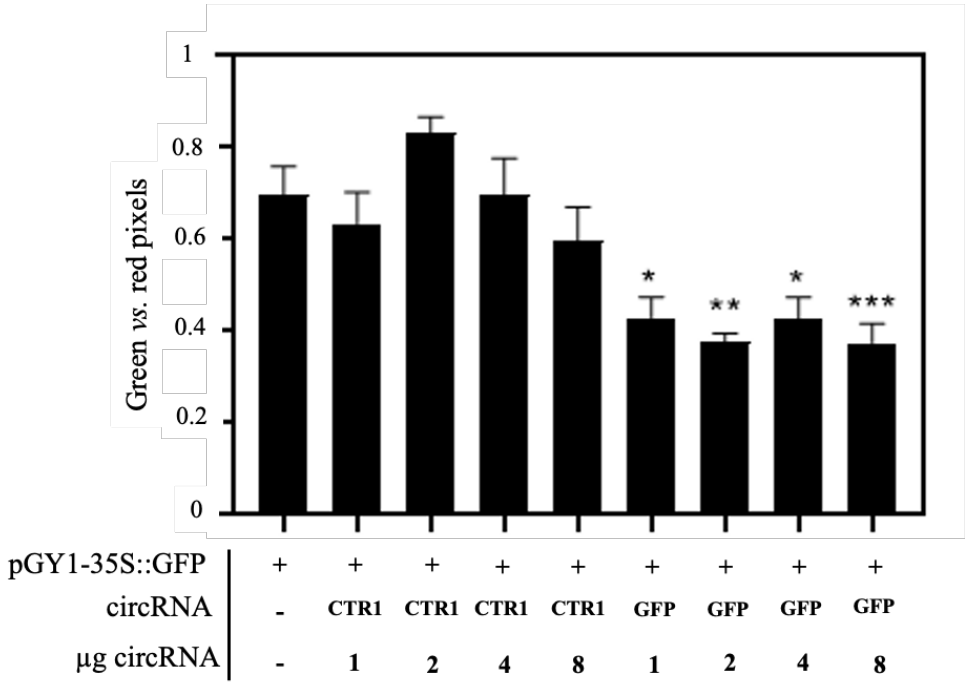

Figure 21: GFP signal quantification based on the green and red pixel ratio after ImageJ analysis. The total amount of the protoplast (red pixels) and GFP fluorescing protoplasts (green pixels) was calculated and analyzed from the images of different places in the buffer containing the protoplast. The doses of circRNA$_{GFP}$ or circRNA$_{CTR1}$ varied from 1 µg, 2 µg, 4 µg, and up to 8 µg. Bars indicate an average of at least 3 different pictures with SEM. Statistical analysis was performed by using one-way ANOVA. Statistical significance is indicated by the asterisks (*P < 0.05; **P < 0.01; ***P < 0.001 to the control group; Dunnett's test).

3.9 Immunoblotting analysis of different doses of circRNAs

Previous experiments showed that 4 µg of circRNAs can reduce GFP protein expression. To gain further knowledge about the mode of action, a dosing experiment was carried out from a minimum amount of 1 µg and up to 8 µg of circRNA. Both the control and the antisense circRNA were used in the same concentrations. The effect of circRNA$_{CTR1}$ showed a steady state condition, and the circRNA$_{GFP}$ showed an effect of GFP inhibition into the *A thaliana* protoplasts expression (Fig. 22). At all the doses, circRNA$_{CTR1}$ showed no changes in the protein expression level. On the other hand, increasing doses of circRNA$_{GFP}$ showed increased inhibition of the GFP accumulation. Two µg of antisense circRNA$_{GFP}$ reduced by the 30% the GFP accumulation, while the inhibition increased up to 44% using a maximum of 8 µg against the 20 µg of plasmid.

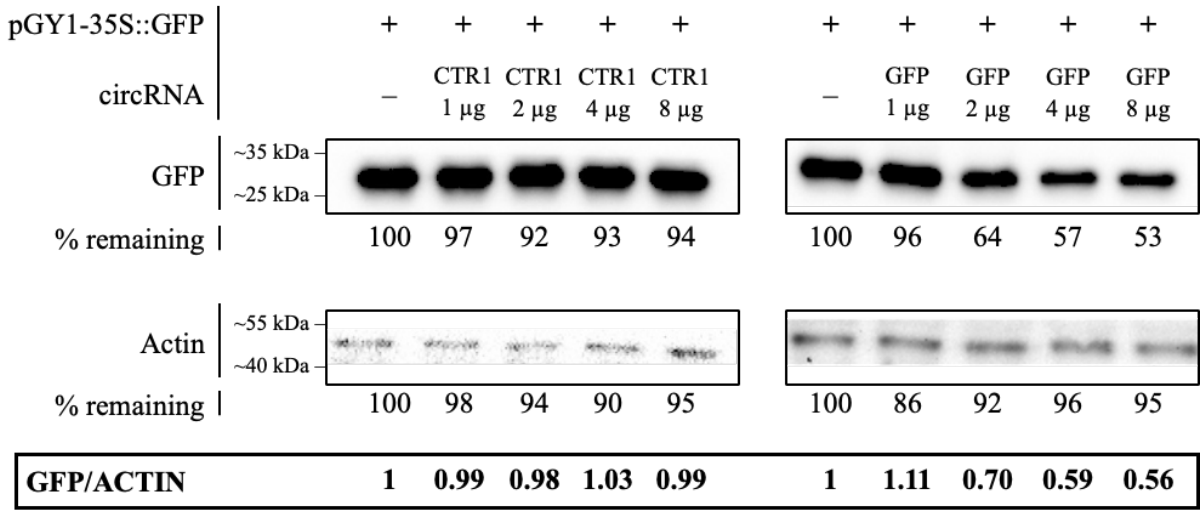

Figure 22: Application of different doses of circRNAs in WT *A. thaliana* protoplasts. Protoplast transfection was carried out with different amounts of circRNAs starting from 1µg to 8 µg at the same time point of 18 hours. Control protoplasts were used without any circRNAs. Values under each band indicated the amount of remaining proteins as a percentage. An anti-Actin antibody was used as an internal loading control. The GFP protein band always appeared in a minute at ~26.9 kDa, whereas the Actin band appeared in between 10 to 15 minutes at ~45 kDa. The ratio of GFP**:**Actin shows the effect of protein reduction in the co-transfection process.

3.10 The impact of sequence-specific circRNA$_{GFP}$ compared to linRNA$_{GFP}$ on GFP

To investigate the inhibitory effect of circRNA in protein accumulation over time, we conducted a time-course experiment. This experiment would enable us to track protein inhibition levels at multiple time points throughout the protein inhibition process by circRNAs and their non-circularized linear form. To this end, the following experiments were conducted in three different time points starting from 10 h, 18 h, which was a standard time point for all the previous experiments, and 32 h as an ending time point. We used two different types of antisense RNA, circular RNA (circRNA$_{GFP}$) and linear RNAs (linRNA$_{GFP}$). linRNA$_{GFP}$ has the same nucleotide sequence and is single stranded. They are not circularized but contain the same antisense sequence-like activity.

The inhibition of GFP accumulation by circRNA$_{GFP}$ took place at all time points, even in 10 h and lasting until 32 h after co-transfection (Fig. 23). On the other hand, linRNA$_{GFP}$ showed a slight reduction in the protein level at 10 h time point but the reduction effect got lost over the time (Fig. 23). Taken together, our results showed that circRNA$_{GFP}$ exerted a stronger form-

specific effect on the accumulation of GFP protein compared to the linRNA$_{GFP}$. Consequently, our findings provide a hint that circRNA is superior to linear RNA in the antisense targeting of plant genes.

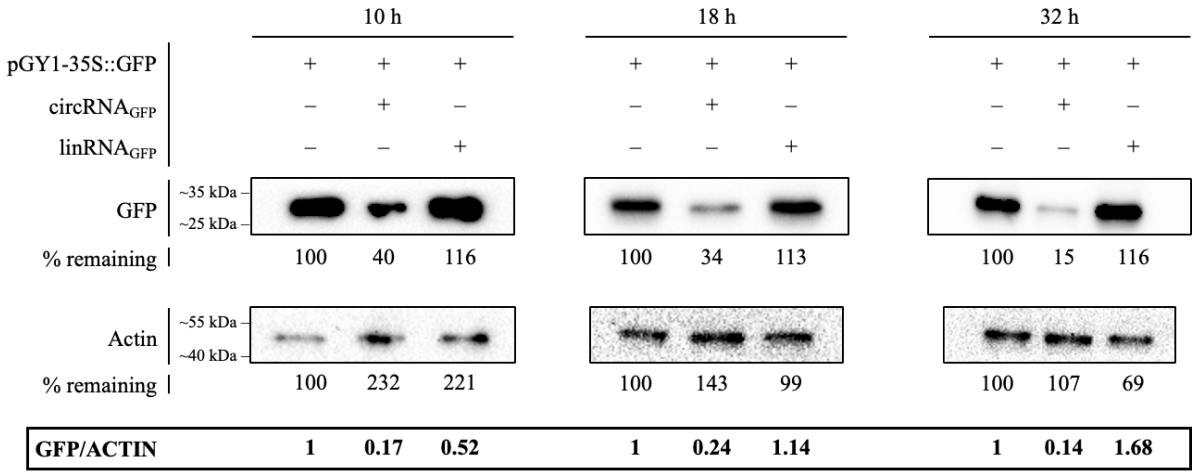

Figure 23: Time-course of antisense activity of designated circRNAs against the GFP protein. *A. thaliana* (WT) protoplasts were co-transfected with plasmid and antisense circRNA$_{GFP}$ or its linear counterpart (linRNA$_{GFP}$) individually. Three individual experiments were conducted at different time points such as 10 h, 18 h, and 32 h. As a loading control, an anti-Actin antibody was used. The ratio between the GFP and Actin represents the downregulation of protein content at different time points. At each time point, protoplasts cotransfected with only plasmid (pGY1-35S::GFP), plasmid (pGY1-35S::GFP) with antisense circRNA$_{GFP}$, and antisense linRNA$_{GFP}$ with a plasmid (pGY1-35S::GFP) represented at the loading well from left to right.

3.11 Topical application of circRNA$_{GFP}$ in *GFP*-expressing *Arabidopsis thaliana*

Until now, besides CRISPR/Cas9, the application of dsRNA is one of the effective methods to silence endogenous genes in different plants. By exploting RNAi methods, genes can be downregulated using dsRNA, as well as siRNA. However, the method is already getting challenging due to poor uptake, degradation and as well as lack of efficient delivery strategies (Nitnavare et al. 2021). Due to the longer half-life, and design specificity circRNA provides advantages over the dsRNA (Patop et al. 2019; Pfafenrot et al. 2021). Similarly, to the direct application of dsRNA, circRNA could be used as a significant tool for protein inhibition. Consequently, we set an experiment to test the effect of antisense circRNA against endogenously expressed *GFP* in *A. thaliana* (*AtW33*) (Harvey et al. 2022).

Two different types of RNA, $dsRNA_{GFP}$ and $circRNA_{GFP}$ were applied to plant leaf to target the *GFP* gene for the inhibition of protein expression. As a consequence, dsRNA was prepared without any off-target effect by using bioinformatic approaches. Both RNAs were applied along with their negative controls, including an intronic $dsRNA_{Clp\text{-}1}$ and $circRNA_{CTR1}$ into the leaf surface. In the experimental procedure, we applied 10 µg of $dsRNA_{GFP}$ as well as the same amount of $circRNA_{GFP}$ in the plant leaf separately as a drop inoculation (Fig. 24). Several controls were used for this experiment including the water control (dH_2O).

Figure 24: Direct application of dsRNA and circRNA against the endogenous gene *GFP*. From left to right, dH_2O (control), intronic $dsRNA_{Clp\text{-}1}$ derived from an intron contained in the *Verticillium longisporum Clp-1* gene (control), $dsRNA_{GFP}$, $circRNA_{CTR1}$ (control), and $circRNA_{GFP}$ were applied as a drop onto the leaf surface. The amounts of RNAs were consistently 10 µg in each inoculation. To support the leaf, parafilm paper was used. After 48 h, plant leaves were collected for further microscopic analysis.

3.12 Microscopic image analysis after topical application of different types of RNAs

After 48 hours of treatment, the plants were directly observed under the microscope to check the initial effect of dsRNAs and circRNAs. By using the GFP filter, there was no particular difference observed throughout the leaf surface (Fig. 25). Therefore, further analysis proceeded to check the direct effect of different RNAs on the protein biosynthesis process.

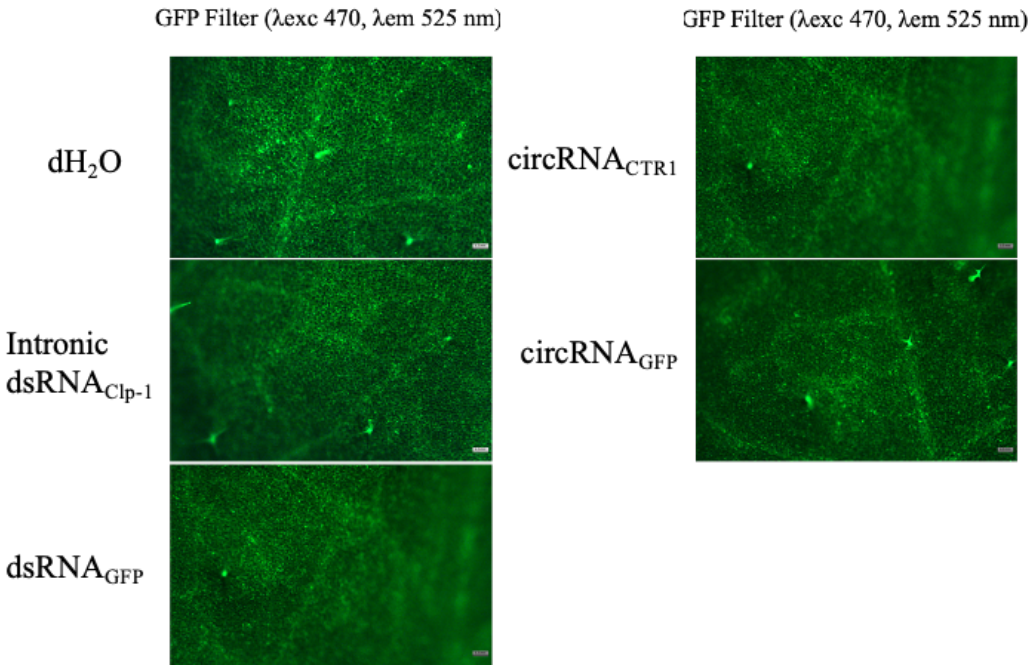

Figure 25: Observation under the microscope for downregulation of GFP. The images were captured from the side of inoculation under a *GFP* filter ranging from 470 nm (λexc) to 525 nm (λem). dH_2O control, intronic $dsRNA_{Clp-1}$, $daRNA_{GFP}$ (on the left side), $circRNA_{CTR1}$, and $circRNA_{GFP}$ images don't show any significant differences under the GFP filter.

3.13 Immunoblotting analysis of the reduction in foliar GFP accumulation

At 48 hours of drop inoculation, samples were collected for total protein extraction. To characterize the accumulation of GFP protein, all the samples went through immunoblotting analysis. From the immunoblotting analysis, we observed that $circRNA_{GFP}$ treatment did not lead to a reduction in foliar GFP accumulation (Fig. 26). Similarly, drop-treatment of leaves with 10 µg of 476 bp GFP dsRNA or with 10 µg of 431 bp Clp-1 dsRNA are serving as controls along with another two controls dH_2O and $circRNA_{CTR1}$. Due to the sequence specificity of $dsRNA_{GFP}$ and $circRNA_{GFP}$, there is a possibility that RNAs will show inhibitory effect on GFP accumulation. However, the unspecific controls should not show any effect on GFP protein accumulation on the foliar application.

Taken together, this result denotes that both types of RNA did not show any huge changes in the GFP expression pattern, only a slight reduction was observed with $circRNA_{GFP}$ (Fig 26). Although more experiments are needed to investigate this slight reduction by sequence-specific antisense circRNA.

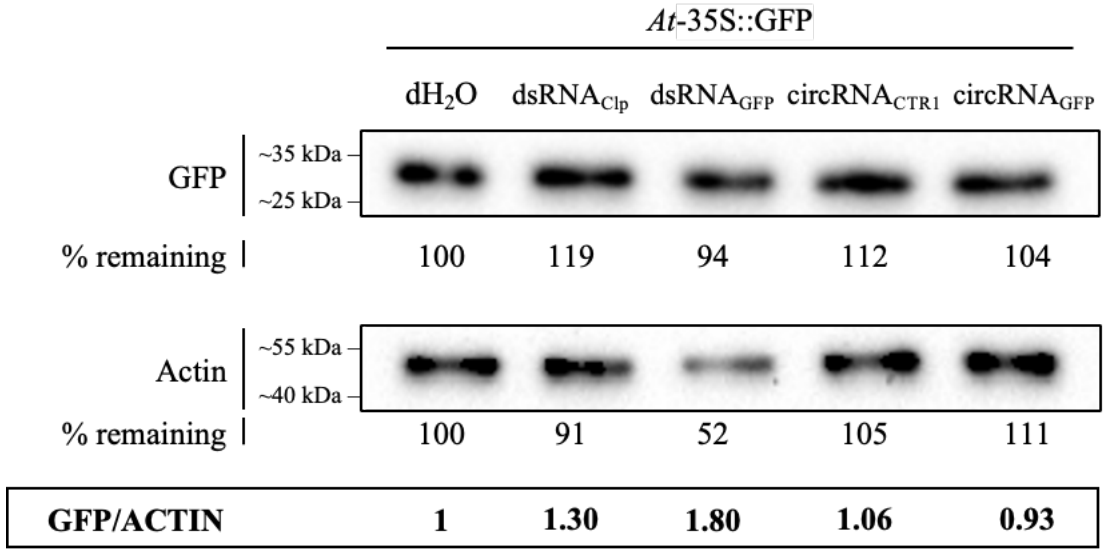

Figure 26: Protein accumulation after 48 h of drop treatment with dsRNA and circRNAs. Three-week-old *A. thaliana* expressing *GFP* leaves were inoculated by droplets containing10 µg of $circRNA_{GFP}$ and $dsRNA_{GFP}$, to inhibit the GFP protein accumulation, alongside dH_2O and non-targeting controls $circRNA_{CTR1}$ and $dsRNA_{Clp-1}$. All the samples were collected at 48 hours for immunoblotting analysis. As a loading control, an anti-Actin antibody was utilized. The percentage of GFP reduction and the ratio of GFP protein accumulation (expressed as the ratio between GFP and Actin signals) is indicated below each band.

3.14 Additional approach to investigate the GFP inhibition by antisense circRNAs

For further investigation, it was necessary to generate a plasmid that can simultaneously express *GFP* and *RFP*. This dual reporter system can measure the GFP inhibition which is normalized to the RFP contained in the same plasmid. The simultaneous expression of dual reporter systems in the same protoplast would provide better information about the transfection efficiency, based on the GFP and RFP expression ratio.

Here, we have demonstrated the co-transfection of protoplast using $circRNA_{GFP}$ and the plasmid (pGY1-35S::GFP:RFP) by following the previous method. The results showed less GFP fluorescence in the sample co-transfected by $circRNA_{GFP}$ in microscopic image analysis (Fig. 27). The graph illustrates the reduction of GFP expression in the $circRNA_{GFP}$-treated sample compared to the plasmid control (pGY1-35S::GFP:RFP) and also showed a significance GFP fluorescence reduction compared to the non-specific control ($circRNA_{CTR1}$).

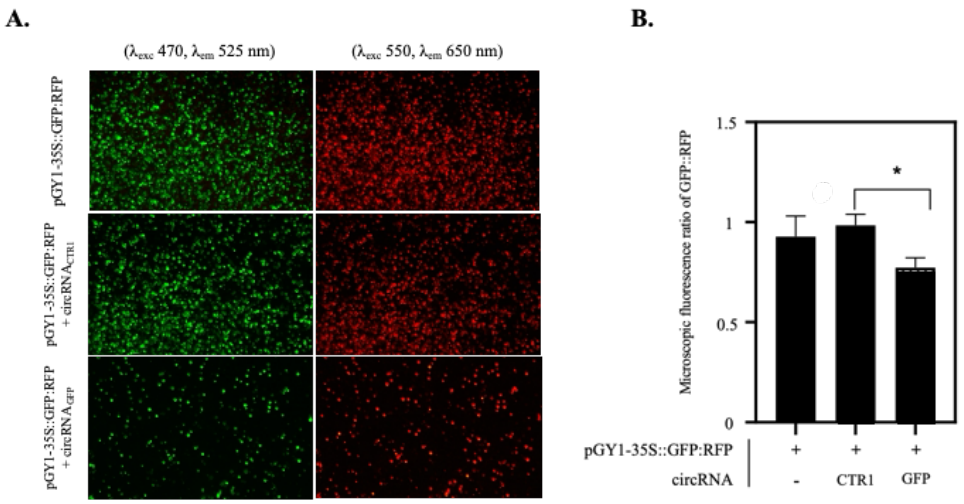

Figure 27: Microscopic image analysis of the *GFP* and *RFP* expression ratio of *Arabidopsis thaliana* protoplasts after co-transfection. (A) The transfection of protoplast was performed with 20 µg of plasmid pGY1-35S::GFP:RFP, and co-transfected with the same amount of plasmid and 4 µg of antisense $circRNA_{GFP}$. As an additional control, co-transfection of protoplast with 20 µg pGY1-35S::GFP:RFP and 4 µg of $circRNA_{CTR1}$ was performed. (B) The fluorescence ratio between GFP (λexc 470, λem 525 nm) and RFP (λexc 550, λem 650 nm) was calculated using microscopic images and then analyzed using ImageJ software. The bar represents the measurement of SEM (Standard Error of Mean) based on different images taken from three various spots. Statistical analysis was conducted using t-test, where '*' denotes $p \leq 0.05$ significance to the $circRNA_{CTR1}$-treated protoplasts.

4. Discussion

4.1 Synthesis and designing of antisense circRNA (circRNA$_{GFP}$)

Apart from the presence of circRNAs within mammalian cells, it can be synthesized artificially *in vitro*. In general, there are three main approaches for producing circRNAs in a system that doesn't involve cells. These methods comprise chemical techniques (such as cyanogen bromide treatment), enzymatic processes (employing enzymes RNA or DNA ligases), and ribozymatic methods (utilizing self-splicing introns). These procedures have been discussed in detail in previous publications (Beaudry & Perreault 1995; Petkovic & Müller 2015; Wesselhoeft et al. 2018).

The use of exogenous circRNA for plant systems is less studied. To our knowledge, there is only another study by Zhang et al. (2021) about antisense circRNA against RuBisCO. Therefore, in this study, we specifically utilized antisense circRNA (AS-circRNA) to impede the translation of green fluorescent protein (*GFP*). Our target was the Open Reading Frame (ORF) region. We identified this region by bioinformatical analysis as one of the effective target sites for circRNA interference. ORF holds a very important role due to its sequence and structural significance, integral to the plant life cycle. It has also been reported that the ORF region is recognized as a crucial target for designer antisense circRNA according to the previous report (Pfafenrot et al. 2021).

Through the utilization of AS-circRNAs directed at distinct ORF regions of the *GFP* gene. It has been noted that the target sequence of our antisense circRNA (circRNA$_{GFP}$) is highly efficient in the binding process with *GFP* mRNA due to the sequence complementarity. To establish a potential tool for selectively targeting plant genes with exogenous RNA, we synthesized a circRNA specifically targeting the ORF of a *GFP* reporter gene (Fig. 5). The selection of antisense sequences was identified by a secondary structure model of the ORF region (Fig. 6) and their mRNA accessibility (Fig. 7), resulting in the preparation of an artificial 50 nucleotide antisense circRNA (circRNA$_{GFP}$). This artificially generated circRNA contained a 30-nucleotide anti-GFP sequence with perfect complementarity and 20 nt of backbone. As a control, one non-specific circRNAs with randomized sequences of comparable length were synthesized (Fig. 8).

4.2 The influence of antisense circRNA$_{GFP}$ on fungal protoplast co-transfection

Gene silencing method based on RNAi has been used since the beginning of the 21st century to study gene functions in different organisms and has been shown a great achievement in plant protection against fungal species (Abdurakhmonov et al. 2016; Nguyen et al. 2008; Majumdar et al. 2017).

In this study, protoplasts have been isolated from a necrotrophic fungal species known as *Botrytis cinerea*. With a combination of different enzymes, we achieved an efficient production of the fungal protoplasts (Fig. 9). Several studies have reported on fungal protoplast transfection by using different techniques for various purposes (Ish-Shalom et al. 2011; Turgeon et al. 2010). The purpose of our transfection was to study the expression and protein inhibition in *B. cinerea* protoplasts by co-transfection method using antisense circRNA and a GFP-expressing plasmid. The transfection process allowed the expression of the reporter gene, which could be detected based on its expression level in the protoplast culture (Fig. 10 and 11). However, the transfection efficiency must be higher to achieve the desired experimental success (Wubie et al. 2014). In this study, we used two different plasmids (Fig. 04A, and 04B) to determine the transfection rate. Afterward, based on the higher rate of transfection (Fig. 10 and Fig. 11) we selected the plasmid pBGgHg-pgpd::GFP (Fig. 04B) for further experiments. Plasmid pBGgHg-pgpd::GFP contained GFP, which can express properly through the fungus transfection process (Chen et al. 2000). By using the selected plasmid for the co-transfection process, it was noteworthy to notice that the GFP proteins were expressed properly in the protoplast system (Fig. 10).

Protoplasts from *B. cinerea* were co-transfected with the desired plasmid and antisense circRNA$_{GFP}$ by using PEG (Polyethyleneglycol). After transfection, it was observed that the GFP protein expressed at 24 h. A higher amount of GFP protein expression was observed after 72 hours (Fig. 11). It's important to notice that the regeneration time of *B. cinerea* protoplasts is very fast (Pollastro et al. 1995). The regeneration of protoplasts is a critical stage and serves as the primary constraining element after post-transfection (Rehman et al. 2016). However, in this experiment, the fungal protoplast was regenerated from 10 h of post-transfection by growing small mycelia and also contained huge mycelial debris. Then the immunoblotting of the fungus sample was performed 72 h later of co-transfection using antisense circRNA. From the immunoblotting, it was confirmed that the GFP protein was not expressed as expected in the transfected or co-transfected protoplasts (Fig. 12). There are several possible reasons, among them, the most important was transfection efficiency. The rate of transfection was low as found in the microscopic analysis (Fig. 10 and 11). The size of the plasmid also has a crucial

impact on the efficiency of transfection and expression of the *GFP* gene. Earlier research suggested that enlarging the plasmid's size leads to a reduction in transfection efficiency in the fungal system (Chan et al. 2002; Ohse et al. 1995). Another reason could be the codon optimization of the GFP protein expression in fungal protoplasts. Based on these results, it was noticed that the use of antisense circRNA against the fungal protoplast was not an ideal way to investigate the effect of antisense activity of circRNAs.

It is crucial to acknowledge that the efficiencies observed in our study are dependent upon fungal protoplast transfection efficiency in our specific culture conditions. Our fungal protoplast transfection rate is very low (Fig. 11). Therefore, the experimental conditions of circRNA transfection and the *in vitro* stabilities of circRNA should be further enhanced through systematic optimization of circRNA delivery, evaluation of backbone sequences and structure, or the incorporation of RNA modifications or peptide conjugation.

4.3 Effect of antisense circRNA (circRNA$_{GFP}$) on Arabidopsis protoplast co-transfection

There is plenty of evidence on the initiation of gene expression in the plant protoplast by transfection (Bart et al. 2006; Jiang et al. 2010; Cao et al. 2014). Transient expression systems using plant protoplasts have also been built and developed in numerous non-model plant species that lack established transfection methods or face challenges in producing transgenic plants through regeneration (Sheen. 2001; Fraiture et al. 2014). In this study, we focused on how antisense circular RNA affects the cellular system, particularly its ability to inhibit the expression of a target gene. Based on the recent publication (Pfafenrot et al. 2021), we applied the idea of antisense circRNA against GFP targeting their coding ORF region in a versatile protoplast co-transfection system. Based on predictive structural models, we have identified a specific effective target region for antisense circRNA in the *GFP* sequence. Notably, the antisense circRNA demonstrated strong interference with protein expression, resulting in an approximate reduction of 40% in GFP protein expression according to microscopic analysis of red (total protoplast) vs green pixels (Fig. 13). Furthermore, the protoplast co-transfected with antisense circRNA$_{GFP}$ showed a significant inhibitory effect on the GFP expression level (Fig. 16A). In the microscopic images for the red vs. green pixel analysis, we observed less GFP expression in the circRNA$_{GFP}$ treated sample after 18 h of co-transfection (Fig.13, Fig.14, Fig.15). Our results indicated that the reduction of protein content is always similar in diverse experimental setups. We next wondered whether GFP inhibition was due to the RNAi mechanism. Therefore, we continued with various Arabidopsis mutant analyses, especially with Δ*Atago1* and Δ*Atdcl1*. The mutants *ago1* and *dcl-1* lack RNAi activity. However,

similarly to the WT, we found the same type of GFP reduction in the mutant protoplasts lacking these important RNAi components (Fig. 16A,16B, and 16C). These mutant plants also showed 49% (*ago1*) and 57% (*dcl1*) GFP protein reduction in their co-transfection with antisense circRNA (circRNA$_{GFP}$) compared to the plasmid control and control circRNA$_{CTR1}$ (Fig. 16). We observed that the GFP protein in two mutant lines (*ago1* and *dcl1*) was reduced in the same way as the GFP reduction in WT plants protoplast after co-transfected with circRNA$_{GFP}$. Additionally, we also conducted another immunoblotting experiment using three more mutant lines such as *dcl2,3,4, ago2-1,* and *ago4-1*. We also noticed the same type of protein reduction in the mutant protoplasts after co-transfection with plasmid and circRNA$_{GFP}$. Our results suggest that the circRNA$_{GFP}$ reduced the GFP protein abundance in a sequence-specific manner whereas the circRNA$_{CTR1}$ did not show any kind of GFP protein reduction.

4.4 Antisense circRNA$_{GFP}$ inhibits protein biosynthesis independent of the RNAi process

RNAi is an important process in plants and other organisms that impedes gene expression at both transcriptional and post-transcriptional levels. Previously, several mechanisms of RNAi have been extensively studied which are involved in the regulation of gene expression within cellular systems (Fjose et al. 2001; Agrawal et al. 2003; Rosa et al. 2018). This process utilizes three main groups of proteins to defend against pathogenic invasion (Muhammad et al. 2019; Borges et al. 2015). RNAi involves the production of small RNA molecules, typically 20 to 26 nucleotides long, through key components like DCL (Dicer-like protein), AGO (Argonaute protein), and also RDRs (RNA-dependent RNA polymerase). DCL proteins generate sRNAs from dsRNA precursors, incorporating them into RNA-induced silencing complexes (RISCs) (Vaucheret 2006). These sRNAs, classified as either siRNAs or microRNAs (miRNAs), guide AGO proteins within RISCs to impact DNA methylation, endonuclease activity, or translational suppression of mRNAs. RDR enzymes synthesize dsRNAs from single-stranded RNAs (ssRNAs), serving as templates for further RNAi activity by Dicer-like proteins in the plant cells (Baulcombe 2004; Park et al. 2021).

It has already been reported that plenty of techniques are involved to mitigate the risk of disease in plants using RNAi against viruses, fungal diseases, insects, and nematodes (Mitter et al. 2017; Koch et al. 2016; Jain et al. 2021). Exogenous dsRNA, clay nanoparticle-based dsRNA delivery, and even high-pressure sprays of dsRNA have fully or partially achieved the goal of protein or gene inhibition in recent decades (Das et al. 2020; Yong et al. 2022; Koch et al. 2016; Dalakouras et al. 2016). Still, some controversies and challenges exist about the exact

location and the action of dsRNA in the cellular system. Apart from that, alternative techniques are getting the attention of scientists to inhibit particular protein expression. In our study, we investigated the effect of antisense circRNA$_{GFP}$ as a dsRNA alternative. Likewise, we wanted to show the effect of antisense circRNA$_{GFP}$, and how it interferes with the GFP protein expression in plant protoplast.

To explore the mechanism, we used the Arabidopsis plant protoplast from mutant lines *ago1-27* and *dcl1-11*. Here, the mutant lines are defective or lack a particular function and have pleiotropic developmental and morphological deficiencies. Initially, we found that antisense circRNA$_{GFP}$ cannot downregulate the *GFP* transcript in the wild type and two Arabidopsis mutants after protoplast co-transfection (Fig. 18A,18B, and 18C). However, we noticed that the wild-type and mutant plants revealed protein reduction in the previous experiment (Fig. 16A, 16B, and 16C).

Additionally, we also tested another three mutant lines to explore the effect of antisense circRNA$_{GFP}$ in the mRNA level. After analyzing all possible ways, we found the same kind of results in our experiments where antisense circRNA$_{GFP}$ doesn't show any mRNA downregulation in the mutant lines *dcl2,3,4, ago2-1*, and *ago4-1*.

Our experiments with Arabidopsis *DCL* and *AGO* mutants, including ago1-27, *dcl1-11, dcl2,3,4, ago2-1,* and *ago4-1*, strongly suggest that the reduction in GFP protein in protoplast co-transfection is not associated with RNAi. Our results consistently revealed no significant downregulation of *GFP* transcripts in both wild type and the additional *DCL* and *AGO* mutant lines protoplasts (Fig. 18, Fig. 19). We can conclude that antisense circRNA$_{GFP}$ modulates GFP protein levels at the translational level in a nucleotide sequence-specific manner, but independent of RNAi activity. Antisense circRNA$_{GFP}$ clearly showed a blockage-type effect against *GFP*. Moreover, this mechanism showed the same type of blockage mechanism observed in the circRNA-induced inhibition of coronavirus proliferation in a cell culture system (Pfafenrot et al. 2021).

4.5 Impact of different amounts of circRNAs on GFP protein accumulation

Consistent with the efficiency of antisense circRNA$_{GFP}$ in WT and mutant plant co-transfection experiments, we have applied different circRNA concentrations in the experimental process. In these experiments, we aimed to investigate the minimal doses of circRNA, at which a reduction of GFP can occur.

Our results showed that circRNA activity is very specific since circRNA$_{CTR1}$ didn't show any significant inhibition even in higher doses on the GFP expression (Fig. 20, Fig. 21, Fig. 22).

On the other hand, antisense circRNA$_{GFP}$ exhibited a reduction in GFP protein accumulation, when applied in higher amounts during the co-transfection process (Fig. 22). In addition, despite the high concentration of circRNAs, we found as lower as 2 µg of antisense circRNA$_{GFP}$ efficiently inhibited the GFP protein until 30% of *Arabidopsis thaliana* protoplasts. The efficient downregulation of GFP protein was closely comparable when using 8 µg, as observed with 4 µg (Fig. 22). Additional studies involving the microscopic analysis also strongly support the immunoblotting analysis (Fig. 20, Fig. 21). Furthermore, we also demonstrated the inhibitory potency of the linear and circular versions of antisense sequences against GFP. Following a 10 h treatment of protoplasts with circRNA$_{GFP}$, we observed a significant decrease in GFP protein levels, reaching up to 83%, whereas linRNA$_{GFP}$ exhibited a reduction of up to 48% (Fig. 23). Notably, at later time points, circRNA$_{GFP}$ sustained its potent inhibitory activity on GFP accumulation in comparison to protoplasts treated with the control (circRNA$_{CTR1}$), while its linear counterpart no longer exhibited inhibitory effects. This enduring inhibitory effect of circRNAs is likely attributed to their high metabolic stability compared to linear forms, rendering them more resistant to exonuclease degradation. Here, it has been proved that the use of antisense circRNA$_{GFP}$ is superior to the linear antisense RNA against the same target region (Fig. 23).

This is probably because circular RNAs tend to have a relatively strong resistance to metabolic stability. Moreover, the individual structural features and limitations that influence how the complementary sequence is presented in a circular arrangement might also play a role in the effectiveness of antisense circRNA (Pfafenrot et al. 2021).

We used different time points for collecting data to gather information on the duration and sequence of events related to the phenomenon of circRNA activities. This aids in developing a more complete understanding of the underlying mechanisms of our circRNAs. We conducted the time course experiment at three different time points. Except for the standard time point of 18 h, others showed a different kind of activity of antisense circRNA$_{GFP}$. We found antisense activity already at the 10 h time point, while 32 h later the antisense activity also showed protein inhibition. After 32 h bacterial contamination of the protoplast medium is a risk, and eventually, protoplasts continue to burst. However, we conducted co-transfection experiments using antisense circRNA$_{GFP}$ and antisense linRNA$_{GFP}$, which confirmed the inhibitory effect is diverse at various time points.

4.6 Topical application of circRNAs against endogenously expressed *GFP* gene of *A. thaliana*

After the successful implementation of antisense circRNA$_{GFP}$ against GFP in the *in-vitro* system, we also applied the same antisense circRNA$_{GFP}$ against endogenously expressed GFP protein topically on the leaf of *A. thaliana*. In this topical application dsRNAs and circRNAs were directly put onto the plant leaves for local gene silencing without any special preparation or additional tools (e.g., without any kind of mechanical elements or steps to pressurize the RNAs). This type of application is also regarded as an environmentally friendly approach, where RNAs can degrade in the environment over time after a specific function. One of the advantages of this technique is to avoid the lethal effect on the whole plant. It's also relatively quicker than the other existing methods which provides faster results in 48 h of post-inoculation. Moreover, the application of RNA directly onto the plant leaves to target plant endogenous genes shows difficulty in entering plant cells due to the necessity of overcoming various barriers, which include plant cuticles, cell walls, etc. Moreover, the application of RNA directly onto plant leaves to target endogenous genes poses challenges in entering the cellular system (Bennett et al. 2020). Apart from that, there is successful application of dsRNA has already been reported recently in the insect from plants (Pampolini et al. 2023). Recently reported by Delgado-Martín et al. showed the successful application of dsRNA against the control of the virus in cucurbits (Delgado-Martín et al. 2022). Those applications of dsRNA gave us a hint to apply antisense RNAs against endogenous genes in our experiment.

The *A. thaliana GFP* reporter line Δ*At-35SGFP* (L-W33) has been extensively used for the study of protein inhibition using antisense circRNAs. The plant line Δ*At-35SGFP* (L-W33) is a highly *GFP*-expressed line, where the GFP protein can be expressed all over the leaf in every plant sample (Harvey et al. 2022). After initial visualization by a microscope, all the plant sample was selected for the further application of dsRNA and circRNAs. In this study, we were trying to reduce the gene expression on a local silencing basis where antisense RNA was applied as a drop inoculation method without harming the leaf mechanically or chemically. With further microscopic study, we observed that the *GFP* silencing was not visible as expected after 48 h of the experimental setup (Fig. 24 and Fig. 25). Then we continued with the immunoblotting with our control (dH_20) and RNA applicated plant sample to observe the activity of antisense circRNA$_{GFP}$ as well as the effect of antisense dsRNA$_{GFP}$ on *GFP* expressed leaf. We didn’t notice any significant reduction of foliar GFP accumulation under in-vivo conditions. Even though we haven’t seen any systemic downregulation of GFP protein all over the plant leaf surface. However, we noticed a slight tendency of less GFP protein using the

antisense circRNA$_{GFP}$ (Fig. 26). From our experiment, it is still unclear why GFP was not reduced by exogenous circRNA application. One reason could be that the *GFP* under the 35S promoter is expressed too strongly in the *A. thaliana* plant (Niedz et al. 1995). Also, the exogenous application of dsRNA results in its accumulation in the xylem (Liu et al. 2021). Consistent with this, when dsRNA is applied to leaves and enters through the petioles, it leads to the accumulation of RNA in the xylem tissues only (Dalakouras et al. 2018, 2020). It is widely acknowledged that the absorption of large molecules from xylem tissue involves exo/endocytosis mechanisms (Botha et al. 2008; Słupianek et al. 2019). When considering all these findings taken together, it appears that the high-level expression of certain *GFP* genes is a critical characteristic that hinders the effective local silencing in the *ΔAt-35SGFP* (L-W33) line when initiated using the drop inoculation method.

In summary, our experiment provides a hint that other mechanical delivery methods for example high-pressure sprays or formulations of RNAs may be required to facilitate the effective circRNA or dsRNA entry inside the plant cells.

4.7 Dual reporter system to confirm the interaction between circRNA and *GFP*

The question arose about the mechanism of protein inhibition of GFP by antisense circRNAs. To investigate the inhibitory process, we have introduced a dual-reporter system that can evaluate the mechanism of the inhibition process. The dual reporter system carries two different genes *RFP* (Red fluorescence protein) and *GFP* (Green fluorescence protein) in the same plasmid (pGY1-35S::GFP:RFP). After co-transfection with antisense circRNA$_{GFP}$, we noticed the reduction of *GFP* expression by analyzing the GFP and RFP expression ratio (Fig. 27). Due to the same size of the *RFP* and *GFP*, we could not confirm GFP protein inhibition by immunoblotting. In a nutshell, our dual-reporter system only provides information based on the ratio of GFP and RFP expression. From the GFP and RFP expression ratio, it was confirmed that the antisense circRNA$_{GFP}$ reduced the GFP expression in the protoplast co-transfection process in a sequence-specific manner. In the future, it's necessary to improve the immunoblotting system to enable precise measurement of protein inhibition by analyzing the concentration of the protein samples.

4.8 Conclusion and Future Outlook

My Ph.D. project aimed to investigate the role of artificially designed antisense circRNA$_{GFP}$ in the protein biosynthesis process. To achieve this, we used the transient transfection system with protoplasts to investigate protein biosynthesis in plants and fungi. We also attempted to determine the binding process or mechanism by using the dual reporter system. We showed that the antisense circRNA$_{GFP}$ successfully inhibits the expression of the GFP target protein in *Arabidopsis thaliana* and its RNAi mutant's protoplasts. We also discovered that it is possible to reduce protein accumulation independent of the RNAi machinery through a co-transfection process in protoplasts.

Furthermore, we also investigated the activity of antisense circRNA$_{GFP}$ in the fungal protoplast system. We noticed that antisense circRNA$_{GFP}$ doesn't show any protein inhibition in the *Botrytis cinerea* protoplast co-transfection process. This could happen due to its transfection efficiency. Moreover, fungi are very fast growing in the artificial medium. Due to its complex co-transfection system, it's not an ideal way to observe the antisense activity of circRNA$_{GFP}$ in fungal protoplasts. Alternatively, direct topical application is also not a proper way to conduct experimental procedures in plants due to its limited efficiency. This research serves as a foundation for understanding the function of the initial aspects of antisense circRNA$_{GFP}$ in the plant protoplast co-transfection process. Such insights could potentially enhance our understanding of how antisense circRNA can be used in the future for plant protection independent of RNAi.

5. Summary

As single-stranded molecules, circRNAs have gathered increasing attention in recent years due to their distinct covalently closed circular structure. In mammalian cells, circRNAs are recognized for their diverse functional roles, contributing to the intricate regulation of gene expression and protein function. Emerging evidence also suggests that circRNAs play special roles in plants, influencing plant development, providing resistance against biotic stress, and enhancing tolerance to abiotic stress.

Our study aimed at addressing a relevant agricultural question: is it possible to apply exogenous circRNAs to regulate endogenous plant proteins or genes in a sequence-specific manner? We conducted experiments using *GFP*-expressing Arabidopsis protoplasts and found that treatment with a designer 50-nt *GFP* antisense circRNA (circRNA$_{GFP}$) resulted in a dose-dependent reduction in the cellular accumulation of the reporter protein. Interestingly, the corresponding sequence-identical linear form of the circRNA (linRNA$_{GFP}$) had no apparent effect on protein reduction. Importantly, the inhibitory activity of circRNA$_{GFP}$ persisted even in Arabidopsis ARGONAUTE and DICER-like mutants with impaired RNAi pathways. The results prompt consideration of the potential for circRNAs to influence the regulation of endogenous plant genes, suggesting a potential application as a bioherbicide in the future. Expanding our investigation, we extended the application of antisense circRNA$_{GFP}$ to pathogenic fungi, specifically *Botrytis cinerea*, to explore its impact on reporter GFP accumulation in this fungus and explore the possibility of using circRNA as a fungicide.

In sum, my study contributes to the emerging understanding of the versatile roles of antisense circRNAs on both fungal and plant systems, shedding light on their potential applications in agriculture for targeted gene regulation and crop protection.

6. Zusammenfassung

Als einzelsträngige Moleküle haben zirkuläre RNAs (circRNAs) aufgrund ihrer ausgeprägten kovalent geschlossenen zirkulären Struktur in den letzten Jahren zunehmend an Aufmerksamkeit gewonnen. In Säugetierzellen sind circRNAs für ihre vielfältigen funktionellen Aufgaben bekannt, die zur Regulierung der Genexpression und der Proteinfunktion beitragen. Neue Erkenntnisse deuten darauf hin, dass circRNAs in Pflanzen eine besondere Rolle spielen, indem sie die Pflanzenentwicklung beeinflussen, Resistenz gegen biotischen Stress vermitteln und die Toleranz gegenüber abiotischem Stress erhöhen.

Ziel unserer Studie war es, eine für die Landwirtschaft relevante Frage zu klären: Ist es möglich, exogene circRNAs einzusetzen, um die Produktion von endogenen Pflanzenproteinen auf sequenzspezifische Weise zu regulieren? Wir haben Experimente mit GFP-exprimierenden Arabidopsis-Protoplasten durchgeführt und festgestellt, dass die Behandlung mit einem Designer 50-nt-GFP-Antisense-circRNA ($circRNA_{GFP}$) zu einer dosisabhängigen Verringerung der zellulären Akkumulation des Reporterproteins führt. Interessanterweise hatte die lineare Form der circRNA ($linRNA_{GFP}$) keine offensichtliche Auswirkung auf die Proteinbildung.

Wichtig ist, dass diese hemmende Wirkung von $circRNA_{GFP}$ sogar in Arabidopsis ARGONAUTE und DICER-ähnlichen Mutanten mit beeinträchtigten RNAi-Wegen erhalten bleibt. Die Ergebnisse regen dazu an, das Potenzial von circRNAs zur Beeinflussung endogener Pflanzengene in Betracht zu ziehen, und auf eine mögliche künftige Anwendung als Bioherbizid zu analysieren. In Erweiterung unserer Untersuchung haben wir die Anwendung von Antisense-$circRNA_{GFP}$ auf pathogene Pilze, insbesondere *Botrytis cinerea*, ausgedehnt, um ihre Auswirkungen auf die transiente GFP Akkumulation in den Protoplasten zu untersuchen.

Diese Studie trägt zum wachsenden Verständnis der vielseitigen Rolle von Antisense-circRNAs, sowohl in Pilz-, als auch in Pflanzensystemen bei. Sie weist auf eine potenziellen agronomische Anwendungen von circRNA zur gezielten Genregulierung in Kulturpflanzen und damit zur Anwendung im Pflanzenschutz.

7. References

Abdurakhmonov, I. Y., Ayubov, M. S., Ubaydullaeva, K. A., Buriev, Z. T., Shermatov, S. E., Ruziboev, H. S., Shapulatov, U. M., Saha, S., Ulloa, M., Yu, J. Z., Percy, R. G., Devor, E. J., Sharma, G. C., Sripathi, V. R., Kumpatla, S. P., van der Krol, A., Kater, H. D., Khamidov, K., Salikhov, S. I., Jenkins, J. N., Abdukarimov, A. and Pepper, A. E. (2016) RNA Interference for Functional Genomics and Improvement of Cotton (Gossypium sp.). Frontiers in plant science 7, 202.

Abe, N., Matsumoto, K., Nishihara, M., Nakano, Y., Shibata, A., Maruyama, H., Shuto, S., Matsuda, A., Yoshida, M., Ito, Y., & Abe, H. (2015). Rolling Circle Translation of Circular RNA in Living Human Cells. Scientific Reports, 5(1), 1–9.

Agrawal, N., Dasaradhi, P. V. N., Mohmmed, A., Malhotra, P., Bhatnagar, R. K., & Mukherjee, S. K. (2003). RNA interference: biology, mechanism, and applications. Microbiology and molecular biology reviews, 67(4), 657-685.

Alder, M. N., Dames, S., Gaudet, J., & Mango, S. E. (2003). Gene silencing in Caenorhabditis elegans by transitive RNA interference. Rna, 9(1), 25-32.

Alexander, P., Brown, C., Arneth, A., Finnigan, J., Moran, D., & Rounsevell, M. D. (2017). Losses, inefficiencies and waste in the global food system. Agricultural systems, 153, 190-200.

Amselem, J., Cuomo, C. A., van Kan, J. A., Viaud, M., Benito, E. P., Couloux, A., & Dickman, M. (2011). Genomic analysis of the necrotrophic fungal pathogens Sclerotinia sclerotiorum and Botrytis cinerea. PLoS genetics, 7(8), e1002230.

Araújo, A. E., Maffia, L. A., Mizubuti, E. S., Alfenas, A. C., Capdeville, G. D., & Grossi, J. A. (2005). Survival of Botrytis cinerea as mycelium in rose crop debris and as sclerotia in soil. Fitopatologia Brasileira, 30, 516-521.

Arnaiz, E., Sole, C., Manterola, L., Iparraguirre, L., Otaegui, D., & Lawrie, C. H. (2019). CircRNAs and cancer: Biomarkers and master regulators. In Seminars in Cancer Biology (Vol. 58, pp. 90–99). Academic Press.

Arnaiz, E., Sole, C., Manterola, L., Iparraguirre, L., Otaegui, D., & Lawrie, C. H. (2019). CircRNAs and cancer: Biomarkers and master regulators. In Seminars in Cancer Biology (Vol. 58, pp. 90–99). Academic Press.

Ashwal-Fluss, R., Meyer, M., Pamudurti, N. R., Ivanov, A., Bartok, O., Hanan, M., Evantal, N., Memczak, S., Rajewsky, N., & Kadener, S. (2014). CircRNA Biogenesis competes with Pre-mRNA splicing. Molecular Cell, 56(1), 55–66.

Aufiero, S., Reckman, Y. J., Pinto, Y. M., & Creemers, E. E. (2019). Circular RNAs open a new chapter in cardiovascular biology. In Nature Reviews Cardiology (Vol. 16, Issue 8, pp. 503–514). Nature Publishing Group.

Bachmayr-Heyda, A., Reiner, A. T., Auer, K., Sukhbaatar, N., Aust, S., Bachleitner-Hofmann, T., Mesteri, I., Grunt, T. W., Zeillinger, R., & Pils, D. (2015). Correlation of circular RNA abundance with proliferation exemplified with colorectal and ovarian cancer, idiopathic lung fibrosis, and normal human tissues. Scientific Reports, 5, 8057.

Barrett, S. P., & Salzman, J. (2016). Circular RNAs: Analysis, expression and potential functions. Development (Cambridge), 143(11), 1838–1847.

Barrett, S. P., Wang, P. L., & Salzman, J. (2015). Circular RNA biogenesis can proceed through an exon-containing lariat precursor. ELife, 4(JUNE), 1–18.

Bart, R., Chern, M., Park, C. J., Bartley, L., & Ronald, P. C. (2006). A novel system for gene silencing using siRNAs in rice leaf and stem-derived protoplasts. Plant methods, 2(1), 1-9.

Baulcombe, D. (2004). RNA silencing in plants. Nature, 431(7006), 356-363.

Beaudry, D., & Perreault, J. P. (1995). An efficient strategy for the synthesis of circular RNA molecules. Nucleic acids research, 23(15), 3064.

Borges, F., & Martienssen, R. A. (2015). The expanding world of small RNAs in plants. Nature reviews Molecular cell biology, 16(12), 727-741.

Borrelli, V. M., Brambilla, V., Rogowsky, P., Marocco, A., & Lanubile, A. (2018). The enhancement of plant disease resistance using CRISPR/Cas9 technology. Frontiers in plant science, 9, 1245.

Botha, C. E. J., Aoki, N., Scofield, G. N., Liu, L., Furbank, R. T., & White, R. G. (2008). A xylem sap retrieval pathway in rice leaf blades: evidence of a role for endocytosis?. Journal of Experimental Botany, 59(11), 2945-2954.

Breuer, J., & Rossbach, O. (2020). Production and purification of artificial circular RNA sponges for application in molecular biology and medicine. Methods and protocols, 3(2), 42.

Brown, J. R., & Chinnaiyan, A. M. (2020). The potential of circular RNAs as cancer biomarkers. Cancer Epidemiology Biomarkers and Prevention, 29(12), 2541–2555.

Burd, C. E., Jeck, W. R., Liu, Y., Sanoff, H. K., Wang, Z., & Sharpless, N. E. (2010). Expression of Linear and Novel Circular Forms of an INK4/ARF-Associated Non-Coding RNA Correlates with Atherosclerosis Risk. PLoS Genetics, 6(12), e1001233.

Buyse, M., Michiels, S., Sargent, D. J., Grothey, A., Matheson, A., & De Gramont, A. (2011). Integrating biomarkers in clinical trials. In Expert Review of Molecular Diagnostics (Vol. 11, Issue 2, pp. 171–182). Expert Rev Mol Diagn.

Cao, J., Yao, D., Lin, F., & Jiang, M. (2014). PEG-mediated transient gene expression and silencing system in maize mesophyll protoplasts: a valuable tool for signal transduction study in maize. Acta Physiologiae Plantarum, 36, 1271-1281.

Capelari, É. F., da Fonseca, G. C., Guzman, F., & Margis, R. (2019). Circular and micro RNAs from Arabidopsis thaliana flowers are simultaneously isolated from AGO-IP libraries. Plants, 8(9).

Cerutti, H., & Casas-Mollano, J. A. (2006). On the origin and functions of RNA-mediated silencing: from protists to man. Current genetics, 50, 81-99.

Chan, V. I. C. K. Y., Dreolini, L. F., Flintoff, K. A., Lloyd, S. J., & Mattenley, A. A. (2002). The effect of increasing plasmid size on transfection efficiency in Escherichia coli. Journal of Experimental Microbiology and Immunology, 2, 207-223.

Chen, C. Y., & Sarnow, P. (1995). Initiation of protein synthesis by the eukaryotic translational apparatus on circular RNAs. Science, 268(5209), 415–417.

Chen, R. X., Chen, X., Xia, L. P., Zhang, J. X., Pan, Z. Z., Ma, X. D., Han, K., Chen, J. W., Judde, J. G., Deas, O., Wang, F., Ma, N. F., Guan, X., Yun, J. P., Wang, F. W., Xu, R. H., & Dan Xie. (2019). N 6-methyladenosine modification of circNSUN2 facilitates cytoplasmic export and stabilizes HMGA2 to promote colorectal liver metastasis. Nature Communications, 10(1).

Chen, Y. G., Chen, R., Ahmad, S., Verma, R., Kasturi, S. P., Amaya, L., Broughton, J. P., Kim, J., Cadena, C., Pulendran, B., Hur, S., & Chang, H. Y. (2019). N6-Methyladenosine Modification Controls Circular RNA Immunity. Molecular Cell, 76(1), 96-109.e9.

Chen, Y. G., Kim, M. V., Chen, X., Batista, P. J., Aoyama, S., Wilusz, J. E., Iwasaki, A., & Chang, H. Y. (2017). Sensing Self and Foreign Circular RNAs by Intron Identity. Molecular Cell, 67(2), 228-238.e5.

Cheung, N., Tian, L., Liu, X., & Li, X. (2020). The destructive fungal pathogen *Botrytis cinerea* Insights from genes studied with mutant analysis. Pathogens, 9(11), 923.

Chi, S. W., Zang, J. B., Mele, A., & Darnell, R. B. (2009). Argonaute HITS-CLIP decodes microRNA-mRNA interaction maps. Nature, 460(7254), 479–486.

Chu, Q., Bai, P., Zhu, X., Zhang, X., Mao, L., Zhu, Q. H., Fan, L., & Ye, C. Y. (2018). Characteristics of plant circular RNAs. Briefings in Bioinformatics, 21(1), 135–143.

Chu, Q., Zhang, X., Zhu, X., Liu, C., Mao, L., Ye, C., Zhu, Q. H., & Fan, L. (2017). PlantcircBase: A Database for Plant Circular RNAs. In Molecular Plant (Vol. 10, Issue 8, pp. 1126–1128). Cell Press.

Conlon, E. G., & Manley, J. L. (2017). RNA-binding proteins in neurodegeneration: Mechanisms in aggregate. In Genes and Development (Vol. 31, Issue 15, pp. 1509–1528). Cold Spring Harbor Laboratory Press.

Conn, S. J., Pillman, K. A., Toubia, J., Conn, V. M., Salmanidis, M., Phillips, C. A., Roslan, S., Schreiber, A. W., Gregory, P. A., & Goodall, G. J. (2015). The RNA binding protein quaking regulates formation of circRNAs. Cell, 160(6), 1125–1134.

Conn, V. M., Hugouvieux, V., Nayak, A., Conos, S. A., Capovilla, G., Cildir, G., Jourdain, A., Tergaonkar, V., Schmid, M., Zubieta, C., & Conn, S. J. (2017). A circRNA from SEPALLATA3 regulates splicing of its cognate mRNA through R-loop formation. Nature Plants, 3.

Dalakouras, A., Jarausch, W., Buchholz, G., Bassler, A., Braun, M., Manthey, T., & Wassenegger, M. (2018). Delivery of hairpin RNAs and small RNAs into woody and herbaceous plants by trunk injection and petiole absorption. Frontiers in Plant Science, 9, 1253.

Dalakouras, A., Wassenegger, M., Dadami, E., Ganopoulos, I., Pappas, M. L., & Papadopoulou, K. (2020). Genetically modified organism-free RNA interference: exogenous application of RNA molecules in plants. Plant Physiology, 182(1), 38-50.

Dalakouras, A., Wassenegger, M., McMillan, J. N., Cardoza, V., Maegele, I., Dadami, E., & Wassenegger, M. (2016). Induction of silencing in plants by high-pressure spraying of in vitro-synthesized small RNAs. Frontiers in plant science, 7, 1327.

Darbani, B., Noeparvar, S., & Borg, S. (2016). Identification of circular RNAs from the parental genes involved in multiple aspects of cellular metabolism in barley. Frontiers in Plant Science.

Das, P. R., & Sherif, S. M. (2020). Application of exogenous dsRNAs-induced RNAi in agriculture: Challenges and triumphs. Frontiers in Plant Science, 11, 946.

Dean, R., Van Kan, J. A., Pretorius, Z. A., Hammond-Kosack, K. E., Di Pietro, A., Spanu, P. D., & Foster, G. D. (2012). The Top 10 fungal pathogens in molecular plant pathology. Molecular plant pathology, 13(4), 414-430.

Delgado-Martín, J., Ruiz, L., Janssen, D., & Velasco, L. (2022). Exogenous application of dsRNA for the control of viruses in cucurbits. Frontiers in Plant Science, 13, 895953.

Dodds, P. N., & Rathjen, J. P. (2010). Plant immunity: towards an integrated view of plant–pathogen interactions. Nature Reviews Genetics, 11(8), 539-548.

Druege, U., Franken, P., & Hajirezaei, M. R. (2016). Plant hormone homeostasis, signaling, and function during adventitious root formation in cuttings. Frontiers in Plant Science, 7, 381.

Du, W. W., Yang, W., Chen, Y., Wu, Z. K., Foster, F. S., Yang, Z., Li, X., & Yang, B. B. (2017). Foxo3 circular RNApromotes cardiac senescence by modulating multiple factors associated with stress and senescence responses. European Heart Journal, 38(18), 1402–1412.

Du, W. W., Yang, W., Li, X., Awan, F. M., Yang, Z., Fang, L., Lyu, J., Li, F., Peng, C., Krylov, S. N., Xie, Y., Zhang, Y., He, C., Wu, N., Zhang, C., Sdiri, M., Dong, J., Ma, J., Gao, C., Yang, B. B. (2018). A circular RNA circ-DNMT1 enhances breast cancer progression by activating autophagy. Oncogene, 37(44), 5829–5842.

Dubin, R. A., Kazmi, M. A., & Ostrer, H. (1995). Inverted repeats are necessary for circularization of the mouse testis Sry transcript. Gene, 167(1–2), 245–248.

Ebbesen, K. K., Kjems, J., & Hansen, T. B. (2016). Circular RNAs: Identification, biogenesis and function. In Biochimica et Biophysica Acta Gene Regulatory Mechanisms. Elsevier B.V.

Ebert, M. S., Neilson, J. R., & Sharp, P. A. (2007). MicroRNA sponges: Competitive inhibitors of small RNAs in mammalian cells. Nature Methods, 4(9), 721–726.

Fan, J., Quan, W., Li, G. B., Hu, X. H., Wang, Q., Wang, H., Li, X. P., Luo, X., Feng, Q., Hu, Z. J., Feng, H., Pu, M., Zhao, J. Q., Huang, Y. Y., Li, Y., Zhang, Y., & Wang, W. M. (2020). CircRNAs are involved in the rice-magnaporthe oryzae interaction. Plant Physiology, 182(1), 272–286.

Finkel, O. M., Castrillo, G., Paredes, S. H., González, I. S., & Dangl, J. L. (2017). Understanding and exploiting plant beneficial microbes. Current opinion in plant biology, 38, 155-163.

Fire, A. (1999). RNA-triggered gene silencing. Trends in Genetics, 15(9), 358-363.

Fischer, J. W., & Leung, A. K. L. (2017). CircRNAs: A regulator of cellular stress. Critical Reviews in Biochemistry and Molecular Biology, 52(2), 220–233.

Fjose, A., Ellingsen, S., Wargelius, A., & Seo, H. C. (2001). RNA interference: mechanisms and applications.

Fraiture, M., Zheng, X., & Brunner, F. (2014). An Arabidopsis and tomato mesophyll protoplast system for fast identification of early MAMP-triggered immunity-suppressing effectors. Plant-Pathogen Interactions: Methods and Protocols, 213-230.

Franco-Zorrilla, J. M., Valli, A., Todesco, M., Mateos, I., Puga, M. I., Rubio-Somoza, I., Leyva, A., Weigel, D., García, J. A., & Paz-Ares, J. (2007). Target mimicry provides a

new mechanism for regulation of microRNA activity. Nature Genetics, 39(8), 1033–1037.

Gan, W. C., & Ling, A. P. (2022). CRISPR/Cas9 in plant biotechnology: applications and challenges. BioTechnologia, 103(1), 81-93.

Gao, Y., Zhang, J., & Zhao, F. (2018). Circular RNA identification based on multiple seed matching. Briefings in Bioinformatics, 19(5), 803–810.

Gao, Z., Li, J., Luo, M., Li, H., Chen, Q., Wang, L., Song, S., Zhao, L., Xu, W., Zhang, C., Wang, S., & Ma, C. (2019). Characterization and cloning of grape circular rnas identified the cold resistance-related vv-circats1. Plant Physiology, 180(2), 966–985.

Gentile, A. C. (1954). Carbohydrate metabolism and oxalic acid synthesis by Botrytis cinerea. Plant Physiology, 29(3), 257.

Ghorbani, A., Izadpanah, K., Peters, J. R., Dietzgen, R. G., & Mitter, N. (2018). Detection and profiling of circular RNAs in uninfected and maize Iranian mosaic virus-infected maize. Plant Science, 274, 402–409.

Glažar, P., Papavasileiou, P., & Rajewsky, N. (2014). CircBase: A database for circular RNAs. RNA, 20(11), 1666–1670.

Grapp, M., Wrede, A., Schweizer, M., Hüwel, S., Galla, H. J., Snaidero, N., Simons, M., Bückers, J., Low, P. S., Urlaub, H., Gärtner, J., & Steinfeld, R. (2013). Choroid plexus transcytosis and exosome shuttling deliver folate into brain parenchyma. Nature Communications, 4.

Guo, J. U., Agarwal, V., Guo, H., & Bartel, D. P. (2014). Expanded identification and characterization of mammalian circular RNAs. Genome Biology, 15(7).

Hamakawa, M., & Hirotsu, T. (2017). Establishment of Time-and Cell-Specific RNAi in Caenorhabditis elegans. Eukaryotic Transcriptional and Post-Transcriptional Gene Expression Regulation, 67-79.

Hanan, M., Simchovitz, A., Yayon, N., Vaknine, S., Cohen-Fultheim, R., Karmon, M., & Kadener, S. (2020). A Parkinson's disease Circ RNA s resource reveals a link between circ SLC 8A1 and oxidative stress. EMBO molecular medicine, 12(9), e11942.

Hansen, T. B., Jensen, T. I., Clausen, B. H., Bramsen, J. B., Finsen, B., Damgaard, C. K., & Kjems, J. (2013). Natural RNA circles function as efficient microRNA sponges. Nature, 495(7441), 384–388.

Hansen, T. B., Wiklund, E. D., Bramsen, J. B., Villadsen, S. B., Statham, A. L., Clark, S. J., & Kjems, J. (2011). MiRNA-dependent gene silencing involving Ago2-mediated cleavage of a circular antisense RNA. EMBO Journal, 30(21), 4414–4422.

Harland, R., & Misher, L. (1988). Stability of RNA in developing Xenopus embryos and identification of a destabilizing sequence in TFIIIA messenger RNA. In Development (Vol. 102).

Hentze, M. W., & Preiss, T. (2013). Circular RNAs: Splicing's enigma variations. The EMBO Journal, 32(7), 923–925.

Hoffmann, S., Otto, C., Doose, G., Tanzer, A., Langenberger, D., Christ, S., Kunz, M., Holdt, L. M., Teupser, D., Hackermüller, J., & Stadler, P. F. (2014). A multi-split mapping algorithm for circular RNA, splicing, trans-splicing and fusion detection. Genome Biology, 15(2), 34.

Holdt, L. M., Stahringer, A., Sass, K., Pichler, G., Kulak, N. A., Wilfert, W., Kohlmaier, A., Herbst, A., Northoff, B. H., Nicolaou, A., Gäbel, G., Beutner, F., Scholz, M., Thiery, J., Musunuru, K., Krohn, K., Mann, M., & Teupser, D. (2016). Circular non-coding RNA ANRIL modulates ribosomal RNA maturation and atherosclerosis in humans. Nature Communications, 7(1), 1–14.

Hong, Y. H., Meng, J., Zhang, M., & Luan, Y. S. (2020). Identification of tomato circular RNAs responsive to Phytophthora infestans. Gene, 746.

Hsu, M. T., & Coca-Prados, M. (1979). Electron microscopic evidence for the circular form of RNA in the cytoplasm of eukaryotic cells [24]. In Nature (Vol. 280, Issue 5720, pp. 339–340). Nature Publishing Group.

Huang, C., Liang, D., Tatomer, D. C., & Wilusz, J. E. (2018). A length-dependent evolutionarily conserved pathway controls nuclear export of circular RNAs.

Huang, L., Li, Y., Chen, S., Periyannan, S., & Fahima, T. (2023). Advances in crop resistance breeding using modern genomic tools. Frontiers in Plant Science, 14, 1143689.

Ish-Shalom, S., Gafni, A., Lichter, A., & Levy, M. (2011). Transfection of *Botrytis cinerea* by direct hyphal blasting or by wound-mediated transfection of sclerotia. BMC microbiology, 11, 1-8.

Jain, R. G., Robinson, K. E., Asgari, S., & Mitter, N. (2021). Current scenario of RNAi-based hemipteran control. Pest management science, 77(5), 2188-2196.

Jarvis, W. R. (1962). The infection of strawberry and raspberry fruits by *Botrytis cinerea* Fr. Annals of applied Biology, 50(3), 569-575.

Jeck, W. R., & Sharpless, N. E. (2014). Detecting and characterizing circular RNAs. In Nature Biotechnology (Vol. 32, Issue 5, pp. 453–461). Nature Publishing Group.

Jeck, W. R., Sorrentino, J. A., Wang, K., Slevin, M. K., Burd, C. E., Liu, J., Marzluff, W. F., & Sharpless, N. E. (2013). Circular RNAs are abundant, conserved, and associated with ALU repeats. RNA, 19(2), 141–157.

Jens, M. (2014). Circular RNAs Are a Large Class of Animal RNAs with Regulatory Potency (pp. 69–80).

Jiang, L., Wang, J., Liu, Z., Wang, L., Zhang, F., Liu, G. C., & Zhong, Q. (2010). Silencing induced by inverted repeat constructs in protoplasts of Nicotiana benthamiana. Plant Cell, Tissue and Organ Culture (PCTOC), 100, 139-148.

Jones, J. D., & Dangl, J. L. (2006). The plant immune system. nature, 444(7117), 323-329.

Jost, I., Shalamova, L. A., Gerresheim, G. K., Niepmann, M., Bindereif, A., & Rossbach, O. (2018). Functional sequestration of microRNA-122 from Hepatitis C Virus by circular RNA sponges. RNA Biology, 15(8), 1032–1039.

Kachroo, A., & Kachroo, P. (2007). Salicylic acid-, jasmonic acid-and ethylene mediated regulation of plant defense signaling. Genetic engineering: Principles and methods, 55-83.

Kamthan, A., Chaudhuri, A., Kamthan, M., & Datta, A. (2015). Small RNAs in plants: recent development and application for crop improvement. Frontiers in plant science, 6, 208.

Katan, T. (1982). Persistence of dicarboximide-fungicide resistance in populations of Botrytis cinerea in a warm, dry temperate agroclimate. Phytoparasitica, 10, 209-211.

Kim, S., Cho, Y. J., Song, E. S., Lee, S. H., Kim, J. G., & Kang, L. W. (2016). Time-resolved pathogenic gene expression analysis of the plant pathogen Xanthomonas oryzae pv. oryzae. BMC genomics, 17(1), 1-15.

Kleaveland, B., Shi, C. Y., Stefano, J., & Bartel, D. P. (2018). A Network of Noncoding Regulatory RNAs Acts in the Mammalian Brain. Cell, 174(2), 350-362.e17.

Koch, A., Biedenkopf, D., Furch, A., Weber, L., Rossbach, O., Abdellatef, E., & Kogel, K. H. (2016). An RNAi-based control of Fusarium graminearum infections through spraying of long dsRNAs involves a plant passage and is controlled by the fungal silencing machinery. PLoS pathogens, 12(10), e1005901.

Koch, A., Höfle, L., Werner, B. T., Imani, J., Schmidt, A., Jelonek, L., & Kogel, K. H. (2019). SIGS vs HIGS: a study on the efficacy of two dsRNA delivery strategies to silence Fusarium FgCYP51 genes in infected host and non-host plants. Molecular plant pathology, 20(12), 1636-1644.

Koch, A., Kumar, N., Weber, L., Keller, H., Imani, J., & Kogel, K. H. (2013). Host-induced gene silencing of cytochrome P450 lanosterol C14α-demethylase–encoding genes confers strong resistance to Fusarium species. Proceedings of the National Academy of Sciences, 110(48), 19324-19329.

Kos, A., Dijkema, R., Arnberg, A. C., Van Der Meide, P. H., & Schellekens, H. (1986). The hepatitis delta (δ) virus possesses a circular RNA. Nature, 323(6088), 558–560.

Kramer, M. C., Liang, D., Tatomer, D. C., Gold, B., March, Z. M., Cherry, S., & Wilusz, J. E. (2015). Combinatorial control of Drosophila circular RNA expression by intronic repeats, hnRNPs, and SR proteins. Genes and Development, 29(20), 2168–2182.

Lapin, D., & Van den Ackerveken, G. (2013). Susceptibility to plant disease: more than a failure of host immunity. Trends in plant science, 18(10), 546-554.

Legnini, I., Di Timoteo, G., Rossi, F., Morlando, M., Briganti, F., Sthandier, O., Fatica, A., Santini, T., Andronache, A., Wade, M., Laneve, P., Rajewsky, N., & Bozzoni, I. (2017). Circ-ZNF609 Is a Circular RNA that Can Be Translated and Functions in Myogenesis. Molecular Cell, 66(1), 22-37.e9.

Leroch, M., Mernke, D., Koppenhoefer, D., Schneider, P., Mosbach, A., Doehlemann, G., & Hahn, M. (2011). Living colors in the gray mold pathogen Botrytis cinerea: codon-optimized genes encoding green fluorescent protein and mCherry, which exhibit bright fluorescence. Applied and environmental microbiology, 77(9), 2887-2897.

Li, B., Zhang, X. Q., Liu, S. R., Liu, S., Sun, W. J., Lin, Q., & Qu, L. H. (2017). Discovering the Interactions between Circular RNAs and RNA-binding Proteins from CLIP-seq Data using circScan. BioRxiv, 115980.

Li, J., Sun, D., Pu, W., Wang, J., & Peng, Y. (2020). Circular RNAs in Cancer: Biogenesis, Function, and Clinical Significance. In Trends in Cancer (Vol. 6, Issue 4, pp. 319–336). Cell Press.

Li, S., Teng, S., Xu, J., Su, G., Zhang, Y., Zhao, J., Zhang, S., Wang, H., Qin, W., Lu, Z. J., Guo, Y., Zhu, Q., & Wang, D. (2018). Microarray is an efficient tool for circRNA profiling. Briefings in Bioinformatics, 20(4),1420–1433.

Li, Y., Zheng, Q., Bao, C., Li, S., Guo, W., Zhao, J., Chen, D., Gu, J., He, X., & Huang, S. (2015). Circular RNA is enriched and stable in exosomes: A promising biomarker for cancer diagnosis. In Cell Research (Vol. 25, Issue 8, pp. 981–984). Nature Publishing Group.

Li, Z., Huang, C., Bao, C., Chen, L., Lin, M., Wang, X., & Shan, G. (2017). Corrigendum: exon-intron circular RNAs regulate transcription in the nucleus. Nature structural & molecular biology, 24(2), 194.

Litholdo, C. G., & da Fonseca, G. C. (2018). Circular RNAs and Plant Stress Responses. In J. Xiao (Ed.), Circular RNAs: Biogenesis and Functions (pp. 345–353). Springer.

Liu, C. X., Li, X., Nan, F., Jiang, S., Gao, X., Guo, S. K., Xue, W., Cui, Y., Dong, K., Ding, H., Qu, B., Zhou, Z., Shen, N., Yang, L., & Chen, L. L. (2019). Structure and Degradation of Circular RNAs Regulate PKR Activation in Innate Immunity. Cell, 177(4), 865-880.e21.

López-Carrasco, A., & Flores, R. (2017). Dissecting the secondary structure of the circular RNA of a nuclear viroid in vivo: A “naked” rod-like conformation similar but not identical to that observed in vitro. RNA biology, 14(8), 1046-1054.

Lü, L., Sun, J., Shi, P., Kong, W., Xu, K., He, B., Zhang, S., Wang, J., Lü, L., Sun, J., Shi, P., Kong, W., Xu, K., He, B., Zhang, S., & Wang, J. (2017). Identification of circular RNAs as a promising new class of diagnostic biomarkers for human breast cancer. Oncotarget, 8(27), 44096–44107.

Lu, R., Malcuit, I., Moffett, P., Ruiz, M. T., Peart, J., Wu, A. J., & Baulcombe, D. C. (2003). High throughput virus-induced gene silencing implicates heat shock protein 90 in plant disease resistance. The EMBO journal, 22(21), 5690-5699.

Lu, T., Cui, L., Zhou, Y., Zhu, C., Fan, D., Gong, H., Zhao, Q., Zhou, C., Zhao, Y., Lu, D., Luo, J., Wang, Y., Tian, Q., Feng, Q., Huang, T., & Han, B. (2015). Transcriptome-wide investigation of circular RNAs in rice. RNA, 21(12), 2076–2087.

Lu, Z., Filonov, G. S., Noto, J. J., Schmidt, C. A., Hatkevich, T. L., Wen, Y., Jaffrey, S. R., & Gregory Matera, A. (2015). Metazoan tRNA introns generate stable circular RNAs in vivo. RNA, 21(9), 1554–1565.

Maass, P. G., Glažar, P., Memczak, S., Dittmar, G., Hollfinger, I., Schreyer, L., Sauer, A. V., Toka, O., Aiuti, A., Luft, F. C., & Rajewsky, N. (2017). A map of human circular RNAs in clinically relevant tissues. Journal of Molecular Medicine, 95(11), 1179–1189.

Macho, A. P., & Zipfel, C. (2014). Plant PRRs and the activation of innate immune signaling. Molecular cell, 54(2), 263-272.

Majumdar, R., Rajasekaran, K. and Cary, J. W. (2017) RNA Interference (RNAi) as a Potential Tool for Control of Mycotoxin Contamination in Crop Plants: Concepts and Considerations. Frontiers in plant science 8, 200.

Martin, T. C., Ilieva, K. M., Visconti, A., Beaumont, M., Kiddle, S. J., Dobson, R. J. B., Mangino, M., Lim, E. M., Pezer, M., Steves, C. J., Bell, J. T., Wilson, S. G., Lauc, G., Roederer, M., Walsh, J. P., Spector, T. D., & Karagiannis, S. N. (2020). Dysregulated Antibody, Natural Killer Cell and Immune Mediator Profiles in Autoimmune Thyroid Diseases. Cells, 9(3), 665.

Memczak, S., Jens, M., Elefsinioti, A., Torti, F., Krueger, J., Rybak, A., Maier, L., Mackowiak, S. D., Gregersen, L. H., Munschauer, M., Loewer, A., Ziebold, U., Landthaler, M., Kocks, C., Le Noble, F., & Rajewsky, N. (2013). Circular RNAs are a large class of animal RNAs with regulatory potency. Nature, 495(7441), 333–338.

Meng, S., Zhou, H., Feng, Z., Xu, Z., Tang, Y., Li, P., & Wu, M. (2017). CircRNA: Functions and properties of a novel potential biomarker for cancer. In Molecular Cancer (Vol. 16, Issue 1). BioMed Central Ltd.

Metge, F., Czaja-Hasse, L. F., Reinhardt, R., & Dieterich, C. (2017). FUCHS-towards full circular RNA characterization using RNAseq. PeerJ, 2017(2), e2934.

Meyer, K. D., Patil, D. P., Zhou, J., Zinoviev, A., Skabkin, M. A., Elemento, O., Pestova, T. V., Qian, S. B., & Jaffrey, S. R. (2015). 5′ UTR m6A Promotes Cap-Independent Translation. Cell, 163(4), 999–1010.

Millar, A. A., & Waterhouse, P. M. (2005). Plant and animal microRNAs: similarities and differences. Functional & integrative genomics, 5, 129-135.

Mitter, N., Worrall, E. A., Robinson, K. E., Li, P., Jain, R. G., Taochy, C., & Xu, Z. P. (2017). Clay nanosheets for topical delivery of RNAi for sustained protection against plant viruses. Nature Plants, 3(2), 1-10.

Mogensen, T. H. (2009). Pathogen recognition and inflammatory signaling in innate immune defenses. Clinical microbiology reviews, 22(2), 240-273.

Morel, J. B., Godon, C., Mourrain, P., Béclin, C., Boutet, S., Feuerbach, F., & Vaucheret, H. (2002). Fertile hypomorphic ARGONAUTE (ago1) mutants impaired in post-transcriptional gene silencing and virus resistance. The Plant Cell, 14(3), 629-639.

Morris, K. V., & Mattick, J. S. (2014). The rise of regulatory RNA. In Nature Reviews Genetics (Vol. 15, Issue 6, pp. 423–437). Nature Publishing Group.

Muhammad, T., Zhang, F., Zhang, Y., & Liang, Y. (2019). RNA interference: a natural immune system of plants to counteract biotic stressors. Cells, 8(1), 38.

Müller, S., & Appel, B. (2017). In vitro circularization of RNA. RNA biology, 14(8), 1018-1027.

Neri, F., Cappellin, L., Spadoni, A., Cameldi, I., Algarra Alarcon, A., Aprea, E., & Biasioli, F. (2015). Role of strawberry volatile organic compounds in the development of *Botrytis cinerea* infection. Plant Pathology, 64(3), 709-717.

Nguyen, Q. B., Kadotani, N., Kasahara, S., Tosa, Y., Mayama, S. and Nakayashiki, H. (2008) Systematic functional analysis of calcium-signalling proteins in the genome of the riceblast fungus, Magnaporthe oryzae, using a high-throughput RNA-silencing system. Molecular microbiology 68, 1348–1365.

Niedz, R. P., Sussman, M. R., & Satterlee, J. S. (1995). Green fluorescent protein: an in vivo reporter of plant gene expression. Plant Cell Reports, 14, 403-406.

Nigro, J. M., Cho, K. R., Fearon, E. R., Kern, S. E., Ruppert, J. M., Oliner, J. D., Kinzler, K. W., & Vogelstein, B. (1991). Scrambled exons. Cell, 64(3), 607–613.

Nishimoto, R. (2019). Global trends in the crop protection industry. Journal of pesticide science, 44(3), 141-147.

Nitnavare, R. B., Bhattacharya, J., Singh, S., Kour, A., Hawkesford, M. J., & Arora, N. (2021). Next generation dsRNA-based insect control: Success so far and challenges. Frontiers in Plant Science, 12, 673576.

Nosaka, M., Itoh, J. I., Nagato, Y., Ono, A., Ishiwata, A., & Sato, Y. (2012). Role of transposon-derived small RNAs in the interplay between genomes and parasitic DNA in rice.

Nwilene, F. E., Nwanze, K. F., & Youdeowei, A. (2008). Impact of integrated pest management on food and horticultural crops in Africa. Entomologia experimentalis et applicata, 128(3), 355-363.

Nybakken, K., Vokes, S. A., Lin, T. Y., McMahon, A. P., & Perrimon, N. (2005). A genome-wide RNA interference screen in Drosophila melanogaster cells for new components of the Hh signaling pathway. Nature Genetics, 37(12), 1323-1332.

O'Sullivan, D., Sanin, D. E., Pearce, E. J., & Pearce, E. L. (2019). Metabolic interventions in the immune response to cancer. In Nature Reviews Immunology (Vol. 19, Issue 5, pp. 324–335). Nature Publishing Group.

Oerke, E. C., & Dehne, H. W. (2004). Safeguarding production losses in major crops and the role of crop protection. Crop protection, 23(4), 275-285.

Ohse, M., Takahashi, K., Kadowaki, Y., & Kusaoke, H. (1995). Effects of plasmid DNA sizes and several other factors on transfection of Bacillus subtilis ISW1214 with plasmid DNA by electroporation. Bioscience, biotechnology, and biochemistry, 59(8), 1433-1437.

Pamudurti, N. R., Bartok, O., Jens, M., Ashwal-Fluss, R., Stottmeister, C., Ruhe, L., Hanan, M., Wyler, E., Perez-Hernandez, D., Ramberger, E., Shenzis, S., Samson, M., Dittmar, G., Landthaler, M., Chekulaeva, M., Rajewsky, N., & Kadener, S. (2017). Translation of CircRNAs. Molecular Cell, 66(1), 9-21.e7.

Pampolini, F., & Rieske, L. K. (2023). Foliar Application of dsRNA to Induce Gene Silencing in Emerald Ash Borer: Systemic Distribution, Persistence, and Bioactivity. Forests, 14(9), 1853.

Pan, T., Sun, X., Liu, Y., Li, H., Deng, G., Lin, H., & Wang, S. (2018). Heat stress alters genome-wide profiles of circular RNAs in Arabidopsis. Plant Molecular Biology, 96(3), 217–229.

Panda, A., & Gorospe, M. (2018). Detection and Analysis of Circular RNAs by RT-PCR. BIO-PROTOCOL, 8(6).

Papp, I., Mette, M. F., Aufsatz, W., Daxinger, L., Schauer, S. E., Ray, A., & Matzke, A. J. (2003). Evidence for nuclear processing of plant micro RNA and short interfering RNA precursors. Plant Physiology, 132(3), 1382-1390.

Park, S., Kang, I., & Shin, C. (2021). MicroRNA clustering on the biogenesis of suboptimal microRNAs. Applied Biological Chemistry, 64, 1-9.

Perriman, R., & Ares, M. (1998). Circular mRNA can direct translation of extremely long repeating- sequence proteins in vivo. RNA, 4(9), 1047–1054.

Petkovic, S., & Müller, S. (2015). RNA circularization strategies in vivo and in vitro. Nucleic acids research, 43(4), 2454-2465.

Pfafenrot, C., & Preußer, C. (2019). Establishing essential quality criteria for the validation of circular RNAs as biomarkers. Biomolecular Detection and Quantification, 17, 100085.

Pfafenrot, C., Schneider, T., Müller, C., Hung, L.-H., Schreiner, S., Ziebuhr, J., & Bindereif, A. (2021). Inhibition of SARS-CoV-2 coronavirus proliferation by designer antisense-circRNAs. Nucleic Acids Research, 49(21), 12502–12516.

Piwecka, M., Glažar, P., Hernandez-Miranda, L. R., Memczak, S., Wolf, S. A., Rybak-Wolf, A., Filipchyk, A., Klironomos, F., Jara, C. A. C., Fenske, P., Trimbuch, T., Zywitza, V., Plass, M., Schreyer, L., Ayoub, S., Kocks, C., Kühn, R., Rosenmund, C., Birchmeier, C., & Rajewsky, N. (2017). Loss of a mammalian circular RNA locus causes miRNA deregulation and affects brain function. Science, 357(6357).

Plasterk, R. H. (2002). RNA silencing: the genome's immune system. Science, 296(5571), 1263-1265.

Pollastro, S., Santomauro, A., Miazzi, M., Contesini, A., & Faretra, F. (1995). Protoplast production from the mycelium of Botryotinia fuckeliana (Botrytis cinerea). Phytopathologia Mediterranea, 38-44.

Pratt, A. J., & MacRae, I. J. (2009). The RNA-induced silencing complex: a versatile gene-silencing machine. Journal of Biological Chemistry, 284(27), 17897-17901.

Prusky, D., & Lichter, A. (2007). Activation of quiescent infections by postharvest pathogens during transition from the biotrophic to the necrotrophic stage. FEMS microbiology letters, 268(1), 1-8.

Qin, M., Liu, G., Huo, X., Tao, X., Sun, X., Ge, Z., Yang, J., Fan, J., Liu, L., & Qin, W. (2016). Hsa-circ-0001649: A circular RNA and potential novel biomarker for hepatocellular carcinoma. Cancer Biomarkers, 16(1), 161–169.

Quinn, J. J., & Chang, H. Y. (2016). Unique features of long non-coding RNA biogenesis and function. In Nature Reviews Genetics (Vol. 17, Issue 1, pp. 47–62). Nature Publishing Group.

Rehman, L., Su, X., Guo, H., Qi, X., & Cheng, H. (2016). Protoplast transfection as a potential platform for exploring gene function in *Verticillium dahliae*. BMC biotechnology, 16, 1-9.

Rosa, C., Kuo, Y. W., Wuriyanghan, H., & Falk, B. W. (2018). RNA interference mechanisms and applications in plant pathology. Annual review of phytopathology, 56, 581-610.

Russell, C. D., Unger, S. A., Walton, M., & Schwarze, J. (2017). The human immune response to respiratory syncytial virus infection. In Clinical Microbiology Reviews (Vol. 30, Issue 2, pp. 481–502). American Society for Microbiology.

Sainju, U. M., Lenssen, A. W., Allen, B. L., Stevens, W. B., & Jabro, J. D. (2017). Soil total carbon and crop yield affected by crop rotation and cultural practice. Agronomy Journal, 109(1), 388-396.

Salzman, J., Chen, R. E., Olsen, M. N., Wang, P. L., & Brown, P. O. (2013). Cell-Type Specific Features of Circular RNA Expression. PLoS Genetics, 9(9).

Salzman, J., Gawad, C., Wang, P. L., Lacayo, N., & Brown, P. O. (2012). Circular RNAs Are the Predominant Transcript Isoform from Hundreds of Human Genes in Diverse Cell Types. PLoS ONE, 7(2), e30733.

Sanger, H. L., Klotz, G., Riesner, D., Gross, H. J., & Kleinschmidt, A. K. (1976). Viroids are single stranded covalently closed circular RNA molecules existing as highly base paired rod like structures. Proceedings of the National Academy of Sciences of the United States of America, 73(11), 3852–3856.

Sanger, H. L., Klotz, G., Riesner, D., Gross, H. J., & Kleinschmidt, A. K. (1976). Viroids are single stranded covalently closed circular RNA molecules existing as highly base paired rod like structures. Proceedings of the National Academy of Sciences of the United States of America, 73(11), 3852–3856.

Sasanuma, I., & Suzuki, T. (2016). Effect of calcium on cell-wall degrading enzymes of Botrytis cinerea. Bioscience, biotechnology, and biochemistry, 80(9), 1730-1736.

Sato, F. (2005). RNAi and functional genomics. Plant Biotechnology, 22(5), 431-442.

Schindewolf, C., Braun, S., & Domdey, H. (1996). In vitro generation of a circular exon from a linear pre-mRNA transcript. Nucleic Acids Research, 24(7), 1260–1266.

Schreiner, S., Didio, A., Hung, L. H., & Bindereif, A. (2021). Design and application of circular RNAs with protein-sponge function. Nucleic Acids Research, 48(21), 12326–12335.

Schumacher, J. (2012). Tools for Botrytis cinerea: new expression vectors make the gray mold fungus more accessible to cell biology approaches. Fungal genetics and biology, 49(6), 483-497.

Schweizer P, Pokorny J, Abderhalden O, Dudler R (1999) A transient assay system for the functional assessment of defense-related genes in wheat. Mol Plant Microbe Interact 12: 647–654.

Sheen, J. (2001). Signal transduction in maize and Arabidopsis mesophyll protoplasts. Plant Physiology, 127(4), 1466-1475.

Słupianek, A., Kasprowicz-Maluśki, A., Myśkow, E., Turzańska, M., & Sokołowska, K. (2019). Endocytosis acts as transport pathway in wood. New Phytologist, 222(4), 1846-1861.

Srivastava, P. K., Singh, V. P., Singh, A., Tripathi, D. K., Singh, S., Prasad, S. M., & Chauhan, D. K. (Eds.). (2020). Pesticides in crop production: physiological and biochemical action. John Wiley & Sons.

Staats, M., van Baarlen, P., & van Kan, J. A. (2005). Molecular phylogeny of the plant pathogenic genus Botrytis and the evolution of host specificity. Molecular biology and Evolution, 22(2), 333-346.

Starke, S., Jost, I., Rossbach, O., Schneider, T., Schreiner, S., Hung, L. H., & Bindereif, A. (2015). Exon circularization requires canonical splice signals. Cell Reports, 10(1), 103–111.

Sun, X., Wang, L., Ding, J., Wang, Y., Wang, J., Zhang, X., Che, Y., Liu, Z., Zhang, X., Ye, J., Wang, J., Sablok, G., Deng, Z., & Zhao, H. (2016). Integrative analysis of Arabidopsis thaliana transcriptomics reveals intuitive splicing mechanism for circular RNA. FEBS Letters, 590(20), 3510–3516.

Suzuki, H., Zuo, Y., Wang, J., Zhang, M. Q., Malhotra, A., & Mayeda, A. (2006). Characterization of RNase R-digested cellular RNA source that consists of lariat and circular RNAs from pre-mRNA splicing. Nucleic Acids Research, 34(8).

Tabak, H. F., van der Horst, G., Smit, J., Winter, A. J., Mul, Y., & Koerkamp, G. M. J. a. (1988). Discrimination between RNA circles, interlocked RNA circles and lariats using two-dimensional polyacrylamide gel electrophoresis. Nucleic Acids Research, 16(14), 6597–6605.

Tang, C., Xie, Y., Yu, T., Liu, N., Wang, Z., Woolsey, R. J., Tang, Y., Zhang, X., Qin, W., Zhang, Y., Song, G., Zheng, W., Wang, J., Chen, W., Wei, X., Xie, Z., Klukovich, R., Zheng, H., Quilici, D. R., & Yan, W. (2020). M6A-dependent biogenesis of circular RNAs in male germ cells. Cell Research, 30(3), 211–228.

Tang, M., Kui, L., Lu, G., & Chen, W. (2020). Disease-Associated Circular RNAs: From Biology to Computational Identification. In BioMed Research International (Vol. 2020). Hindawi Limited.

Turgeon, B. G., Condon, B., Liu, J., & Zhang, N. (2010). Protoplast transfection of filamentous fungi. Molecular and cell biology methods for fungi, 3-19.

Vaucheret, H. (2006). Post-transcriptional small RNA pathways in plants: mechanisms and regulations. Genes & development, 20(7), 759-771.

Vincent, H. A., & Deutscher, M. P. (2006). Substrate recognition and catalysis by the exoribonuclease RNase R. Journal of Biological Chemistry, 281(40), 29769–29775.

Vo, J. N., Cieslik, M., Zhang, Y., Shukla, S., Xiao, L., Zhang, Y., Wu, Y. M., Dhanasekaran, S. M., Engelke, C. G., Cao, X., Robinson, D. R., Nesvizhskii, A. I., & Chinnaiyan, A. M. (2019). The Landscape of Circular RNA in Cancer. Cell, 176(4), 869-881.e13.

Waage, J. K., & Greathead, D. J. (1988). Biological control: challenges and opportunities. Philosophical Transactions of the Royal Society of London. B, Biological Sciences, 318(1189), 111-128.

Wang, J., Lin, J., Wang, H., Li, X., Yang, Q., Li, H., & Chang, Y. (2018). Identification and characterization of circRNAs in Pyrus betulifolia Bunge under drought stress. PLOS ONE, 13(7), e0200692.

Wang, J., Yang, Y., Jin, L., Ling, X., Liu, T., Chen, T., Ji, Y., Yu, W., & Zhang, B. (2018). Re-analysis of long non-coding RNAs and prediction of circRNAs reveal their novel roles in susceptible tomato following TYLCV infection. BMC Plant Biology, 18(1).

Wang, K., Wang, C., Guo, B., Song, K., Shi, C., Jiang, X., Wang, K., Tan, Y., Wang, L., Wang, L., Li, J., Li, Y., Cai, Y., Zhao, H., & Sun, X. (2019). CropCircDB: A comprehensive circular RNA resource for crops in response to abiotic stress. Database, 2019(1).

Wang, P. L., Bao, Y., Yee, M. C., Barrett, S. P., Hogan, G. J., Olsen, M. N., Dinneny, J. R., Brown, P. O., & Salzman, J. (2014). Circular RNA is expressed across the eukaryotic tree of life. PLoS ONE, 9(3).

Wang, Q., & Carmichael, G. G. (2004). Effects of length and location on the cellular response to double-stranded RNA. Microbiology and Molecular Biology Reviews, 68(3), 432-452.

Wang, Y., Yang, M., Wei, S., Qin, F., Zhao, H., & Suo, B. (2017). Identification of circular RNAs and their targets in leaves of Triticum aestivum L. under dehydration stress. Frontiers in Plant Science, 7.

Wang, Z., Liu, Y., Li, D., Li, L., Zhang, Q., Wang, S., & Huang, H. (2017). Identification of circular rnas in kiwifruit and their species-specific response to bacterial canker pathogen invasion. Frontiers in Plant Science, 8.

Weigelt, C. M., Sehgal, R., Tain, L. S., Cheng, J., Eßer, J., Pahl, A., Dieterich, C., Grönke, S., & Partridge, L. (2020). An Insulin-Sensitive Circular RNA that Regulates Lifespan in Drosophila. Journal of Cleaner Production, 79(2), 268-279.e5.

Werner, B. T., Gaffar, F. Y., Schuemann, J., Biedenkopf, D., & Koch, A. M. (2020). RNA-spray-mediated silencing of Fusarium graminearum AGO and DCL genes improve barley disease resistance. Frontiers in Plant Science, 11, 476.

Wesselhoeft, R. A., Kowalski, P. S., & Anderson, D. G. (2018). Engineering circular RNA for potent and stable translation in eukaryotic cells. Nature communications, 9(1), 2629.

Westholm, J. O., Miura, P., Olson, S., Shenker, S., Joseph, B., Sanfilippo, P., Celniker, S. E., Graveley, B. R., & Lai, E. C. (2014). Genome-wide Analysis of Drosophila Circular RNAs Reveals Their Structural and Sequence Properties and Age-Dependent Neural Accumulation. Cell Reports, 9(5), 1966–1980.

Whetzel, H. H. (1945). A synopsis of the genera and species of the Sclerotiniaceae, a family of stromatic inoperculate discomycetes. Mycologia, 37(6), 648-714.

Williamson, B., Tudzynski, B., Tudzynski, P., & Van Kan, J. A. (2007). Botrytis cinerea: the cause of grey mould disease. Molecular plant pathology, 8(5), 561-580.

Wilson, R. C., & Doudna, J. A. (2013). Molecular mechanisms of RNA interference. Annual review of biophysics, 42, 217-239.

Wubie, A. J., Hu, Y., Li, W., Huang, J., Guo, Z., Xu, S., & Zhou, T. (2014). Factors analysis in protoplast isolation and regeneration from a chalkbrood fungus, Ascosphaera apis. Int J Agric Biol, 16, 89-96.

Xiang, L., Cai, C., Cheng, J., Wang, L., Wu, C., Shi, Y., Luo, J., He, L., Deng, Y., Zhang, X., Yuan, Y., & Cai, Y. (2018). Identification of circularRNAs and their targets in Gossypium under Verticillium wilt stress based on RNA-seq. PeerJ, 2018(3).

Xu, T., Wu, J., Han, P., Zhao, Z., & Song, X. (2017). Circular RNA expression profiles and features in human tissues: A study using RNA-seq data. BMC Genomics, 18(S6), 680.

Yang, B., Yang, S., Zheng, W., & Wang, Y. (2022). Plant immunity inducers: From discovery to agricultural application. Stress Biology, 2(1), 5.

Yang, L., Wilusz, J. E., & Chen, L. L. (2022). Biogenesis and regulatory roles of circular RNAs. Annual review of cell and developmental biology, 38, 263-289.

Yang, W., Li, Y., Song, X., Xu, J., & Xie, J. (2017). Genome-wide analysis of long noncoding RNA and mRNA co-expression profile in intrahepatic cholangiocarcinoma tissue by RNA sequencing.Oncotarget, 8(16), 26591–26599.

Yang, X. S., Wu, J., Ziegler, T. E., Yang, X., Zayed, A., Rajani, M. S., Zhou, D., Basra, A. S., Schachtman, D. P., Peng, M., Armstrong, C. L., Caldo, R. A., Morrell, J. A., Lacy, M., & Staub, J. M. (2011). Gene expression biomarkers provide sensitive indicators of in planta nitrogen status in maize. Plant Physiology, 157(4), 1841–1852.

Yang, X., Mei, J., Wang, H., Gu, D., Ding, J., & Liu, C. (2020). The emerging roles of circular RNAs in ovarian cancer. In Cancer Cell International (Vol. 20, Issue 1, p. 265). BioMed Central.

Yang, Y., Fan, X., Mao, M., Song, X., Wu, P., Zhang, Y., Jin, Y., Yang, Y., Chen, L. L., Wang, Y., Wong, C. C. L., Xiao, X., & Wang, Z. (2017). Extensive translation of circular RNAs driven by N6-methyladenosine. Cell Research, 27(5), 626–641.

Ye, C. Y., Chen, L., Liu, C., Zhu, Q. H., & Fan, L. (2015). Widespread noncoding circular RNAs in plants. New Phytologist, 208(1), 88–95.

Ye, J., Wang, L., Li, S., Zhang, Q., Zhang, Q., Tang, W., Wang, K., Song, K., Sablok, G., Sun, X., & Zhao, H. (2019). AtCircDB: A tissue-specific database for Arabidopsis circular RNAs. Briefings in Bioinformatics, 20(1), 58–65.

Yong, J., Wu, M., Zhang, R., Bi, S., Mann, C. W., Mitter, N., & Xu, Z. P. (2022). Clay nanoparticles efficiently deliver small interfering RNA to intact plant leaf cells. Plant Physiology, 190(4), 2187-2202.

You, X., & Conrad, T. O. (2016). Acfs: Accurate circRNA identification and quantification from RNA-Seq data. Scientific Reports, 6(1), 1–11.

Zhai, Z., Sooksa-nguan, T., & Vatamaniuk, O. K. (2009). Establishing RNA interference as a reverse-genetic approach for gene functional analysis in protoplasts. Plant physiology, 149(2), 642-652. Zhang, J., Hao, Z., Yin, S., & Li, G. (2020). GreenCircRNA: a database for plant circRNAs that act as miRNA decoys. Database, 2020, 39.

Zhang, P., Fan, Y., Sun, X., Chen, L., Terzaghi, W., Bucher, E., Li, L., & Dai, M. (2019). A large-scale circular RNA profiling reveals universal molecular mechanisms responsive to drought stress in maize and Arabidopsis. Plant Journal, 98(4), 697–713.

Zhang, P., Meng, X., Chen, H., Liu, Y., Xue, J., Zhou, Y., & Chen, M. (2017). PlantCircNet: A database for plant circRNA-miRNA-mRNA regulatory networks. Database : The Journal of Biological Databases and Curation, 2017.

Zhang, X. O., Wang, H. Bin, Zhang, Y., Lu, X., Chen, L. L., & Yang, L. (2014). Complementary sequence-mediated exon circularization. Cell, 159(1), 134–147.

Zhang, Y., Zhang, X. O., Chen, T., Xiang, J. F., Yin, Q. F., Xing, Y. H., Zhu, S., Yang, L., & Chen, L. L. (2013). Circular Intronic Long Noncoding RNAs. Molecular Cell, 51(6), 792–806.

Zhao, W., Cheng, Y., Zhang, C., You, Q., Shen, X., Guo, W., & Jiao, Y. (2017). Genome-wide identification and characterization of circular RNAs by high throughput sequencing in soybean. Scientific Reports, 7(1).

Zhao, W., Zhang, C., Shen, X., Xiao, L., Lu, J., Zhang, Y., Guo, W., & Jiao, Y. (2017). Characterization of circRNAs associated with resistance to defoliating insects in soybean. 2(1), 23–37.

Zhao, Z., Li, X., Jian, D., Hao, P., Rao, L., & Li, M. (2017). Hsa_circ_0054633 in peripheral blood can be used as a diagnostic biomarker of pre-diabetes and type 2 diabetes mellitus. Acta Diabetologica, 54(3), 237–245.

Zheng, F., Yu, X., Huang, J., & Dai, Y. (2017). Circular RNA expression profiles of peripheral blood mononuclear cells in rheumatoid arthritis patients, based on microarray chip technology. Molecular Medicine Reports, 16(6), 8029–8036.

Zhong, S., Zhang, J., & Zhang, G. Z. (2019). Botrytis polyphyllae: A new botrytis species causing gray mold on Paris polyphylla. Plant disease, 103(7), 1721-1727.

Zhou, C., Molinie, B., Daneshvar, K., Pondick, J. V., Wang, J., Van Wittenberghe, N., Xing, Y., Giallourakis, C. C., & Mullen, A. C. (2017). Genome-Wide Maps of m6A circRNAs Identify Widespread and Cell-Type-Specific Methylation Patterns that Are Distinct from mRNAs. Cell Reports, 20(9), 2262–2276.

Zhu, Y.X., Jia, J., Yang, L., Xia, Y.C., Zhang, H., Jia, J.-B., Zhou, R., Nie, P.-Y., Yin, J., Ma, D., & Liu, L.C. (2019). Identification of cucumber circular RNAs responsive to salt stress. BMC Plant Biology.

Zuker, M. (2003) Mfold web server for nucleic acid folding and hybridization prediction. Nucleic acids research, *31*(13), 3406-3415.

Zuo, J., Wang, Q., Zhu, B., Luo, Y., & Gao, L. (2016). Deciphering the roles of circRNAs on chilling injury in tomato. Biochemical and Biophysical Research Communications, 479(2), 132–138.

Zuo, J., Wang, Y., Zhu, B., Luo, Y., Wang, Q., & Gao, L. (2018). Analysis of the Coding and Non-Coding RNA Transcriptomes in Response to Bell Pepper Chilling. International Journal of Molecular Sciences, 19(7), 2001.

8. Attachment

8.1 List of Table

8.2 List of Figures

8.3 List of sequences used in this study

Name	Sequences (5'-3')
circRNA$_{GFP}$	GGGAGUAAGCUCGUGCUGCUUCAUGUGGUCGGGGUAGCGGGCUUACAGUA
circRNA$_{CTR1}$	GGGAGUAAGCAGAUGCGCACCGCACAGAUGCGCACGCUUACAGUA
circRNA$_{CTR2}$	GGGAGUAAGCAAAAGUCAGUGAGUCAGUGUAAUACGGGAGGAUACCCGCUGUCAAAGCUUACAGUA
GFP-dsRNA sequence (476 bp)	ACCACAUGAAGCAGCACGACUUCUUCAAGUCCGCCAUGCCCGAAGGCUACGUCCAGGAGCGCACCAUCUUCUUCAAGGACGACGGCAACUACAAGACCCGCGCCGAGGUGAAGUUCGAGGGCGACACCCUGGUGAACCGCAUCGAGCUGAAGGGCAUCGACUUCAAGGAGGACGGCAACAUCCUGGGGCACAAGCUGGAGUACAACUACAACAGCCACAACGUCUAUAUCAUGGCCGACAAGCAGAAGAACGGCAUCAAGGUGAACUUCAAGAUCCGCCACAACAUCGAGGACGGCAGCGUGCAGCUCGCCGACCACUACCAGCAGAACACCCCCAUCGGCGACGGCCCCGUGCUGCUGCCCGACAACCACUACCUGAGCACCCAGUCCGCCCUGAGCAAAGACCCCAACGAGAAGCGCGAUCACAUGGUCCUGCUGGAGUUCGUGACCGCCGCCGGGAUCACUCUCGGCAUGGAC
Clp1-dsRNA (431 bp) Intronic sequence of the Ca^{2+}-dependent cysteine protease (*Clp-1*) gene from *Verticillium longisporum* (BN1708_013046)	GAUUCAGGCCAGAGAGUGCGUGUGCGACUCGUCUUCCUAUUUUCCUUCUGGCGUGCUUCUAGGUCAGAGACGGCGCGAGGCGCCAAAGGUUUCGGCGUUGAAGCGGCGCACCGAGAAAUGGGACGAGACGGAACAAACUGAUGCGGAAAGUAUUGCUAGGUCCGACAGUCUAACAGAGCGAAGAAGAAACCUUCCUAGGAUUUAUCACGAUGAAAGACAAUGUCAACAGACCAGUGGGGGCUGGCAAUGUUCAGACAGGAUAGUGUGGACGAGUGUACAGCUCGCCAAGCCAGUGCUGUCUUGCUUUGGGUACUCCGCCACCGUUCGCCUCCAGCCUCCAUUAAUCUUCACACCUAUGCUAGGUAUUUUCUUGCAAUUUCUUUGACUGCUAUGAGAGCCUAUCCGCUGGUCACGUCGGGAGAAUUGCCUUC
ORF_GFP sequence (718 bp)	TTTGGAGAGGACAGGGTACCCATCATACTAGTAGATCTGCGATCTAAGTAAGCTTGGCATTCCGGTACTGTTGGTAAAGCCACCATGGTGAGCAAGGGCGAGGAGCTGTTCACCGGGGTGGTGCCCATCCTGGTCGAGCTGGACGGCGACGTAAACGGCCACAAGTTCAGCGTGTCCGGCGAGGGCGAGGGCGATGCCACCTACGGCAAGCTGACCCTGAAGTTCATCTGCACCACCGGCAAGCTGCCCGTGCCCTGGCCCACCCTCGTGACCACCTTGACCTACGGCGTGCAGTGCTTCGCCCGCTACCCCGACCACATGAAGCAGCACGACTTCTTCAAGTCCGCCATGCCCGAAGGCTACGTCCAGGAGCGCACCATCTTCTTCAAGGACGACGGCAACTACAAGACCCGCGCCGAGGTGAAGTTCGAGGGCGACACCCTGGTGAACCGCATCGAGCTGAAGGGCATCGACTTCAAGGAGGACGGCAACATCCTGGGGCACAAGCTGGAGTACAACTACAACAGCCACAAGGTCTATATCACCGCCGACAAGCAGAAGAACGGCATCAAGGTGAACTTCAAGACCCGCCACAACATCGAGGACGGCAGCGTGCAGCTCGCCGACCACTACCAGCAGAACACCCCCATCGGCGACGGCCCCGTGCTGCTGCCCGACAACCACTACCTGAGCACCCAGTCCGCCCTGAGCAAAGACCCCAACGAGAAGCGCGATCACATGGTCCTGCTGGAGTTCGTGACCGCCGCCGGGATCACTCTCGGCATGGACGAGCTGTACAAGTAACTCGACTAGAGTCGGGGCGGCCGGGGATCCTCTAGAGTCGACCTGCAGGCATGCCGCTGAAATCACCAGTCTCTC

9. Acknowledgment

I express my heartfelt gratitude to everyone who has been an indispensable part of my Ph.D. journey. The completion of this study would not have been possible without the unwavering support and guidance from each one of you.

First and foremost, I am deeply thankful to **Prof. Dr. Karl-Heinz Kogel** for providing me with the invaluable opportunity to undertake this Ph.D. journey. His exceptional scientific acumen and academic expertise have been a guiding force throughout my four years of study. I am grateful for the chance to study in such an enriching environment and to have encountered so many wonderful individuals. Your academic approach and critical thinking have left a lasting impact on me, and I will carry these valuable lessons with me always.

I extend my sincere appreciation to **Prof. Dr. Albrecht Bindereif** from the Department of Biochemistry at Justus-Liebig University, Giessen, for agreeing to be my second supervisor. His continuous support and advice have been instrumental in shaping the trajectory of my research. Also, thanks to **Prof. Dr. Patrick Schäfer** from the Institute of Phytopathology for being my supervisor. Furthermore, I express my gratitude and special thanks to **Dr. Jafargholi Imani**, whose mentorship has been invaluable. His guidance in experiment setup and problem-solving has not only enhanced my research skills but has also left a lasting impact on my personal and professional life. Dr. Jafargholi Imani's unwavering support, motivation, and kindness have been a source of my strength, especially during challenging times. Also, thanks to **Dr. Maria José Ladera Carmona** for her guidance and help in the writing process in the last year of my Ph.D. journey. I would also like to express my gratitude to our technicians Ute Micknass, Cornelia Dechert, Eugen Swidtschenko, and our gardeners Juliette Kellermann and Christina Birkenstock. Their technical competence and experience have greatly contributed to the success of my research work. I extend my appreciation to my colleagues at the Institute of Phytopathology and Biochemistry, including Dr. Shaoshuai Liu, M.Sc. Rina Mahmuti and Dr. Christina Pfafenrot. Your support and advice have enriched my research and daily life. I would like to acknowledge DAAD, TransMIT Gesellschaft für Technologietransfer mbH, and Deutsche Forschungsgemeinschaft (DFG) for the financial support that covered my living expenses during my study.

Last but not least, my deepest gratitude goes to my wife, **Dr. Ishrat Jahan**, and my parents. Their unconditional love, support, and encouragement have been the driving force behind every step of my journey. With their support, my journey continues, and I look forward to the future with unwavering determination.